

AUS Repository

Shear Capacity of Fiber Reinforced Lightweight Concrete

Item Type	Thesis
Authors	El Shazly, Mariam Hesham
Download date	2026-06-08 17:49:55
Link to Item	http://hdl.handle.net/11073/16424

SHEAR CAPACITY OF FIBER REINFORCED LIGHTWEIGHT CONCRETE

by

Mariam Hesham El Shazly

A Thesis presented to the Faculty of the
American University of Sharjah
College of Engineering
In Partial Fulfillment
of the Requirements
for the Degree of

Master of Science in
Civil Engineering

Sharjah, United Arab Emirates

November 2018

Approval Signatures

We, the undersigned, approve the Master's Thesis of Mariam Hesham El Shazly
Thesis Title: Shear Capacity of Fiber Reinforced Lightweight Concrete

Signature

Date of Signature

(dd/mm/yyyy)

Dr. Sherif Yehia
Professor, Department of Civil Engineering
Thesis Advisor

Dr. Rami A. Hawileh
Professor, Department of Civil Engineering
Thesis Committee Member

Dr. Wael Abuzaid
Assistant Professor, Department of Mechanical Engineering
Thesis Committee Member

Dr. Irtishad U. Ahmad
Head, Department of Civil Engineering

Dr. Ghaleb Hussein
Associate Dean for Graduate Affairs and Research
College of Engineering

Dr. Richard Schoephoerster
Dean, College of Engineering

Dr. Mohamed El-Tarhuni
Vice Provost for Graduate Studies

Acknowledgment

I would like to express my utmost gratitude to my advisor Prof. Sherif Yehia for providing me with a lot of knowledge, motivation, guidance and help throughout the stages of my research. His continuous support was fundamental to the whole process, and without him, I would not have reached to this stage. I have been lucky to have a supervisor who cared so much about my work, and who responded to my questions and queries so promptly, to ensure I am on the right track. I am also extremely thankful to Dr. Wael Abuzaid for his generous help, support, encouragement, patience and his great contribution to my thesis work. He was a great inspiration to me, provided me with a lot of motivation, confidence, precious advices, pushed me to work harder, and raised my spirits during stressful times. Additionally, I owe many thanks to Prof. Aqeel Ahmed for always making time for me and the fruitful discussions we used to have despite his busy schedule. He always provided me with immense guidance to keep me on the right track and was always a source of constant motivation and support. Furthermore, I would like to thank Eng. Waleed Nawaz for always helping me with my research, operating complex machinery during my experiments and encouraging me whenever I was demotivated or frustrated. I would also like to thank Mr. Anis Zakaria for his continuous help in the development of my master's thesis, especially with difficulties I encountered that were related to IT. In addition, I would like to thank Mr. Arshi Faridi and Mr. Mohammed Ansari for their help while conducting my experiments in the lab. I would like to thank Eng. Muhammad Qasim for always motivating me and offering help even though we are not from the same major. I am thankful as well to my colleagues Munir Basmaji, Abdallah Ghomeim and Youssef Awera for helping me in the preparation of my samples. I am also grateful to Coach Natalie Kondrat (my AUS Swimming coach) for being a second mother and my teammates for being great sisters. I would like to express my gratitude towards my dearest friends, Sabrin Dar-Amer, Sara Ahmed, Nouran EL-Mesalami, Hanin Atwany, Anfal Al-Abdulla and Zainab Feroz, who have always been there for me and making my AUS journey an amazing one. Finally, I would like to acknowledge the financial support I received from AUS during my studying period.

Dedication

Dedicated to my beloved parents and sisters for their unconditional love, endless support, encouragement and sacrifices.

Abstract

In this study, shear capacity of fiber reinforced High-strength Lightweight Self Consolidated Concrete (HSLWSCC) was investigated. Lightweight aggregate, size 4-8 mm coarse aggregate, was utilized in the evaluation. Steel (3D and 5D), synthetic and hybrid fibers (mix of steel (5D) and synthetic fibers) with a volume fraction of 0.75 % were added to the concrete matrix to prepare eight beams. In addition, four beams were prepared without fibers as control specimens. The twelve beams were prepared to cover the following six categories: 1) lightweight concrete (ALWSCC); 2) lightweight with partial normal-weight coarse-aggregate replacement (PRLWSCC); 3) lightweight with partial replacement and 3D steel fiber; 4) lightweight with partial replacement and 5D steel fiber; 5) lightweight with partial replacement and synthetic fiber; and 6) lightweight with partial replacement and hybrid fibers (mix of steel (5D) and synthetic fibers). The aim of the experimental program was to evaluate the effect of: 1) the normal-weight coarse-aggregate replacement; 2) the addition of fibers and 3) the steel fiber configuration on the shear capacity of lightweight concrete. It was concluded that the 12% replacement ratio of normal weight aggregate has insignificant effect on the shear capacity of the ALWSCC beams. The addition of the fibers showed a great enhancement in the ultimate load in the range of 91.6% to 137% compared to that of the control specimens (PRLWSCC). Furthermore, the fiber reinforced concrete beams showed improved crack distribution, post cracking and ductile behavior. The improvement was influenced by the fiber type and configuration. The experimental results of the four control beams were compared to the corresponding predicted values from the American, the Canadian and the European codes. It was concluded that, the Euro code, followed by the Canadian code, are better matching the experimental results in this investigation as compared to the ACI code. Moreover, the results of the fiber-reinforced beams were compared with the predicted values calculated from the ACI modified equation and previously proposed equations by other researchers, that accounts for the fiber effect. It was found that the ACI modified equation best matches the experimental results of the fiber reinforced concrete beams.

Keywords: *concrete shear capacity, lightweight concrete, partial normal-weight coarse-aggregate replacement, fibres*

Table of Contents

Abstract	6
List of Figures	10
List of Tables	13
Chapter 1. Introduction	15
1.1. Overview	15
1.2. Thesis Objectives.....	17
1.3. Research Significance	17
1.4. Thesis Organization.....	18
Chapter 2. Background and Literature Review.....	19
2.1. Factors Affecting Shear Strength in FRC.....	19
2.1.1. Concrete compressive strength.	19
2.1.2. Longitudinal reinforcement ratio.	20
2.1.3. Shear reinforcement.	20
2.1.4. Shear span to depth ratio.....	21
2.1.5. Beam size	22
2.1.6. Aggregate size.....	22
2.1.7. Fiber content.	23
2.2. Shear Transfer Mechanisms	24
2.2.1. Shear resistance of concrete compression zone	24
2.2.2. Interlocking action of aggregates	25
2.2.3. Dowel action	25
2.2.4. Arch action.....	25
2.3. Lightweight Aggregate Concrete	26
2.4. Effect of Fibre on Lightweight and Normal weight Concrete.....	26
2.5. Shear in Lightweight Aggregate.....	30
2.6. Partial Replacement of Lightweight Aggregate	30
2.7. Proposed Models for Shear Strength in Fiber Reinforced Lightweight Concrete.....	31
2.8. Different Codes Equations in Predicting Shear Resistance without Web Reinforcement	32
2.8.1. BS 8110.....	33
2.8.2. Euro code 2	33
2.8.3. Canadian code.....	33
2.8.4. ACI code 318.	34
2.8.5. Model code 2010.....	34
2.9. Shear Strength Design Equations for SFRC Beams.....	35

2.10.	Summary of the Effect of Steel Fiber Reinforcement on Concrete.....	35
	Table 2.4: The effect of using fibers on the different properties of FRC concrete.	36
2.11.	An Overview of the DIC and Its Applications	36
2.12.	Summary of Previous Studies	37
Chapter 3. Experimental Program.....		48
3.1.	Material Properties	48
3.1.1.	Lightweight aggregates.....	48
3.1.2.	Fibers.	49
3.1.3.	Steel bars.....	50
3.1.4.	Concrete mixes.	52
3.1.5.	Specimen's configuration.	53
3.2.	Preparation of the Samples.....	54
3.2.1.	Preparing the steel cages.....	54
3.2.2.	Formwork.	55
3.2.3.	Mixing	55
3.2.4.	Casting.....	55
3.2.5.	Curing	55
3.3.	Test Setup and Instrumentation.....	57
3.4.	Mechanical Properties Tests.....	58
3.4.1.	Compressive strength test.....	58
3.4.2.	Flexural strength.	58
3.5.	Summary	59
Chapter 4. Results		60
4.1.	Material Evaluation	60
4.2.	Tests to Determine Concrete Shear Capacity.....	62
4.2.1.	Load-mid span deflection.	62
4.2.2.	Strain Values.....	65
4.2.3.	Crack patterns.	67
4.2.4.	Initial cracking.....	68
4.2.5.	Modes of failure.....	69
4.2.6.	DIC results.....	69
Chapter 5. Discussion of the Results		76
5.1.	Material Evaluation Tests.....	76
5.1.1.	Effect of partial replacement on compressive strength.	76
5.1.2.	Effect of partial replacement on flexural strength.	76
5.1.3.	Effect of the fiber addition on compressive strength.....	76
5.1.4.	Effect of fiber on flexural strength.	77

5.2.	Test to Determine Concrete Shear Capacity	78
5.2.1.	Load _ Deflection response.	78
5.2.2.	Concrete strains.	84
5.2.3.	Steel strains.....	87
5.2.4.	Cracking behavior and mode of failure	87
5.2.5.	Initial cracking and crack widths.....	88
5.2.6.	DIC observations summary	88
5.2.7.	Predication of the shear capacity using codes and proposed equations.....	89
5.2.8	Experimental data vs predicted values from SFRC proposed equations.	90
5.2.9.	Calculating a modification factor to account for lightweight concrete.	92
5.2.10.	Cost of fibers used in all the mixes.....	93
Chapter 6.	Conclusions and Recommendations.....	95
6.1.	Conclusions	95
6.2.	Recommendations	97
References	99
Appendix A	106
Appendix B	109
Appendix C	112
Appendix D	115
Appendix E	118
Appendix F	120
Appendix G	123
Appendix H	132
Appendix I	134
Vita	135

List of Figures

Figure 2.1: Modes of failure for concrete beams of varying a/d ratios [16]	22
Figure 2.2: Schematic of the fiber crossing through the crack [31].....	23
Figure 2.3: Schematic of shear transfer mechanisms [32].....	24
Figure 2.4: Schematic diagram showing the arch action [96].....	25
Figure 2.5: detecting the displacement of point m with time.....	37
Figure 3.1: Pozzolan aggregate.....	48
Figure 3.2: (a) Specific gravity test, (b) Aggregate crushing, and (c) Sieve analysis test.	49
Figure 3.3: (a) Polypropylene fiber, (b) 3D steel fiber, (c) 5D steel fiber.	50
Figure 3.4: Dramix 3D and 5D steel fiber properties (a) strength, (b) anchorage strength, tensile strength, wire ductility/d ratio, steel fiber concrete strength, (c) tensile curves, (d) pull-out test curves [101]	52
Figure 3.5: Stress vs strain curves for tested steel rebars (a) bar 1 (b) bar 2.....	52
Figure 3.6: Specimens configuration.	54
Figure 3.7: Section details (Dimensions in mm).....	54
Figure 3.8: Stages of the samples preparation.	56
Figure 3.9: Experimental setup.	58
Figure 4.1: Typical failure mode of (a) Fiber reinforced concrete cubes, (b) Control sample	60
Figure 4.2: Load versus mid-span deflection responses for the tested beams: (a) Control beams, ALWC-C-2 and PRLWC-C-2; (b) Fiber reinforced beams, PRLWC- 3-1, PRLWC-5D-2, PRLWC-SY-2 and PRLW-HY-1.	63
Figure 4.3: Average ultimate load of all the six mixes.	65
Figure 4.4: Load versus strain for beams (a) PRLWC-C-2, (b) PRLWC-3D-1.	66
Figure 4.5: Load versus strain for beams (a) PRLWC-C-2, (b) PRLWC-3D-1.	67
Figure 4.6: Crack pattern of beam (a) ALWC-C1 and (b) PRLWC-5D-1.....	68
Figure 4.7: Initial part of the load vs strain curve for SG1 or beam PRLWC-C-2.	69
Figure 4.8: Mode of failure and shear angle of beam PRLWC-3D-2.....	69
Figure 4.9: (a) Vertical and (b) horizontal displacement contours of ALWC-C-1 beam.	72
Figure 4.10: Different strain maps (a) ϵ_{xx} (b) ϵ_{yy} (c) ϵ_1	72
Figure 4.11: Shear and flexure crack initiation and propagation of ALWC-C-1 beam.	73
Figure 4.12: Crack vs time plot for beam ALWC-C-1.	75
Figure 4.13: Load vs deflection for beam ALWC-C-1.....	75
Figure 5.1: Average load versus mid-span deflection responses for all groups.....	79
Figure 5.2: Ratios of V_c experimental/ V_c predicted from other codes.	91
Figure 5.3: Ratios of V_n experimental/ V_n predicted from other codes.....	92
Figure A.1: Load versus mid-span deflection responses for Group A beams ALWC-C- 1 and ALWC-C-2.....	106
Figure A.2: Load versus mid-span deflection responses for Group B beams PRLWC- C-1 and PRLWC-C-2.	106
Figure A.3: Load versus mid-span deflection responses for Group C beams PRLWC- 3D-1 and PRLWC-3D-2.....	107

Figure A.4: Load versus mid-span deflection responses for Group D beams PRLWC-5D-1 and PRLWC-5D-2.....	107
Figure A.5: Load versus mid-span deflection responses for Group E beams PRLWC-SY-1 and PRLWC-SY-2.	108
Figure A.6: Load versus mid-span deflection responses for Group F beams PRLWC-HY-1 and PRLWC-HY-2.....	108
Figure B.1: Load versus strain responses for Group A beams (a) ALWC-C-1, (b) ALWC-C-2.....	109
Figure B.2: Load versus strain responses for Group B beams (a) PRLWC-C-1, (b) PRLWC-C-2.....	109
Figure B.3: Load versus strain responses for Group C beams (a) PRLWC-3D-1, (b) PRLWC-3D-2.....	110
Figure B.4: Load versus strain responses for Group D beams (a) PRLWC-5D-1, (b) PRLWC-5D-2.....	110
Figure B.5: Load versus strain responses for Group E beams (a) PRLWC-SY-1, (b) PRLWC-SY-2.	111
Figure B.6: Load versus strain responses for Group F beams (a) PRLWC-HY-1, (b) PRLWC-HY-2.....	111
Figure C.1: Load versus strain responses for Group A beams (a) ALWC-C-1, (b) ALWC-C-2.....	112
Figure C.2: Load versus strain responses for Group B beams (a) PRLWC-C-1.	112
Figure C.3: Load versus strain responses for Group D beams (a) PRLWC-5D-1, (b) PRLWC-5D-2.....	113
Figure C.4: Load versus strain responses for Group E beams (a) PRLWC-SY-1, (b) PRLWC-SY-2.	113
Figure C.5: Load versus strain responses for Group F beams (a) PRLWC-HY-1, (b) PRLWC-HY-2.	114
Figure D.1: Load versus strain initial responses for Group A beams (a) ALWC-C-1, (b) ALWC-C-2.....	115
Figure D.2: Load versus strain initial responses for Group B beams (a) PRLWC-C-1, (b) PRLWC-C-2.	115
Figure D.3: Load versus strain initial responses for Group C beams (a) PRLWC-3D-1, (b) PRLWC-3D-2.	116
Figure D.4: Load versus strain initial responses for Group D beams (a) PRLWC-5D-1, (b) PRLWC-5D-2.	116
Figure D.5: Load versus strain initial responses for Group E beams (a) PRLWC-SY-1, (b) PRLWC-SY-2.....	117
Figure D.6: Load versus strain initial responses for Group F beams (a) PRLWC-HY-1, (b) PRLWC-HY-2.	117
Figure E.1: Modes of failure and angles of cracks of all the twelve beams.....	119
Figure G.1: Shear and flexure crack initiation and propagation of ALWC-C-1.....	123
Figure G.2: Shear and flexure crack initiation and propagation of PRLWC-C-2.....	124
Figure G.3: Shear and flexure crack initiation and propagation of PRLWC-3D-2. ..	125
Figure G.4: Shear and flexure crack initiation and propagation PRLWC-5D-1.....	126
Figure G.5: Shear and flexure crack initiation and propagation for beam PRLWC-SY-1.	127

Figure G.6: Shear and flexure crack initiation and propagation for beam PRLWC-HY-1.....	128
Figure G.7: Crack vs time plot for beam ALWC-C-1.	129
Figure G.8: Crack vs time plot for beam PRLWC-C-2.	129
Figure G.9: Crack vs time plot for beam PRLWC-3D-2.	130
Figure G.10: Crack vs time plot for beam PRLWC-5D-1.	130
Figure G.11: Crack vs time plot for beam PRLWC-SY-1.....	131
Figure G.12: Crack vs time plot for beam PRLWC-HY-1.	131
Figure I.1: Shear and bending moment diagram.....	134

List of Tables

Table 2.1: Different codes minimum shear reinforcement provisions.....	20
Table 2.2: Design constants needed for lightweight modification factor.	32
Table 2.3: Proposed equations for shear strength of fiber reinforced concrete for different authors.	35
Table 2.4: The effect of using fibers on the different properties of FRC concrete.	36
Table 2.5: Summary of previous studies.....	37
Table 3.1: Summary of the physical and mechanical properties of the aggregate.....	48
Table 4.1 Summary of the mechanical properties.....	61
Table 4.2: Summary of the test results.....	64
Table 4.3: Summary of maximum strain values in SG1, SG2, and SG3.....	66
Table 4.4: Summary of maximum strains in SG4, SG5, SG6, and SG7.....	67
Table 4.5: Required loads to develop the cracks (up to crack No. 8).	68
Table 4.6: Initial crack load captured from strain gauges.....	70
Table 4.7: Modes of failure of all the tested beams.	70
Table 5.1: Vc normalizes values for all the test beams.....	81
Table 5.2: Percentage of load increase for all the fiber-reinforced beams with reference to the control beams.	82
Table 5.3: Summary of the material properties.....	85
Table 5.4: Summary of concrete shear capacity	86
Table 5.5: Experimental shear values versus predicted.	90
Table 5.6: Comparing the ratios of Vc experimental/Vc predicted from other codes.	90
Table 5.7: Vn experimental vs Vn predicted from SFRC proposed equations.....	91
Table 5.8: Comparing the ratios of Vn experimental/Vn predicted from other studies.	91
Table 5.9: Shear values (Vc) of all code equations without applying reduction factors.	92
Table 5.10: λ values predicted based on different applied codes.....	93
Table 5.11: Cost of the fibers used in each concrete beam of each mix	93
Table 5.12: A summary of the results obtained from the DIC results.	94

List of Abbreviations

FRC	Fiber Reinforced Concrete
FRSCC	Fiber Reinforced Self Consolidating Concrete
LWA	Light Weight Aggregate
LWC	Light Weight Concrete
NWA	Normal Weight Aggregate
NWC	Normal Weight Concrete
PRLWC	Partially Replaced Light Weight Concrete
SCC	Self Consolidated Concrete
SCLWC	Self Consolidated Lightweight Concrete.

Chapter 1. Introduction

In this chapter, the thesis objectives, significance and contribution is going to be discussed. Then, a summary of the thesis organization is provided.

1.1. Overview

Recently, with the rapid development of high-rise buildings, floating marine structures, larger-sized and long-span concrete bridges, lightweight concrete (LWC) has emerged as a promising modern construction material. Compared to normal weight concrete (NWC); LWC exhibits excellent characteristics such as reduced dead load, higher strength to weight ratio, lower coefficient of thermal expansion, and superior heat and sound insulation [1]. However, a major drawback, which prevents a wider adoption of LWC, is the relatively inferior shear strength compared with that of NWC. According to Taylor et al. [2], 50% of the shear force in slender beams is transferred by aggregate interlock, which suggests that the lower shear capacity of LWC is attributed to degradation in aggregate interlock. To account for this weakness of the lightweight aggregate, a modification factor of 0.7 to 1 was applied to shear strength equations in different codes, as going to be discussed later.

To address the aforementioned limitation of LWC, partial replacement of LWC with NWC (better aggregate interlock) has been proposed as a method to improve the strength. Such an approach aims to improve the shear strength to acceptable magnitudes while still retaining some weight reduction compared to NWC. In the literature, there are few studies conducted on partial replacement of LWC. For instance, Yehia et al. [3] studied the mechanical properties of LWC partially replaced with different percentage of NWA and concluded that a replacement of 12% was most effective, provided that the unit weight does not exceed 2000 kg/m³.

The introduction of fibers into reinforced concrete (RC) enhances toughness; improves resistance to fatigue, impact, blast loading, reduce spalling of the reinforcement cover, improves abrasion resistance, flexural and shear strength [4]. Furthermore, it leads to increase of the ductility and deformability, as a considerable amount of energy is absorbed in deboning and pulling out of fibers from the concrete matrix before the complete concrete failure occurs. As a result, fibers can reduce the spacing and width of diagonal cracks. Therefore, the shear transfer capacity can be

improved due to enhanced aggregate interlock effect. The discretely distributed fibers act as effective shear reinforcement, due to its superior ability in suppressing crack initiation, arresting crack propagation and maintaining the integrity of the concrete structure [5]. However, the extent to which fibers contribute to each mechanical and durability characteristic of FRC largely depends on various factors including fiber type, configuration, length, and volume; water-cement ratio (w/c); aggregate/binder ratio; mortar volume fraction; properties of aggregates; and other mixture parameters [6].

To achieve better shear properties, the use of a Self-Consolidated Concrete (SCC) matrix will be of a great benefit. Greenough et al. [7] showed that Fiber Reinforced Self-Consolidated Concrete (FRSCC) beams with no web reinforcement resulted in a superior shear performance compared with that of conventional FRC beams with no web reinforcement. This might be attributed to, higher workability and the elimination of mechanical vibration led to a more homogeneous distribution of fibers. The construction time and costs as well as the placement of web reinforcement may accordingly be reduced by using FRSCC. Moreover, FRSCC can be easily placed in highly congested structural elements, where it may be very un-practical to keep stirrups. In addition, it helps in obtaining higher quality finishing surfaces [8]. The investigation on FRSCC, which has advantage of both SCC and FRC, is trending. However, investigations on shear toughness of hybrid fiber reinforced RC beams are limited.

Over the past years, significant research effort has been devoted to analyze the mechanical properties and the shear behavior of Steel Fiber Reinforced Concrete (SFRC) members. However, less work was done on the Fiber Reinforced Light Weight Concrete (FRLWC), and, even less research that is concerned with FRSCC. On the other hand, there were no fiber reinforced lightweight self-consolidated (FRLWSC) or partially replaced lightweight concrete (PRLWC) beams studied.

The current study, therefore, aims at investigating two solutions to improve the lightweight concrete performance and choosing the optimum mix in terms of load carrying capacity and ductility, taking the advantage of using SCC concrete that is light in weight combined with fiber and partial replacement with NWC. Effect of partial normal-weight coarse-aggregate replacement as well as addition of steel (3D and 5D),

synthetic and hybrid fibers (mix of steel (5D) and synthetic fibers) with a volume fraction of 0.75 % on shear behavior of lightweight concrete beams without web reinforcement will be evaluated.

An experimental investigation was carried out to evaluate and assess the effectiveness of the two proposed solutions.

1.2. Thesis Objectives

The main objectives of the study are to investigate possible solutions to improve the shear behavior and capacity of lightweight concrete beams. To achieve this goal the following will be evaluated:

- Effect of partial normal weight coarse aggregate replacement on the shear behavior of SCC lightweight concrete beams without web reinforcement.
- Assess the effect of addition of different types of fibers, of fixed volume percentage, on the shear behavior of PRSCCLWC beams without web reinforcement.
- Study the effect of the superior properties of the newly launched 5D steel fiber.
- Study the synergy effect of 5D and polypropylene fiber hybridization on LWSCC.
- Observe the different failure modes for different scenarios.
- Compare the experimental results with different design codes.
- Utilize the Digital Image Correlation technique in detecting and measuring surface displacements.

1.3. Research Significance

The literature, to date, lacks information on the shear behaviour of LWSCC and ways of improving its brittleness. Therefore, to enhance the shear performance of NWC two solutions were proposed. First solution was to assess the effect of inclusion of 12% of NWA into the lightweight concrete mix. This has been investigated earlier on smaller samples to evaluate the effect of partial replacement on compressive strength. However, the effect of the partial replacement on shear performance of beams has not been investigated. The second solution was to evaluate the effect of incorporating various types of fibers, of fixed percentage, on the shear behaviour of PRLWC beams.

Furthermore, the use of the newly launched 5D steel fiber is evaluated as it is recognized as having superior properties when compared to other types of fibers. Additionally, Digital image correlation was used to capture the crack initiation, crack propagation, crack widths, as well as providing full field strain and displacement maps, for the tested beams.

1.4. Thesis Organization

The rest of the thesis is organized as follows: Chapter 2 provides background about shear in partially replaced fiber reinforced lightweight concrete beams. Moreover, works related to this research are discussed. The methodology and experimental program of the study is discussed in Chapter 3. Chapter 4 presents the results and discussion of the conducted experiments. Finally, Chapter 5 concludes the thesis and outlines the future work.

Chapter 2. Background and Literature Review

In this chapter, background information is provided covering the different aspects of the study. This is done through reviewing research efforts found in the literature and discuss their progress in the field to provide baseline on which this study can be built.

2.1. Factors Affecting Shear Strength in FRC

There are several factors affecting the shear strength of fiber reinforced concrete beams, listed as follows:

- Concrete Strength
- Longitudinal Reinforcement Ratio
- Shear Reinforcement
- Shear Span to Depth Ratio (a/d).
- Beam Size.
- Aggregate size
- Fiber content

Influence of individual or combined effect of the above factors on the shear behaviour or strength is briefly discussed in the following subsections.

2.1.1. Concrete compressive strength. The compressive strength of concrete is considered as one of the most important factors influencing the shear strength of concrete beams. A study conducted by kwak et al. [9] demonstrated that the nominal stress at shear cracking and the ultimate shear strength increased by 23% with increasing concrete compressive strength from 31MPa to 65MPa in Steel Fiber-Reinforced Concrete Beams without Stirrups.

Narayanan and Darwish et al. [10] noticed that for a higher volume fraction of steel fibers, the rate of increase in shear strength due to the increase of compressive strength was higher. Due to the stronger bonds that develop between fibers and concrete matrix.

A study performed by Chao et al. [11] showed that the LWC beams without shear reinforcement tends to be brittle, the higher the compressive strength the higher is the brittleness. Mphonde and Frantz et al. [12] showed that as the compressive strength of concrete increases the nominal shear stress also increases.

212. Longitudinal reinforcement ratio. Many studies were carried out to investigate the effect of longitudinal reinforcement ratio on the shear strength of SFRC. Lie et al. [13] noticed that as the longitudinal reinforcement increases, the shear stress at failure increases, when SFRC beams with $\rho=1.1\%$, 2.2% and 3.3% ; respectively were tested. This is mainly attributed to the increased dowel action and reduction in crack width due to crack arresting mechanism. Swamy et al. [14] reported that with the increase in the tensile reinforcement ratio of SFRC, the shear strength increase to a certain limit, beyond which it declines.

213. Shear reinforcement. Shear reinforcement in the form of vertical stirrups does not alter the diagonal cracking strength significantly. However, the presence of stirrups tends to enhance the shear capacity by improving the shear transfer mechanisms by providing better dowel action, restraining crack propagation, minimizing bond-splitting failure and enhancing the contribution of uncracked concrete in the compression zone. In reinforced concrete structures, minimum shear reinforcement in RC elements by the codes of practice is to prevent sudden catastrophic failure as soon as the first diagonal cracking load is reached, to control widening of cracks at service loads and to ensure adequate ductility before failure. Different codes specify a minimum shear reinforcement, as illustrated in Table 2.1. The minimum shear reinforcement is a function of the compressive strength of concrete as per ACI, AASHTO and CSA codes. On the other hand, BS and IS codes consider the minimum shear reinforcement as a function of the strength of shear reinforcement alone as shown in Table 2.1 [15].

Table 2.1: Different codes minimum shear reinforcement provisions.

Equation	(SI)
ACI [16]	$\frac{A_{sv}}{bS_v} \geq \frac{\sqrt{f_c}}{16f_y} \geq \frac{0.33}{f_y}$
AASHTO [17]	$\frac{A_{sv}}{bS_v} \geq \frac{\sqrt{f_c}}{12f_y}$
CSA [18]	$\frac{A_{sv}}{bS_v} \geq \frac{\sqrt{f_c}}{16.6f_y}$
IS 456 [19]	$\frac{A_{sv}}{bS_v} \geq \frac{0.4}{0.87f_y}$
BS 8110 [20]	$\frac{A_{sv}}{bS_v} \geq \frac{0.4}{0.87f_y}$

Where,

- A_{sv} = Area of shear reinforcement
- b = breadth of beam
- d = effective depth in mm,
- f_c = cylindrical compressive strength in MPa
- f_y = yield strength of longitudinal steel
- S_v = Spacing of stirrups

214 Shear span to depth ratio. Shear failure of a reinforced concrete beam is significantly influenced by the shear span to effective depth ratio (a/d). Sinha et al. [21] indicated that shear compression or shear tension failure occurs when shear span to effective depth ratio (a/d) lies within the range of 1 to 2.5. Under this load condition, flexural cracks develop and propagate in the compression zone, Figure 2.1(a). This behavior extended towards the tension reinforcement and propagated along the reinforcement as shown in Figure 2.1(b). The eventual failure will be due to anchorage failure of the tension reinforcement (i.e. shear tension failure) or by crushing of the concrete in the compression zone adjacent to the point load (i.e. shear compression failure). For diagonal tension failure, which occurs for shear span to effective depth ratio (a/d) of 2.5 to 6. In the initial stage, few flexural cracks were formed followed by diagonal flexural cracks propagating towards the compression zone as shown in Figure 2.1(c). As load increases, crack propagates gradually until the sudden shear failure occurs. Before this critical failure occurs, the bottom inclined crack will have widen, with more cracks developing later on.

Kwak et al. [9] indicated that the increase of shear strength was larger (69 to 80%) or smaller a/d ratios (less than 2.5) when compared to larger a/d ratios (shear strength increase by 22 to 38%). Khaloo et al. [22] observed that an increase in shear span to depth ratio causes a decrease in the shear strength, due to the arch action.

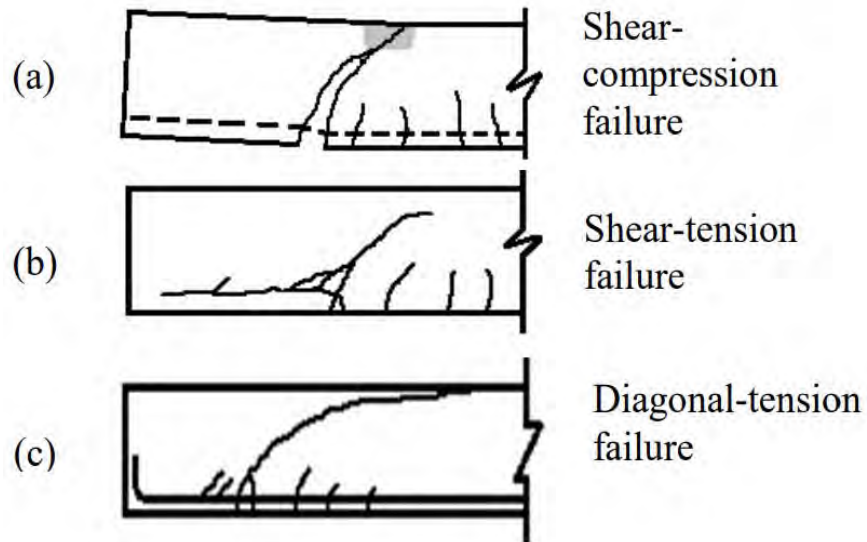


Figure 2.1: Modes of failure for concrete beams of varying a/d ratios [16].

Victor et al. [23] studied the shear strength of beams with a/d , ranging from 1.0 to 4.25. It was concluded that the ultimate shear strength decreases when the a/d ratio increases as shown in Figure 2.3, for reinforcement ratio of 1.1%.

215. Beam size. A study conducted by kani et al. [24], four-beam series of depths 6 in, 12 in, 24 in and 48 in were tested to conclude that the shear strength of concrete beams decrease as the size of the beams increase.

A. Acheampong et al. [25] studied several beams of variable thicknesses from 150 mm to 300 mm depth. It was noticed that the increase of beam depth results in a decrease of the ultimate shear strength of the beam specimens.

216. Aggregate size. According to Keun et al. [26] the shear strength of lightweight concrete (LWC) continuous beams increased with the maximum aggregate size. However, the increasing rate is lower than that of normal weight concrete (NWC) continuous beams.

Sherwood et al. [27] noticed that a reduction in the aggregate maximum size reduces the crack surface roughness and therefore leads to a decrease in the shear stress carried by the aggregate interlock.

Chao et al. [3] concluded that the shear failure paths are smoother in LWC beams than those of the NWC. Normally, the crack paths propagate through the coarse aggregate particles rather than around them. This is attributed to the interlocking of the

cement paste on the rough surface pores of the LWA therefore improving bond strength between aggregate surfaces and cement paste.

Kang et al. [28] indicated that an increase in steel-fiber volume fraction resulted in a change in the failure mode from brittle to ductile. In addition, steel-fiber volume fractions V_f of 0.5 % and 0.75% increased the shear capacities by 13% and 30%, respectively.

217. Fiber content. Mansour et al. [29] observed that an increase in the fiber percentage up to 1% enhances the shear resistance more than the corresponding increase in the bending strength. Therefore, changes the mode of failure from shear to flexure.

Swamy et al. [30] noticed that the ultimate shear strength of SFRLWC beams with fiber volume equals 1% increased load carrying capacity, by 60 to 210% and ductility, by 20 to 150%, when compared to reference beams.

Kang et al. [28] indicated that an increase in steel-fiber volume fraction resulted in a change in the failure mode from brittle to ductile. In addition, steel-fiber volume fractions V_f of 0.5 % and 0.75% increased the shear capacities by 13% and 30%, respectively. This is attributed to the stresses bridging across the cracks and the increased resistance to crack propagation as presented in Figure 2.2.

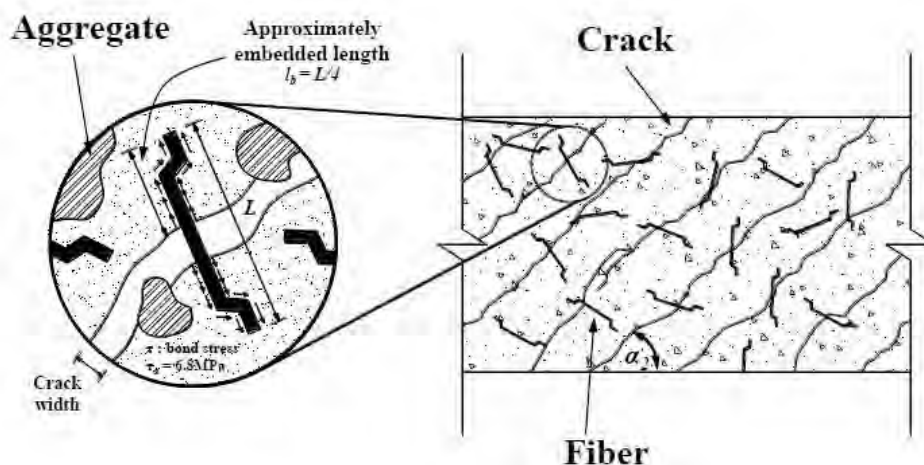


Figure 2.2: Schematic of the fiber crossing through the crack [31].

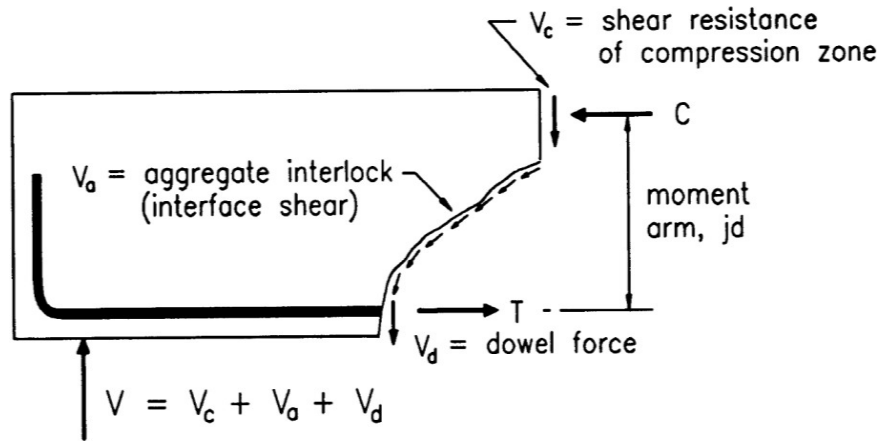


Figure 2.3: Schematic of shear transfer mechanisms [32].

2.2. Shear Transfer Mechanisms

For slender beams where a/d is greater than 2.0 ~ 3.0, shear force in a cracked section is mainly carried by the compression zone, interlocking action of aggregates, and dowel action of longitudinal bars, as shown in Figure 2.3 [32]. After an inclined crack has formed, in rectangular concrete beams, the amount of the shear force transferred by different mechanisms is as follows:

- 20 to 40 % by the un-cracked concrete of compression zone.
- 33 to 50% by aggregate interlock.
- 15 to 25% by dowel action of longitudinal bars.

In shorter beams, the load is directly transferred from the points of load application to the supports, owing to arch action.

2.2.1. Shear resistance of concrete compression zone. After the development of flexure crack, in a reinforced concrete beam, part of the shear is carried by the concrete in the compression zone. The shear failure in the un-cracked concrete is recognized as the failure under combined compression and shear and the area of un-cracked zone. The location of the neutral axis in a beam before it cracks in flexure is mainly dependent on the elastic modulus of concrete and the longitudinal reinforcement ratio. Since, the elastic modulus of steel is almost constant. Therefore, the shear force carried by the un-cracked concrete in the compression zone is greatly influenced by the compressive strength of concrete and the longitudinal steel ratio [32].

2.2.2. Interlocking action of aggregates. A large percentage of the total shear force on a beam without web reinforcement is carried across the cracks by aggregate interlocking. Among different variables, crack width and concrete strength are likely to be the most significant factors. Since the flexural crack width is approximately proportional to the tension reinforcement steel, the crack width at failure load becomes less as the longitudinal steel ratio is increased. In addition, with increasing a/d , the strain of tension reinforcement at failure is increased. Therefore, it is naturally expected that the interlocking force will be increased when the strength of concrete is high [32].

2.2.3. Dowel action. When shear displacement develops along the cracks, a certain amount of shear force is transferred by dowel action of the longitudinal bars mechanism. Although there is some contribution in dowel action by the number and arrangement of longitudinal bars, spacing of flexural cracks, and the amount of concrete cover, etc., the main factors affecting this action are flexural rigidity of the longitudinal bars and the strength of the surrounding concrete [32].

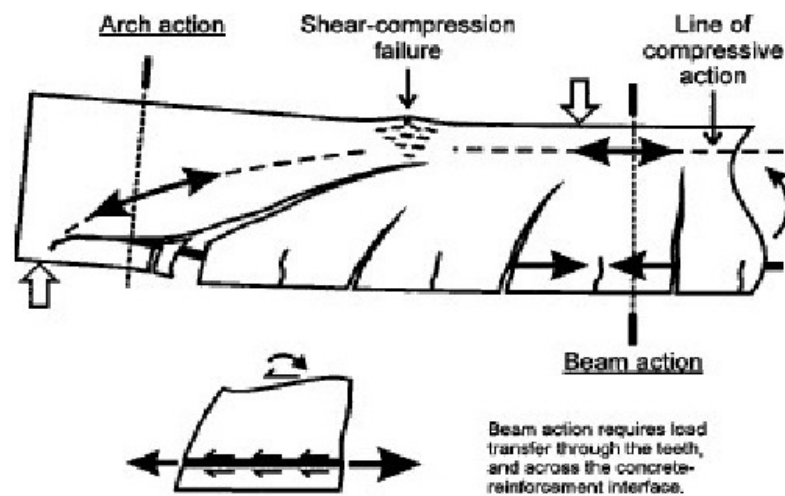


Figure 2.4: Schematic diagram showing the arch action [96].

2.2.4. Arch action. In short beams, the applied loads are carried to the supports directly by arch action. The main factors affecting this action are the span-to-height ratio of the analogous arch and the strength of the compression strut. The strength of the compression strut is proportional to the compressive strength of concrete and the area of tension reinforcement as shown in Figure 2.4 [32].

2.3. Lightweight Aggregate Concrete

Lightweight aggregate concrete is made up of lightweight aggregates of different types like clay, shale, slate materials, etc. LWC is having a density typically in the range of 440-1840kg/m³ as compared to that of NWC lying in the range of 2240-2400kg/m³. Therefore, the lightweight concrete is 20-35% lighter than the normal weight concrete [33].

The lightweight concrete strength for structural application should be of minimum value of 17 MPa in order to show a good performance. Using lightweight aggregate concrete is of great advantage, since, it reduces the dead load carried by the foundations leading to design that is more economical; furthermore, it improves fire resistance and thermal properties. Therefore, the demand on lightweight aggregate concrete is increasing worldwide. On the other hand, the main weakness of lightweight concrete comes from low strength aggregate that results in low compressive strength, tensile strength and shear strength [34].

Taylor et al. [2] concluded from tested slender beams that 50% of the shear force applied could be transferred by aggregate interlock. Due to the brittleness of lightweight aggregate simplified modified compression field theory ignore shear stresses transferred by aggregate interlock in lightweight concrete beams [35]. Therefore, to account for the weakness of the lightweight aggregate in computing shear strength, a modification factor of 0.8 was applied in average in different codes (i.e. ACI code, Euro code, Canadian code) depending on the type of light weight concrete.

2.4. Effect of Fibre on Lightweight and Normal weight Concrete

The addition of fibers to the concrete mix enhances the strength properties of the concrete when compared to that of the reinforced concrete. It improves compressive strength, modulus of rupture, tensile strength and post cracking tensile strength, hence, increasing the shear capacity of concrete [36]. However, the type, geometry, volume and aspect ratio (length/diameter) of the used fiber has a large impact on the strength of the fiber reinforced concrete. Moreover, fiber volume percentage ranging from 0.75% to 1% substantially increases ductility and load capacity of concrete beams [37].

A study done by Choi et al. [38] in which different types of fibers were used to assess their effect on the compressive strength, tensile strength, flexural strength, shear

strength and toughness on light weight concrete samples. Normal weight concrete specimens, with the same compressive strength as the lightweight, were used as a reference. It was concluded that the specimens load capacity increased due to the fiber bridging mechanism. It was shown that the shear strength of steel fiber reinforced lightweight and normal weight concrete specimens were increased by a percentage of 8-40% and 5-43% respectively.

Kwak et al. [9] also studied the effect of steel fibers on beams in which three volume ratios of 0%, 0.5% and 0.75% were investigated and the results showed that as the fiber volume increased, the spacing between the cracks decreased, crack sizes decreased and deformation capacity increased. The ultimate shear strengths of the fiber-reinforced beams ranged from 122 to 180% of the strength of the beams not reinforced with fibers.

Araujo et al. [39] showed that the addition of 1% of fibers content increased the ultimate shear strength of concrete by 87%; meanwhile, adding 2% of steel fiber increased it by 99%. The fibers caused a decrease in shear crack width and in a beam with 2% of steel fibers and low stirrup ratio; they were able to change the failure mode, from shear to bending. Kang et al. [40] demonstrated that a steel fiber content of 0.5% to 0.75% increases ultimate shear strength in SFRLC by around 25% to 45%.

S.K.kulkarni et al. [41] concluded that the increase in fiber content increased the compressive strength of concrete by an increment of 7.77%, for the optimum percentages of the hybrid fibers added (0.7% steel +0.3% glass). Furthermore, the HFRC deep beams showed 11% improvement in shear than the conventional beams due to the improved ductility and post cracking behavior of the beams. In comparison with conventional beams there was an increase of 14% in the first crack load and 11% in load at permissible deflection, this was observed for beams with the optimum fiber mix. Juli et al. [42] demonstrated that the inclusion of fibers increased the shear load capacity by an increment of 40% when compared to conventional beams.

Jianming et al. [43] studied the effect of addition of steel fibers on the mechanical properties of concrete. It was concluded that the addition of fiber extremely improved the flexural strength, the deflection corresponding to the ultimate load with the increase of the fiber volume to 2%, due to the increase in ductility. Jadhav et al. [44]

indicated that there was no propagation of cracks throughout the depth of the beam, if fiber comes across the line of the crack. Further crack generation took place in another direction and the width of the generated cracks were reduced. Wang et al. [45] noticed an increase in the mean value of first crack load and failure strength of SFLWC with fiber volume of 1.5% and 2% increased by 4% and 8.5%, 10% and 13% respectively.

O. Kayali et al. [46] observed that steel fiber at 1.7% by volume of the concrete caused an increase in the direct tensile strength by about 118% and modulus of rupture by about 80%. Furthermore, addition of 0.56% of polypropylene caused an increase of 90% in the indirect tensile strength and 20% increase in the modulus of rupture. On the other hand, the polypropylene fibers did not show significant results for the rest of the mechanical properties. Banthia et al. [47] reported that the addition of the steel, polypropylene and carbon fibers overcome the brittleness of concrete. Chen and liu et al. [48] also showed that the addition of steel fiber significantly enhances the split tensile strength of expanded polystyrene concrete and improve its shrinkage properties.

Rajai et al. [49] reported that the addition of steel and synthetic fibers to the lightweight concrete significantly improved the mechanical properties of the tested specimens. The compressive strength was improved from 2.8% for 0.3% fiber to 11.3% for 1.2% fiber. Splitting tensile strength also showed enhancement from 3.9% for 0.3% fiber to 35.9% for 1.2% fiber. Flexural strength improved from 21.8% for 0.3% fiber to 56.8% for 1.2% fiber. In addition to the significant enhancement of the flexural toughness indexes, post cracking toughness and failure deflections of the tested specimens.

Yinning et al. [50] tested SFRSCC beams to study the influence of steel fibers and the hybrid effect of steel fibers and stirrups on the deflection, cracking, ultimate load and failure pattern. The results demonstrated that the steel fibers enhanced the shear cracking load and ultimate load of SCC beams. For the addition of 60 kg/m^3 of fibers, the shear capacity of SCC beams without stirrups improved by up to 82% over the beam without fibers. Patil et al. [51] investigated the effect of five different steel fiber fractions ranging from 0% to 1.5% on the shear response of SFRC beams. It was found out that the ultimate shear strength of the matrix increased noticeably by adding

fibers to the matrix. Furthermore, it was also noticed that the optimum fiber content used was 0.75%.

Hassan et al. [52] presented the experimental results of 11 slender highly workable SFRC beams tested under four-point loading. It was reported that the combined use of SCC and steel fibers in shear deficient beams resulted in improved shear resistance and flexural ductility. The results of beams cast using SCC mix demonstrated that the increase in fiber content increases shear capacity. An improvement of 63% in shear strength was observed for fiber content of 1% when compared to the control beam. On the other hand, the use of 1.5% fibers did not lead to further increase in capacity.

Balendran et al. [53] studied the effect of inclusion of steel fibers on the tensile strength, flexural strength, compressive strength and toughness of lightweight and normal weight concrete. It was found that a significant enhancement in the splitting tensile strength and toughness at smaller percentages of fibers. Whereas, the compressive strength was not affected that much. Furthermore, it was concluded that the improvement in tensile splitting strength and flexural strength was more observed in the lightweight concrete than the normal weight concrete.

Toubat et al. [54] concluded that the use of macro polypropylene synthetic fibers improved the shear strength of slender beams by 14%, 23% and 30% respectively for fiber fractions of 0.5%, 0.75% and 1%. In addition, it enhanced the shear resistance of fiber reinforced short beams by 20% and 28% for fiber contents of 0.5% and 0.75% respectively.

Chen et al. [55] studied the contribution of hybrid fibers to the workability, mechanical and shrinkage properties of LWC with high strength and workability. The study showed an overall enhancement at different degrees. An improvement of 27.6% and 38.3% were reported for the compressive strength and splitting tensile strength respectively, for the hybrid mix of carbon and steel fibers. Furthermore, the toughness index was significantly enhanced, and brittleness was reduced. Mazaheripour et al. [56] studied the effect of the addition of polypropylene fiber on the lightweight self-consolidating lightweight concrete. It was reported that tensile strength and flexural strength were improved by 14.4% and 10.7% respectively. Pour et al. [57] reported that

the fiber reinforced LWAC showed significantly higher splitting tensile strength when compared to plain LWAC, even at low volume of fibers. Wang et al. [58] concluded that the inclusion of polypropylene fiber and steel fibers are linearly improving flexure and toughness of the lightweight cement composite at a fiber dosage of 0.5%.

2.5. Shear in Lightweight Aggregate

Shear strength is one of the weaknesses in lightweight concrete that needs to be improved due to the reduced shear capacity of lightweight concrete members. ACI code equations [16] were modified by a factor of 0.85 for sand lightweight concrete and 0.75 for all lightweight concrete might be conservatively applied. A study performed by Mattock et al. [59] showed that the shear transfer strength of lightweight concrete is less than that of sand and gravel concrete having the same compressive strength.

Hiroshi et al. [60] carried out a study to correlate the flexural and shear toughness of lightweight fiber reinforced concrete. Since the flexural performance of FRC is better understood than the shear behavior, that cause brittle and catastrophic failures, a clear correlation could lead to a more understood shear behavior. The results showed that there is a linear correlation between the shear strength and flexural strength of FRC.

2.6. Partial Replacement of Lightweight Aggregate

Yehia et al. [61] investigated the partial replacement of lightweight concrete with normal weight concrete. Different percentages of NWA were added to LWA (0%, 12%, 18%, 20%, 25%, 50%) and it was found out that the 88%-12% mix was demonstrating better results given that the unit weight of light weight concrete should not exceed 2000 kg/m³. However, the increase in compressive strength was more remarkable at partial replacement range of 25% to 50% but at these percentages, the concrete is not considered as lightweight any more.

Bhaskar et al. [62] studied the effect of replacing the normal weight aggregate by cinder lightweight aggregate on the compressive strength, tensile strength, modulus of elasticity, density and shear strength. It was concluded that the increase in percentage of the lightweight concrete adversely affected the strength properties of the samples tested.

Abdel Aziz et al. [63] showed that the amount of increase in the compressive strength reached about 15, 30, 50 and 90%, when 35, 50, 60 and 100% NWA were used as a partial replacement for LWA, in an attempt to enhance the properties of the hardened LWSCC. Furthermore, the partial replacement of LWA with NWA also improved the porosity of LWSCC, where increasing the percentage of NWA in LWAC mixes led to a reduction in its porosity results, due to the decrease for pores because of inducing NWA to LWSCC. On the other hand, the density of concrete was increasing because of the addition of NWA reaching 2230 kg/m³ when the LWA was fully replaced with NWA. Therefore, to fulfil density criteria for producing structural LWAC as per (ACI 211.2-81) the maximum content of LWA to be partially replaced by NWA in LWAC mixes should not be more than 50% of the LWA content. Despite, the enhancement in the self-compatibility, the LWSCC lost much of its flow ability and deformability characteristics due to the addition of NWA into LWSCC mixes as shown in the slump flow and air content results. Bogas et al. [64] indicated that there is an almost linear reduction of concrete stiffness as the NW coarse aggregate is replaced by LWA.

2.7. Proposed Models for Shear Strength in Fiber Reinforced Lightweight Concrete

Different scientists [9-10] proposed few shear strength equations for steel fiber reinforced concrete beams. Ashour et al. [65] modified the equation proposed for the steel fiber reinforced concrete to calculate shear strength of fiber reinforced lightweight concrete, in which the lightweight concrete modification factor λ was introduced to account for the effect of lightweight concrete. The equation is represented as follows:

$$V_n = (2.11 \sqrt{\lambda} f_c + 7F \sqrt{\rho \frac{d}{a}}) \quad (\text{MPa}) \text{ for } a/d \geq 2.5 \quad (1)$$

$$V_n = (58.2 \sqrt{\lambda} \frac{2.5}{f_c} + 1015F) \sqrt{\rho \frac{d}{a}} \quad (\text{psi}) \text{ for } a/d \geq 2.5 \quad (2)$$

Furthermore, another equation was proposed by Kang et al. [28] in which he used the model by Ashour and adopted λ^2 and modified it by another term dependent on a/d and the fiber ratio in which it is represented as follows;

$$V_n = [\text{Eq. (1)}] \left(\frac{2.5}{a/d} \right) + V (2.5 - \frac{a}{d}) \quad (\text{MPa; psi}) \text{ for } a/d < 2.5 \quad (3)$$

Moreover, Handson et al. [66] developed equations for the factor λ in which λ is dependent on the type of the lightweight aggregate being used. The developed equation is as follows.

$$\lambda = \frac{C_3\sqrt{f'_c} + C_4 \frac{\rho V_d}{M} (\leq 3.5\sqrt{f'_c})}{1.9\sqrt{f'_c} + 2500 \frac{\rho V_d}{M} (\leq 3.5\sqrt{f'_c})} \quad \text{In US units} \quad (4)$$

$$\lambda = \frac{C_3\sqrt{f'_c} + C_4 \frac{\rho V_d}{M} (\leq 0.292\sqrt{f'_c})}{0.158\sqrt{f'_c} + 17.24 \frac{\rho V_d}{M} (\leq 0.292\sqrt{f'_c})} \quad \text{In SI units} \quad (5)$$

In which the constants C_3 and C_4 are obtained from Table 2.2 depending on the type of aggregates used.

Table 2.2: Design constants needed for lightweight modification factor.

Coarse aggregates	C_3 U. S. Units(SI units)	C_4 U. S. Units(SI units)
Expanded shale (both rounded and angular)	1.1 (0.092)	3750 (25.82)
Expanded slag	1.3 (0.108)	3440 (23.72)
Expanded clay	1.5 (0.125)	3120 (21.52)
Sintered PFA(pulverized fuel ash or fly ash)	1.7 (0.142)	2810 (19.38)
Expanded slate or normal weight concrete aggregate	1.9 (0.158)	2500 (17.24)

2.8. Different Codes Equations in Predicting Shear Resistance without Web Reinforcement

Shear equations were proposed in different codes, in order to predict the shear resistance in beams without web reinforcement. These equations were derived from comprehensive experimental investigation. According to a study done by Ofonime et al. [67] equations from BS 8110, Euro code 2, Canadian code, ACI code 318 and Model code 2010 were compared in order to study the differences between them and the factors taken into consideration based on 435 performed experiments.

2.8.1. BS 8110. Equation (6) is the proposed by the British code (BS8110).

$$V_c = \frac{0.79}{\gamma_m} \left(\frac{100A_s}{bd} \right)^{\frac{1}{3}} \left(\frac{400}{d} \right)^{\frac{1}{4}} \quad (6)$$

Where 0.79 is a factor, taking in to consideration other parameters affecting the shear strength not included in the given equation, $100A_s/bd$ represents the reinforcement ratio, $400/d$ accounts for the size effect. Furthermore, γ_m is the concrete partial factor of safety. If concrete compressive strength (f_{cu}) exceeds the value of 25 N/mm², the above equation should be multiplied by $(f_{cu}/25)^{1/3}$ to account for the effect of higher compressive strength on the shear strength. Moreover, the improvement in shear strength that occur in deep beams due to arching action taken into account by multiplying the calculated shear strength by $2d/av$ for beams with shear span-to-depth ratio $a/d < 2-2.5$.

2.8.2. Euro code 2. Euro code 2 is considered similar to BS 8110 in that it considers the concrete compressive strength, effective depth and reinforcement ratio. Equation (7) is the proposed by the Euro code 2

$$V_{Rd,c} = \frac{0.8}{\gamma_c} (100f_{ck})^{\frac{1}{3}} \left(1 + \sqrt{\frac{200}{d}} \right) b_w d \quad (7)$$

In which f_{ck} represents cylinder compressive strength of concrete in MPa, d is the effective depth in mm, ρ_l is the longitudinal reinforcement ratio given as A_s/bd . γ_c is the concrete partial factor of safety and b_w is the beam width in mm. For beams with short shear span-to-depth ratio ($0.5 \leq a/d \leq 2$), the calculated shear resistance is multiplied by $av/2d$ to take into consideration the arching action.

2.8.3. Canadian code. The Canadian code represents the shear strength of beams without web reinforcement as a function of compressive strength of concrete only. The equation is presented as follows:

$$V_c = 0.2\sqrt{f_c} b_w d \quad (8)$$

In which f'_c , d and b_w are representing concrete compressive strength in MPa, effective depth and width of beam respectively.

2.8.4. ACI code 318. A basic equation was given, taking into consideration the compressive strength of concrete only. The equation is as follows;

$$V_c = \left(\frac{\lambda \sqrt{f'_c}}{6} \right) b_w d \quad (9)$$

For further detailed analysis, the following equation is proposed.

$$V_c = \left(0.16 \sqrt{f'_c} + 17 \rho_w \frac{V_u}{M_u} \right) b_w d \leq 0.29 \sqrt{f'_c} b_w d \quad (10)$$

In which f'_c , ρ_w , b_w and d are representing concrete compressive strength, flexural reinforcement ratio, width and effective depth of beam respectively. λ is a factor that considers the effect of the lightweight concrete on the strength of beams. Furthermore, V_u and M_u are factored shear force and bending moment. In any case, $V_u d / M_u$ should not exceed 1.

2.8.5. Model code 2010. Model code 2010 proposed a more complex compared to other codes considered here. The proposed equation is given as follows;

$$V_{Rdc} = K_v \frac{\sqrt{f_{ck}}}{\gamma_c} b z \quad (11)$$

$$K_v = \frac{0.4}{1 + 1500 \xi} \cdot \frac{1300}{1000 + k_d z} \quad \text{for } \rho_w < 0.08 \sqrt{\frac{f_{ck}}{f_{yk}}}$$

$$K_v = \frac{0.4}{1 + 1500 \xi} \quad \text{for } \rho_w \geq 0.08 \frac{f_{ck}}{f_{yk}}$$

In which f_{ck} is the compressive strength of concrete in MPa, b is the section width in mm and z is the effective shear span depth and is assumed $0.95d$ in reinforced concrete members. γ is the concrete partial factor of safety. The parameter k_v takes into account the effect of strain in the web and the aggregate size. Model code 2010 also proposed

two levels of approximation to determine kv in beams without shear reinforcement. For level 2 approximations,

$$k_{dg} = \frac{32}{16 + d_g} \geq 0.75$$

ε represents the longitudinal strain in the web and k_{dg} is a factor that considers the size of aggregate. For level 1 approximation, equation (1) is simplified more by assuming that strain in the reinforcement is elastic at the point of failure in shear. The strain in the web is assumed to be one-half the yield strain of the flexural reinforcement. In addition, the maximum aggregate size can be assumed 9.6mm; making equation (2) equals 1.25.

2.9. Shear Strength Design Equations for SFRC Beams

Table 2.3 shows a summary of some of the proposed equations for shear strength equations of steel fiber reinforced concrete. All of the equations proposed by different authors are taking into consideration the Fiber factor F that is accounting for the fiber length, diameter, volume fraction and bond factor, which accounts for the shape of the fibers.

Table 2.3: Proposed equations for shear strength of fiber reinforced concrete for different authors.

Author	Proposed equation
Narayanan and Darwish et al. [10]	$V_n = e[0.24f_{sp} + 80\rho_a \frac{d}{a} + v_b] \text{ (MPa)}$
Ashour et al. [65]	$V_n = 2.11\sqrt{f_c} + 7F(\rho_a)^{0.555} \text{ (MPa)}$
Kwak et al. [9]	$V_n = 3.7 e f_{sp}^2 (\rho_a \frac{d}{a})^{\frac{1}{3}} + 0.8v_b \text{ (MPa)}$
Khuntia et al. [68]	$V_n = (0.167\alpha + 0.25F_1\sqrt{f_c}) \text{ (MPa)}$

2.10. Summary of the Effect of Steel Fiber Reinforcement on Concrete

The concrete society UK, 2007, compared the performance of the SFRC to that of the unreinforced concrete. Results were then summarized and presented in Table 2.4. It was clear that there was a remarkable improvement in most of the concrete properties. The major improvements were experienced in impact resistance, shear strength and toughness [69].

Table 2.4: The effect of using fibers on the different properties of FRC concrete.

Property	Comment
Abrasion resistance	Improvement may be achieved as a result of reduced bleeding
Compressive strength	Little change
Electrical resistance	No significant change at fiber dosages generally used
Fatigue resistance	Improvement even at low dosages
Flexural strength	Little change in first crack strength at dosage rates commonly used
Freeze-thaw resistance	Can reduce deterioration caused by freeze thaw cycling
Impact resistance	Major improvements
Modulus of elasticity	No significant change at fiber dosages generally used
Restrained shrinkage	Even at low dosages, better distribution of stresses can reduce crack widths
Shear strength	Improvements even at low dosages can be achieved in combination with reinforcing bars
Spalling resistance	Being dispersed throughout the matrix, steel fiber reinforcement gives superior protection to exposed areas such as the joint arris.
Thermal shock resistance	As with impact resistance , there are improvements even at low dosage rates, a typical application being foundry floors
Toughness	Major improvements, even at low dosages

2.11. An Overview of the DIC and Its Applications

Digital Image Correlation (DIC), also called white light speckle technique, is a non-contact optical, numerical, full field measuring technique. It allows the determination of in-plane displacement fields at the surface of objects subjected to any type of loading.

To obtain good results, the object of interest needs to be fully covered with a speckle pattern, be flat and remain in the same plane parallel to the camera during the loading process. The speckle pattern could be the natural texture of the tested sample or artificially made by spraying white and black paint.

Image correlation analysis involves comparing the change in the grey intensity of the acquired digital images in initial-undeformed and deformed states, to capture the movements and deformations that took place and consequently compute the full-field displacements and strains as shown in Figure 2.5.

Using DIC software, VIC 2D, the movement of the points on the image are calculated by correlating the digital images taken during the testing time. As a result, the DIC system demonstrates high capability in detecting the crack initiation and propagation of the sample under investigation. However, tracking single points is not favorable. Adjacent pixels are used instead, and such collection of pixels creates a window that is called subset.

There are numerous applications of this technique. First, it determines the full-field deformation and strain of materials under various loading conditions. Moreover, it helps in getting some mechanical properties of the tested object such as, young's modulus, poissons ratio, stress intensity factor, residual stress, coefficient of thermal expansion and elastic properties. The major advantage of the DIC is that it is easy to use and cost effective when compared to other methods like speckle interferometry. In addition to being more accurate and subjective than manual measurement techniques.

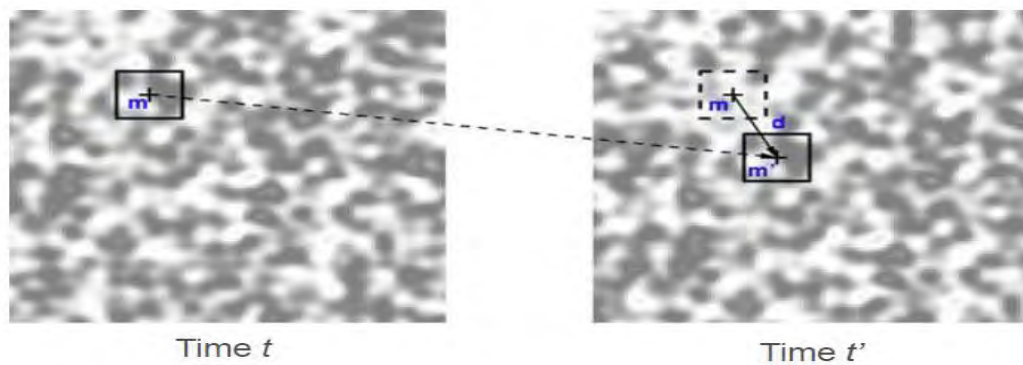


Figure 2.5: detecting the displacement of point m with time.

2.12. Summary of Previous Studies

Table 2.5 shows a summary of the studies conducted previously by other researchers, related to the current study. It presents the author name, fibres used, type of concrete, specimens prepared, parameters tested and conclusions.

Table 2.5: Summary of previous studies.

Mechanical properties of fiber reinforced normal weight concrete					
Author	Fibers used	Type of concrete	Specimens	Parameters tested	Conclusion
A. Samer Ezeldin et al. [70]	Steel	Normal weight	cylinders	Stress strain behavior	Addition of steel fibers to concrete with or without silica fume increases the toughness,

					compressive strength and the strain corresponding to peak stress.
Job Thomas et al. [71]	steel	Normal weight	Cubes cylinders	All Mechanical properties	The fiber matrix interaction effectively enhances the mechanical properties.
A. M. Alhozaimy et al. [72]	0.3% Polypropylene	Normal weight	Cylinders prisms	Compressive strength Flexural strength	No significant effect on compressive strength for the 0.3% used but a more pronounced effect on the flexural strength
M.C. Nataraja et al. [73]	0.5%, 0.75% and 1.0% Round Crimped steel fibers	Normal weight	cylinders	Compressive strength Toughness modulus	Considerable increase in toughness and no significant increase in compressive strength.
P.S. Song et al. [74]	0.5%, 1.0%, 1.5%, and 2.0%. hooked end steel fibers	High strength normal concrete	Cylinders prisms	Compressive strength Splitting tensile Modulus of rupture toughness	Splitting tensile strength increased in the range from 19.0% to 98.3%. modulus of rupture increased in the range from 28.1% to 126.6%. Compressive strength increased 12% for the volume fraction of 1.5%.
Kaiss Sarsam et al. [75]	0% to 2% of straight, hooked, deformed and crimped steel fiber	High strength normal concrete	Cylinders Prisms	compressive strength, axial strain, modulus of elasticity, Poisson's ratio, modulus of rupture, and splitting tensile strength	Increase of 17.5% in compressive strength, 77% in modulus of rupture, and 99% in splitting tensile strength; when using 1.5% volume fraction of

					hooked steel fiber.
Wu Yao[76]	Hybrid combinations of polypropylene (PP) and carbon, carbon and steel, and steel and PP fibers at 0.5%.	Normal weight concrete	Cylinders Prisms	compressive, splitting tensile, and flexural properties	Fibers, when used in a hybrid form, could result in superior composite performance compared to their individual fiber. Carbon steel composite showed the best results
Ahmed Ezeldin et al. [77]	0, 30, 45, and 60 kg/m ³ Hooked end steel fiber	Normal and high strength concrete	Pullout test	bond behavior of normal and high-strength concrete	The slip (relative movement between the bar and the concrete) at maximum bond load increases with increase in fiber content.
B.W. Xu et al. [78]	Steel polypropylene glass fiber	Normal weight concrete	Cylinders Cubes Prisms	Mechanical properties	The inclusion of fibers enhanced the mechanical properties.
N. Banthia et al. [79]	Hybrid (large and small diameter steel fibers)	Normal weight concrete	Cylinders Prisms	Mechanical properties	The results showed that such hybrid FRCs fail to reach the toughness levels demonstrated by the smaller diameter fibers alone. On the other hand, one can successfully enhance the toughness of the concrete by replacing a good amount of big fibers by small fibers.
Antonio et al. [80]	Steel + polypropylene fibers	NWC	Prisms cylinders	Compressive strength bending	HyFRC mixtures with more steel fibers exhibited

					higher post-cracking bending strengths and a tougher behavior. Polypropylene fibers led to lower variability
Shear properties of fiber reinforced normal weight concrete in shear					
Yoon keun et al. [9]	Steel fibers	Normal weight concrete	Beams	Shear	The inclusion of fiber enhanced the shear strength.
A. S. Shelke et al. 2017[16]	Crimped steel +polypropylene	Normal weight concrete	Beams	Shear	Hybrid (Crimped steel- Polypropylene) fiber have significant impact on the shear strength.
Gustavo J. et al. 2006[81]	Crimped and hooked steel fibers	Normal weight concrete	beams	Shear	0.75% of deformed fibers can be used as a minimum shear reinforcement
Achuthankutty A et al. 2013 [82]	Hybrid steel fibers (macro and micro steel fibers)	Normal weight concrete	Beams	Shear	The increase in shear strength of the beam with the use of hybrid micro and macro fiber is greater than the increase in the shear strength of beam when only macro fibers are used
Patil sonail et al. 2015 [51]	Steel fibers	Normal weight concrete	Beams	Shear	Ultimate shear strength of matrix increases significantly by adding fibers to the matrix The optimum content of fibers concluded in the study was 0.75%

Mechanical properties of light weight concrete					
Jisun Choi et al. [83]	Steel vinylon polyethylene	All light weight Artificial Made from shale	Cylinders Small beams	compressive strength splitting tensile strength flexural strength shear strength toughness	steel fibers were the most effective to increasing the toughness of both the all-lightweight and normal concrete
Fatih Altun et al. [84]	Steel	Pumice sand Pumice coarse light weight	Prismatic beams beams	Toughness Ductility	Increased ductility and resist crack formation
Jianming Gao [45]	3 steel fibers with different aspect ratios 46, 58, 70	High strength light weight (expanded clay medium sand)	Cylinders Cubes Prisms	Mechanical properties	Compressive strength was slightly improved 1 to 1.5% showed a huge improved to all other mechanical properties
Harun Tanyildizi et al. 2009[85]	Propylene fibers	Crushed pumice	Cubes prisms	Mechanical properties due to fibers and high temp exposure	
Sedat Kurugoo et al. 2008 [86]	Steel fibers Polymer	Pumice light weight	Cubes	Young's modulus	
Bing Chen et al. 2004[48]	Hybrid fibers (steel fibers carbon fiber polypropylene fibers)	Expanded clay high strength light weight	Cylinders Prisms	Mechanical properties	All the combinations showed good results But propylene fiber reduced the compressive strength a bit
G. Campion et al. 2005[87]	steel	Expanded clay aggregates	prisms	Bond slip behavior	Fibers showed great enhancement
R.V. Balendran et al. 2001[53]	Steel	Light weight Normal weight	Cube Cylinder Prisms	Mechanical properties	Fibers showed great enhancement
Mahmoud Hassanpour et al. 2012[57]	Steel	Pumice light weight	Cubes Cylinder prism	Mechanical properties	Fibers showed great enhancement
H.T. Wang et al. 2013[45]	Steel	High strength shale light weight	Cubes Cylinders Prisms	Mechanical properties	Fibers showed great enhancement
O. Kayali et al. 2003[46]	Polypropylene Steel	Lightweight sintered fly ash aggregate concrete	Cubes Cylinders Prisms	Mechanical properties	Polypropylene fibers at 0.56% by volume of concrete

					resulted in a 90% increase in the value of the indirect tensile strength.
Giuseppe Campione et al. 2003[88]	Steel fibers +stirrups	Pumice stone and expanded clay aggregates	Prism cylinder	Mechanical properties	The reinforcing fibers can partially substitute the transverse reinforcement
Roohollah Bagherzadeh et al. 2016[89]	Polypropylene	Light weight	Cylinders Cubes	Mechanical properties	PP fiber with 12 mm length and proportion 0.35 % performed better in all respects compared to the physical and mechanical properties of reinforced lightweight concrete.
Rajai et al. 2016[49]	Synthetic	Light weight concrete	Cylinders and prisms of different dimensions	Mechanical properties	The compressive strength increased from 2.8 to 11.3% for the 0.3% to 1.2% of fibers Flexural strength increased from 21.8% to 56.8% Increase in post cracking toughness. Crack arresting effect.
Tariq et al. 2013 [90]	polypropylene	Light weight concrete And normal weight	Prismatic beams Cylinders Beams	Flexure Ductility	The addition of the poly propylene fibers improved the ductility ranging from 18% to 98% for different fiber ratios and cement

					ratios when compared to the reference beams
R.V. Balendran et al. 2001 [53]	Steel fibers	Light weight and normal weight	Cube Cylinder Prism Beam Notched beams	Mechanical properties	The improvement in splitting tensile strength and flexural strength is much more for lightweight concrete than for normal weight Concrete.
Aghaee et al. 2014 [91]	Waste steel wires	Light weight concrete and normal weight	Cylinders Cubes Prisms	Mechanical properties	the addition of more than 0.5% of the waste wires and steel fibers decrease the compressive strength of FRC Specimens.
Jianming et al. 1997 [43]	Steel fiber	High strength light weight	Cylinders Cubes prisms	Mechanical properties	Addition of fiber with 1-1.5% volume fraction to high strength light weight concrete is extremely improving the strength and fracture toughness
Shear behavior of fiber reinforced light weight concrete beams					
Angelo Caratelli t al. 2016[93]	Steel fibers	Expanded clay light weight	Beams	Monotonic and reverse cyclic loads were set-up in order to investigate the influence of the fiber reinforcement on the strength, ductility and	steel fibers leads to an increase of about 20% of the ultimate load

				energy dissipation.	
Kang et al. 2011[28]	steel	Pumice Expansive shale Lightweight	Beams	Shear	Steel fiber is more effective in lwc than nwc Shows a high improvement in shear
Kang et al. 2010[40]	steel	Light weight	Beams	Shear	The addition of steel fibers with Vf of 0.5% to 0.75% improves the resistance to structural damage and ultimate shear strength in SFRLC by roughly 25% to 45%
Ayman ababneh et al. 2017[93]	Synthetic fibers stirrups	Light weight	beams	Shear strength	The experimental results showed that the discontinuous structural synthetic fibers improve the ultimate shear strength, ductility, stiffness, and toughness of lightweight The results also showed that addition of discontinuous structural synthetic fibers reduces the crack width of lightweight reinforced concrete Beams. The effectiveness of the discontinuous structural synthetic fibers decreases as

					the stirrups spacing decreases. concrete beams significantly
Mechanical properties of fiber reinforced self-consolidating concrete					
Juli Asni et al. 2016 [94]	Steel	NC SCC	Beams Cylinders Cubes prisms	Mechanical properties shear	Flexural strength enhanced by 57% Tensile strength enhanced by 69% Compressive strength increased by 15% Ultimate load increased by 60% No of cracks decreased
Mustafa Sahmaran et al. [95]	Straight and hooked fiber at a volume of 60kg/m ³	NWSCC	Cylinders Cubes	Mechanical properties	Mechanical properties were enhanced. The longer fibers with hooked ends were more effective.
Shear behavior of steel fiber reinforced self-consolidating concrete					
Hasaan Aoude et al. 2014 [96]	Steel fibers	Self-consolidate concrete SCC	Slender beams	Shear	The addition of steel fibers to a SCC mix improved the shear capacity of the beams and resulted in improved crack control and damage tolerance
Yining Ding et al. 2011[50]	Steel fibers	Self-consolidating concrete	Beams	Shear	Steel fibers enhanced the shear cracking load and ultimate load of SCC, for the addition of 60kg/m ³ , the maximum shear capacity of SCC beams without stirrups was

					increased by up to 82% over that beams with no fibers.
Mechanical properties of steel fiber reinforced light weight self-consolidating concrete					
H. Mazaheripour et al. [56]	Polypropylene fibers	Leca lightweight self-compacting	Cube Cylinder Prisms	Mechanical properties	For compressive strength, 15% was achieved with the inclusion of 1.0% fibers. In spite of little increment observed to the compressive strength of SFSCC, it offered a great contribution to the tensile splitting strength, flexural strength and residual flexural strength of concrete with 69%, 57% and 168% increments
Shahid Iqbal et al. [97]	Straight micro steel fibers	High strength light weight self-consolidating concrete	Cubes Cylinders Prisms	Mechanical properties	12% reduction in compressive strength, 37% and 110% increase in splitting tensile strength and flexural strength respectively, with increase of steel fiber content from 0% to 1.25%, while the modulus of elasticity remains unchanged.
Shear behavior of fiber reinforced self-consolidated lightweight concrete beams.					

No studies are available to date
Mechanical properties on partially replaced fiber reinforced lightweight concrete beams.
No studies are available to date
Shear behavior of fiber reinforced partially replaced light weight concrete beams
No studies are available to date
Mechanical properties on partially replaced fiber reinforced lightweight self-consolidating concrete beams.
No studies are available to date
Shear behavior of fiber reinforced partially replaced lightweight self-consolidating concrete beams
No studies are available to date

Mechanical properties of partially replaced light weight concrete

author	Replacement ratios	Parameters tested	Conclusion
G. E. Abdel Aziz et al. [63]	35%,50%, 60% and 100% NWA were used as a partial replacement of LWA (LWSCC)	Mechanical properties	The amount of increase in the compressive strength reached about 15, 30, 50 and 90%, when 35, 50, 60 and 100% NWA were used as a partial replacement of LWA
Arnon et al. 2001 [98]	Replacing NWC by 25% lightweight concrete.	Autogenous shrinkage	Partial replacement of normal-weight aggregate by SSD lightweight aggregate was effective in eliminating all The autogenous shrinkage in high-strength concrete
J. Alexandre Bogas et al. 2012 [64]	Replacing NWC by LWC	Modulus of elasticity	here is an almost linear reduction of concrete stiffness as the NA coarse aggregate is replaced by LWA

Structural properties of partially replaced light weight concrete

Lie et al. 2016 [99]	Superposed beam SFRLWC+NWC The depth of the SFRLWC varies	Flexure	The superposed beams need to be further studied
-----------------------------	--	---------	---

Chapter 3. Experimental Program

The main objective of this chapter is to present the experimental program, starting from the preparation of the samples to the results collection. The specimens were reinforced with different types of fibers, to enhance the structural shear resistance of the reinforced concrete. Initially, the aggregate properties were tested. Then, the mechanical properties (compressive and flexural strength) of the fiber reinforced concrete samples. Finally, structural load tests were conducted to evaluate the shear behavior of the casted beams.

3.1. Material Properties

3.1.1. Lightweight aggregates. A pozzolan lightweight aggregate with size range of 4 mm to 8 mm, Figure 3.1, was used in the investigation. Sieve analysis test (according to ASTM C136/ C136M), specific gravity and water absorption (according to ASTM C127 - 12) and aggregate crushing value test (according to BS812-110:1990) were conducted to determine the physical and mechanical properties of the aggregate before using in the concrete mixture, as shown in Figure 3.2.



Figure 3.1: Pozzolan aggregate.

Table 3.1 summarizes the results of the crushing value, absorption after 72 hrs, absorption after ½ hr, moisture content and specific gravity.

Table 3.1: Summary of the physical and mechanical properties of the aggregate.

Test	Value
crushing value	27
Absorption after 72 hrs.	15%
Absorption (after soaking for half an hour)	13.4%
Moisture content	0.55%
Specific gravity	1.35



(a)

(b)

(c)

Figure 3.2: (a) Specific gravity test, (b) Aggregate crushing, and (c) Sieve analysis test.

3.1.2. Fibers. Four types of fibers were considered in this research program. Steel fiber with two configurations (3D and 5D), synthetic fiber (polypropylene fibers (strux 90/40)), and hybrid which is a mix of steel fiber (5D) and synthetic fiber as shown in Figure 3.3.

3.1.2.1 Synthetic strux 90/40. STRUX 90/40, shown in Figure 3.3 (a), is a synthetic macro fiber made up of Polypropylene. It is 40 mm long and has an aspect ratio l/d of 90. It is characterized by its high strength and modulus value. When uniformly distributed in the concrete it improves the toughness, the impact resistance and the fatigue resistance. Moreover, it enhances the post cracking performance of the concrete. It was designed to replace different types of reinforcement like welded wire fabric, steel fibers and light rebar reinforcement [100].

3.1.2.2 3D Steel fibers. The 3D steel fibers, shown in Figure 3.3(b), are 60 mm long and has slenderness ratio l/d of 65. 3D steel fibers are known for their durability and ease of use. Furthermore, due to its proper anchorage and tensile strength it is used as a cost-effective solution for most of the applications [101].

3.1.2.3 5D steel fibers. This is a recently introduced type of steel fibers. They are 60 mm long and has a slenderness ratio (l/d) of 65. The perfectly hooked shape of the 5D steel fiber, shown in Figure 3.3 (c), provides high anchorage. Superior enhancements of ductility and tensile stress are introduced in this type of fibers. Therefore, they have higher carrying capacities than other available fiber types [101].

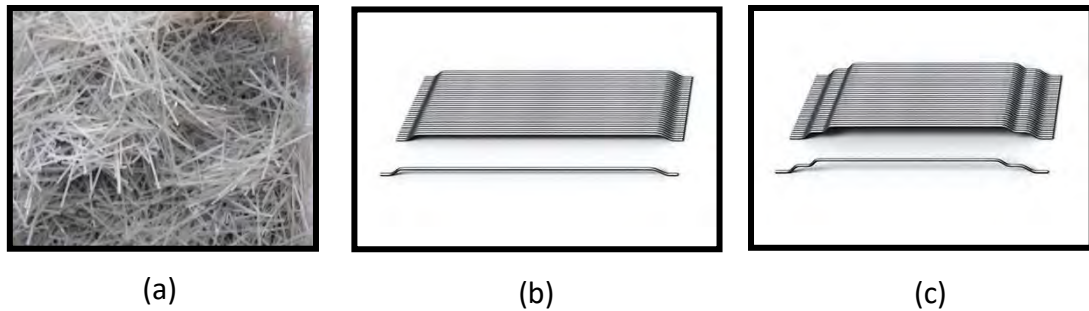


Figure 3.3: (a) Polypropylene fiber, (b) 3D steel fiber, (c) 5D steel fiber.

3.1.2.4 Comparison between 3D and 5D steel fiber. In this section, a comparison between the 3D and the 5D steel fibers is going to be carried out. As shown in Figure 3.4, the 5D fiber has an increased tensile strength with a significant elongation capacity due to its strain hardening behavior resulting in unprecedented levels of ductility. 3D fibers also show very high performance but are significantly lower than those of the 5D (Ultra high). Moreover, and as compared with the 3D type, the stepped anchorage in the and the 5D fiber enables the fiber to utilize higher percentage of its ultimate tensile strength when subject to tension within the concrete matrix. This character is more pronounced in the 5D type, which nearly fails, in a ductile balanced mode of tension and pullout. According to Figure 3.4, 5D shows very high level of strength that was only thought possible with the addition of traditional shear reinforcement. Table 3.2 is showing the characteristics and advantages of the different types of fibers to be used.

3.1.3. Steel bars. The steel bars used are Qatar steel of ASTM A615 Gr 60 grade. They are used as both tensile and compressive reinforcement. 12 mm diameter bars are used in all of the test beams. In order, to determine the stress-strain relationship and to identify the elastic modulus of the steel bars, tensile tests were conducted for two 12 mm rebar samples of 30 cm long. The resulting stress-strain curves are plotted, and the yield stress values were obtained as shown in Figure 3.5. The average value of yielding stress was calculated and considered as 566 MPa. The 1st bar reached an ultimate stress

of 667 MPa and the 2nd bar went up to 636 MPa, giving an average ultimate stress of 652 MPa.

Table 3.2: Dramix 3D steel fiber, Dramix 5D steel fiber and Strux 90/40 synthetic fiber specifications, characteristics and advantages.

Fiber type	Dramix 3D(60/65) steel fiber	Dramix 5D (60/65) steel fiber	Strux (90/40) polypropylene fiber
Specifications	<ul style="list-style-type: none"> ➤ (l) = 60mm ➤ (l/d) =65 ➤ E=210 GPa ➤ Tensile strength: 1.345 MPa 	<ul style="list-style-type: none"> ➤ (l) = 60mm ➤ (l/d) =65 ➤ E=210 GPa ➤ Tensile strength: 2.300 MPa 	<ul style="list-style-type: none"> ➤ (l)=40mm ➤ (l/d) =90 ➤ E=9.5GPa ➤ Tensile strength:620 MPa ➤ Specific gravity 0.92 ➤ Absorption None ➤ Melting point 320°F (160°C) ➤ Ignition point 1,094°F (590°C) ➤ Alkali, acid & salt resistance High
Characteristics	<ul style="list-style-type: none"> ➤ known for their durability ➤ provides original anchorage and standard tensile strength 	<ul style="list-style-type: none"> ➤ perfectly hooked shape of the 5Dsteel fiber provides high performance with superior enhancement of ductility and tensile stress ➤ it can bare higher loads and longer spans 	<ul style="list-style-type: none"> ➤ high strength and modulus ➤ It adds to the toughness of concrete ➤ It adds to fatigue and impact resistance ➤ Enhance post-cracking performance of concrete.

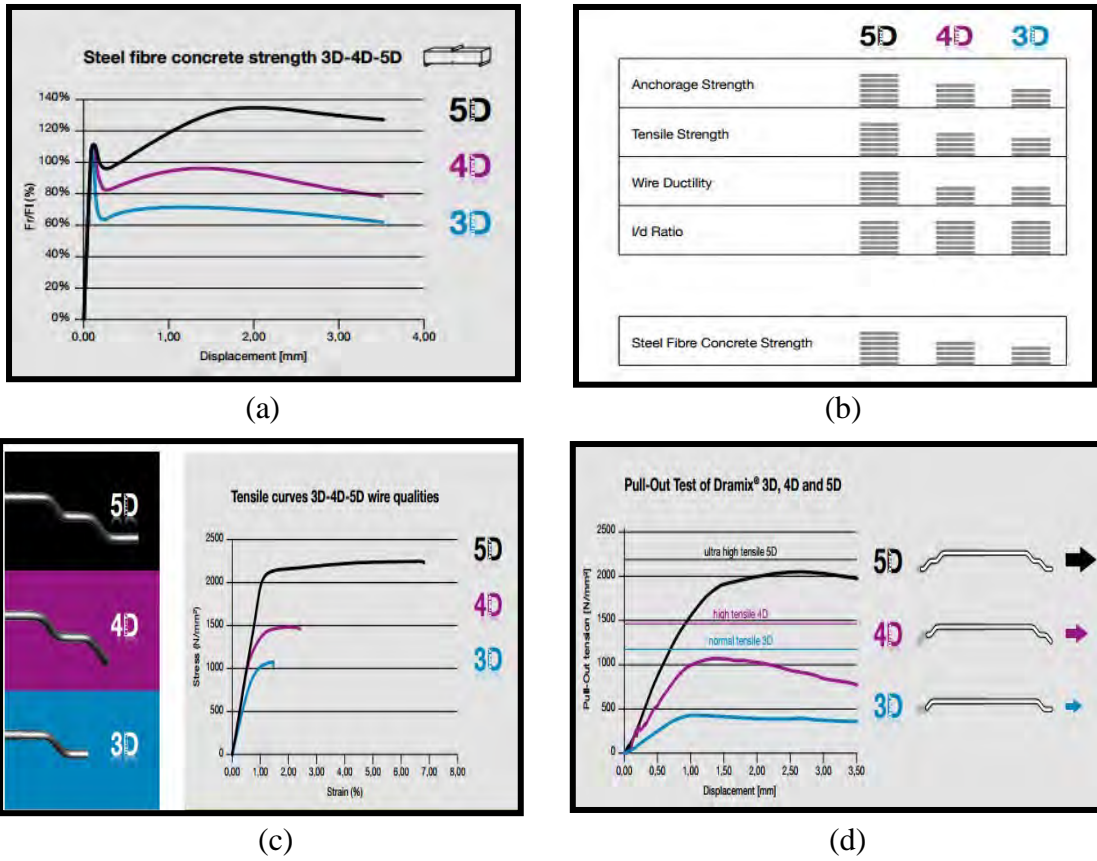


Figure 3.4: Dramix 3D and 5D steel fiber properties (a) strength, (b) anchorage strength, tensile strength, wire ductility/d ratio, steel fiber concrete strength, (c) tensile curves, (d) pull-out test curves [101].

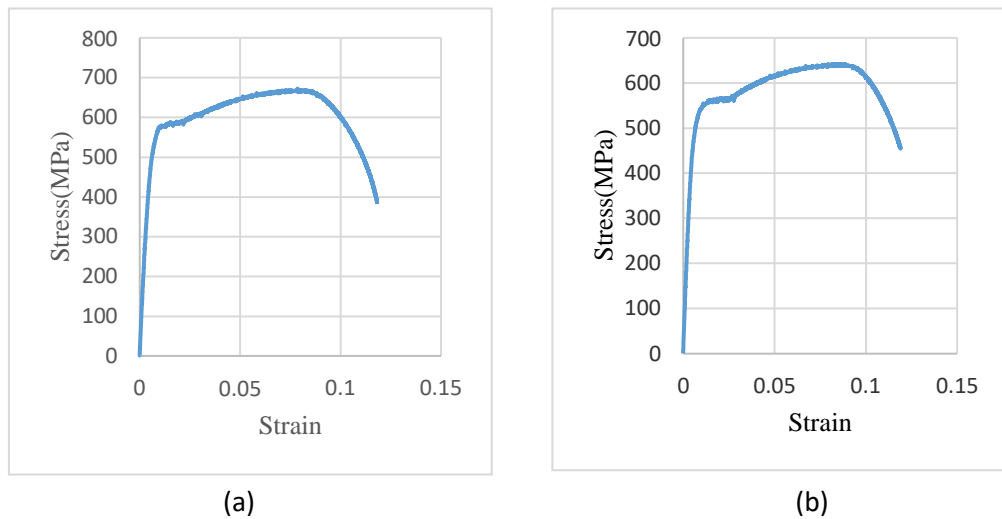


Figure 3.5: Stress vs strain curves for tested steel rebars (a) bar 1 (b) bar 2.

3.14. Concrete mixes. Six lightweight self-consolidated concrete mixes with and without fibers and with and without normal weight aggregates replacement were

prepared in the lab. Each pair of similar beams are prepared in the same mixing operation. Table 3.3 shows the mix proportions for the six mixes. Mix 1 was made for the casting of two beams of high strength self-consolidated lightweight concrete without any shear reinforcement. Mix 2, second pair of beams, is made up of high strength self-consolidated lightweight concrete in which the lightweight aggregates are partially replaced by normal weight aggregates at a percentage of 12%. Mix 3, third pair of beams, is similar to Mix 2 except for the introduction of 0.75% per volume of Dramix 3D steel fibers to enhance the concrete shear strength and ductility. Mixes 4 and 5 adopt two different types of fibers, namely Dramix 5D and strux 90/40, for the fourth and fifth pairs of beams, respectively. Mix 6 and its two beams are characterized by hybrid combination of 50% Strux 90/40 polypropylene synthetic fibers and 50% of the 5D Dramix steel fiber. For all the six mixes, small samples were cast to test their respective mechanical properties at the same test dates as the corresponding structural beams. All the samples were kept for 90 days to cure before testing.

Table 3.3: Mix proportions used in the investigation.

Component	Quantity (kg/5.5ft ³)					
	Mix 1	Mix2	Mix3	Mix4	Mix5	Mix6
Cement	58.7	61.3	61.3	61.3	61.3	61.3
Silica Fume	17.3	18.1	18.1	18.1	18.1	18.1
Water	29.6	30.9	30.9	30.9	30.9	30.9
LW CA	78.8	72.5	72.5	72.5	72.5	72.5
10mmCA	0	18.94	18.9	18.9	18.9	18.9
Cr. Sand	54.6	57.1	56.1	56.1	56.1	56.1
Dune sand	52.6	55	52.9	52.9	52.9	52.9
Fiber	0	0	9.6	9.6	1.123	0.56 (synthetic) + 4.8 (5D)

3.15. Specimen's configuration. Twelve beams are cast in this research work. Four of them were considered as reference beams and the remaining six were reinforced with different types of fibers as shown in Figure 3.6. All beams considered in this work were 1600 mm long, with a rectangular cross-section of 150 mm wide and 200 mm thick. A bottom layer of three 12 mm, ASTM A615 Gr 60, reinforcing bars were used as the tension reinforcement. Also, two 12 mm, ASTM A615 Gr 60, reinforcing bars were placed in the compression zone near the top of the beam. To avoid failure at the supports, 3#8 mm diameter closed stirrups were provided near the edges of the beam.

A schematic showing the beam dimensions and reinforcement details is shown in Figure 3.7.

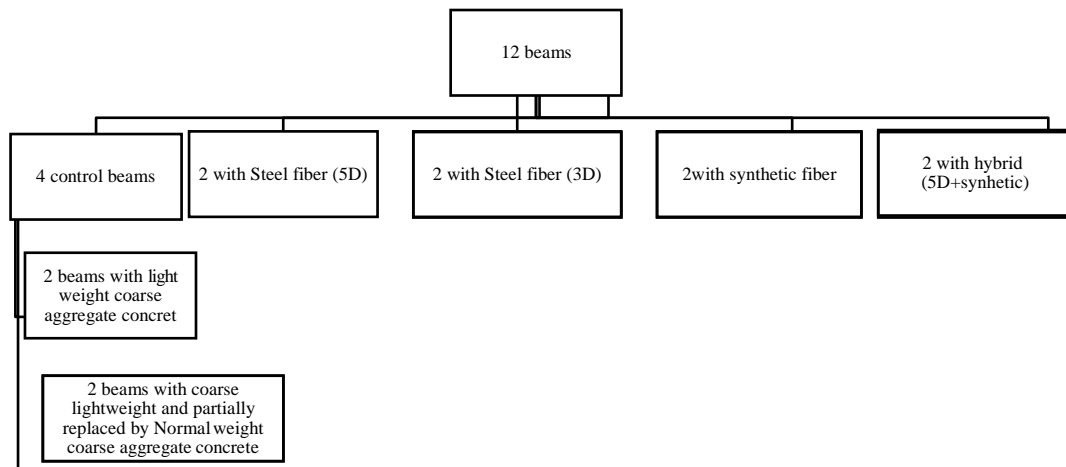


Figure 3.6: Specimens configuration.

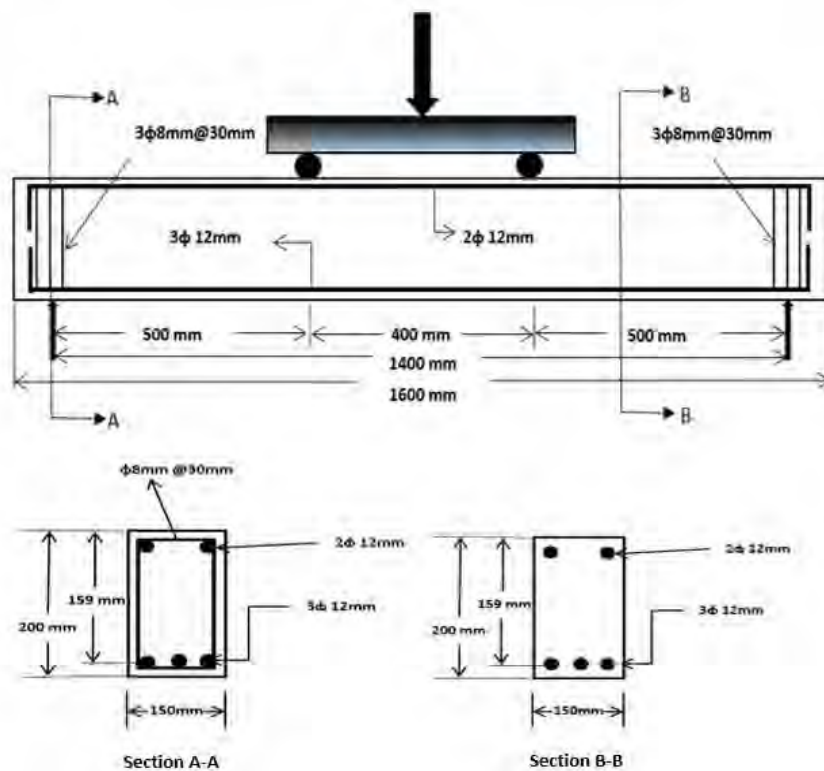


Figure 3.7: Section details (Dimensions in mm).

3.2. Preparation of the Samples

3.2.1. Preparing the steel cages. First step of preparing the samples involved assembling the reinforcement elements and then tying them together as shown in Figure

3.8(a). Three 12 mm diameter, 1540 mm long steel bars were used as a bottom tensile reinforcement. Steel wires were used to tie them together. Two 12 mm steel bars with a similar length were used as top steel. Three 8 mm closed stirrups were placed at the two edges of the reinforcement bars to ensure no failure at the support and to tie the bottom and top bars at these two locations. After tying all the reinforcement elements together, the top and bottom steel bars were grinded at the mid span to prepare their surface for strain gages installation. A pair of strain gages, SG4 and SG5, were fixed on the bottom steel whereas another pair, SG6 and SG7, were fixed on the top bars.

3.22. Formwork. In accordance with the beams dimensions shown in Figure 3.7, the formwork was prepared using plywood. The steel cages were then kept inside the formwork and the spacers were placed to ensure that there would be enough concrete cover on all the sides while pouring the concrete as shown in Figure 3.8(a).

3.23. Mixing. Materials were weighed and prepared as shown in Figure 3.8 (b) according to the mix proportions shown in Table 3.3 to produce a concrete mix, as shown in Figure 3.8(c), of volume 5.5 ft³. The lightweight aggregates were presoaked in 10% of water, 10% of cement and 10% of silica fume for half an hour before the mixing operation started. Later, the rest of the constituents were added into the mixer and the mixing started. The presoaking allows the cement to be absorbed inside the aggregates reducing the aggregate brittleness and thus enhancing the strength of the concrete mix.

3.24. Casting. Following the mixing stage, the concrete mixture was poured into the formwork as shown in Figure 3.8 (d). The vibrator was used to properly compact the concrete layers to avoid weaknesses in the matrix as well as any entrained air voids. Two beams were cast per mix. Furthermore, three 200 mm x 100 mm cylinders, three 150 mm x 150 mm x 150 mm cubes, 500 mm x 100 mm x 100 mm prisms were cast in the glazed molds.

3.25. Curing. Following the casting stage, the formwork was opened as shown in Figure 3.8(e) and the small specimens (non-structural) were demolded after three days. All the prepared samples were sprayed with water daily for up to 14 days as shown in Figure 3.8(g). All the samples were then kept for 90 days to cure as shown in Figure (3.g), to ensure continuous hydration and to reach their target strength.



(a) Sample preparation



(b) Material preparation



(c) Mixing



(d) Beams during concrete casting



(e) Removal of formwork



(f) Samples for the mechanical properties



(h) Sample of concrete with fibers



(g) Curing

Figure 3.8: Stages of the samples preparation.

3.3. Test Setup and Instrumentation

All specimens considered in this investigation were subjected to four-point loading setup using an Instron servo-hydraulic load frame (loading in displacement control at a 0.6 mm/min rate), as shown in Figure 3.9. The shear span is 500 mm and the a/d ratio is 3.1. Four quantities were measured and recorded during the test: load, deflection, crack no. vs load and steel and concrete strain. For concrete, the strain values were recorded at the shear span and midspan while for steel bars readings were only taken at the mid-span. In addition, the specimens were continuously observed during the loading process to mark the crack patterns.

The deflections of the specimens were measured at the beam mid-span with the aid of, Linear Variable Differential Transducer (LVDT). Moreover, in order to capture concrete strain throughout the test, three strain gauges were installed at various locations on the beam surface. The first strain gauge was located at the left shear span of the beam, the second was placed at the compression zone midspan and the third was installed at the right shear span. In addition, strains in the tension reinforcement were recorded using strain gauges mounted at mid-span. Additional two strain gauges were positioned on the compression reinforcement. The applied load, the mid-span deflection, and the strains were recorded every 0.1-second using a data acquisition system.

In addition, optical images were captured during loading to allow for full-field displacement measurements using Digital Image Correlation (DIC). The DIC system consists of three elements: the hardware (i.e. the digital camera and the lighting device), the specimen set up, and VIC snap software that is used for image acquisition and processing. The camera is connected to a PC to record the images at regular time intervals during the test. In addition, lighting was used to ensure high quality images. A preliminary surface treatment was done to create a proper speckle pattern. The camera was placed at a distance of approximately 1m away from the sample. Moreover, scale images were taken using a measuring tape placed diagonally on the sample surface for calibration purposes. Furthermore, a reference-undeformed image was captured prior to the onset of loading. As the load application started, the deformed images were captured every 2 seconds.

3.4. Mechanical Properties Tests

341. Compressive strength test. The Compressive strength test was performed in accordance with the ASTM C39/C39M–17 standard test method. In which, three 100 mm x 200 mm cylinders and three 150 mm x150 mm x150 mm cubes were first prepared with the corresponding structural beams and were tested after curing period of 90 days. The samples were weighed, loaded to failure and the results were recorded and the mode of failure was captured.

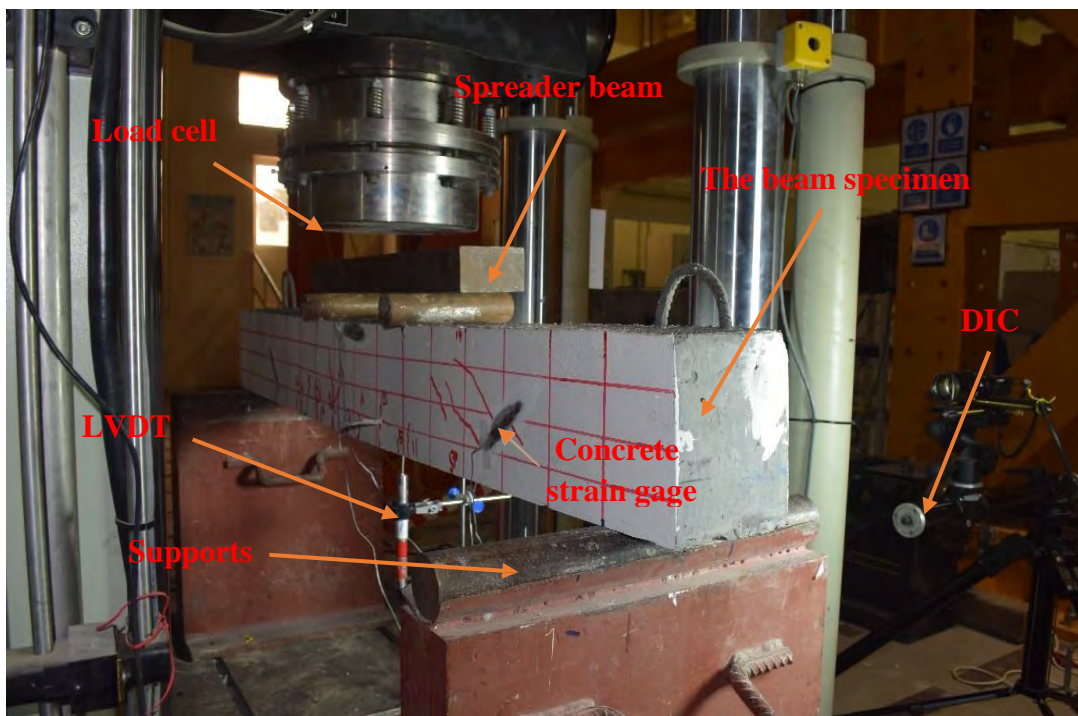


Figure 3.9: Experimental setup.

342. Flexural strength. The Flexural strength test was performed in accordance with ASTM C 78/C78M –16-test method. Three 100mmx100 mmx500 mm prisms were tested, for each mix, after 90 days of curing. Three-point setup was then used to apply the test load until failure. The load at failure was recorded and the following equation is used to get the value for flexural strength

$$\text{Flexural strength} = \frac{3FL}{2bd^2}$$

- F = the load (force) at the fracture point (N).
- L = the length of the supported span of the prism.
- b = width of the prism.
- d = thickness of the prism.

3.5. Summary

Twelve beams are prepared using lightweight concrete with and without partial replacement of normal weight coarse aggregate and left to cure for 90 days. Later, material evaluation was done by testing cubes and prisms under compression and 3-point bending respectively. Load deflection responses were obtained and analyzed to get ultimate load, failure load, shear load, ultimate deflection and stiffness. In addition, strain values at different load levels were collected for steel and concrete.

Chapter 4. Results

The experimental investigation was carried out in two stages. The material properties evaluations were conducted in the first stage to determine the mechanical properties of the concrete mix. In the second stage, the twelve beams were tested to determine the shear strength provided by concrete. The results are presented in this chapter, while the discussion is presented in Chapter 5.

4.1. Material Evaluation

Compressive strength and flexural strength tests were conducted for all the six mixes studied in this research. Three samples were tested for each mix, the average values and percentage increase with reference to the control specimens, are summarized in Table 4.1. The addition of fibers enhanced both properties but was more pronounced in improving flexural strength. On the other hand, it was also noticed that Hybrid and steel fibers had improved results than that of synthetic (polypropylene fibers). In addition, when compared to the control specimens, the fiber-reinforced samples did not have severe failure modes; same observation was also made by Suji et al. [102]. This is attributed to fiber holding concrete parts together, due to fibers capability of bridging stresses across cracks. Therefore, the tested samples had preserved shape with less observed damage shown in Figure 4.1.



Figure 4.1: Typical failure mode of (a) Fiber reinforced concrete cubes, (b) Control sample.

Table 4.1 Summary of the mechanical properties.

	Average Cube compressive strength(N/mm ²)	Average cylinder compressive strength	Average Prismatic flexural strength (N/mm ²)	% increase in cube compressive strength*	% increase in cylinder compressive strength*	% increase in flexural strength*
Mix 1 (all light weight)	56	30.96	3.9	-	-	-
Mix 2 (partially replaced)	52	30.77	4.425	-7.1	-0.61	13.46
Mix 3 (3D steel fiber)	68	39.39	11.66	30.7	27.2	198.97
Mix 4 (5D steel fiber)	74	47.635	15.95	42.3	53.8	308.97
Mix 5 (SY fiber)	63	37.48	5.613	21.1	21.05	43.92
Mix 6 (HY fiber)	71	45.02	12.07	36.5	45.41	209.48

*compared to Mix1

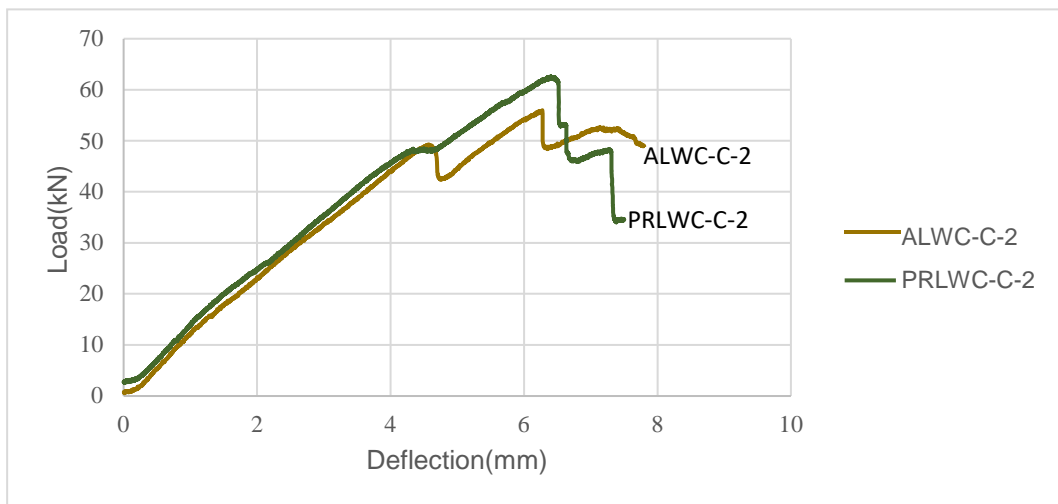
4.2. Tests to Determine Concrete Shear Capacity

4.2.1. Load-mid span deflection. Figure 4.2 shows the load vs deflection for six different beams (One beam from each set). Responses of the load vs deflection for the second set of beams (repeated beams) are provided in Appendix A. Ultimate load, failure load, shear load, ultimate deflection and stiffness of all the twelve beams are shown in Table 4.2.

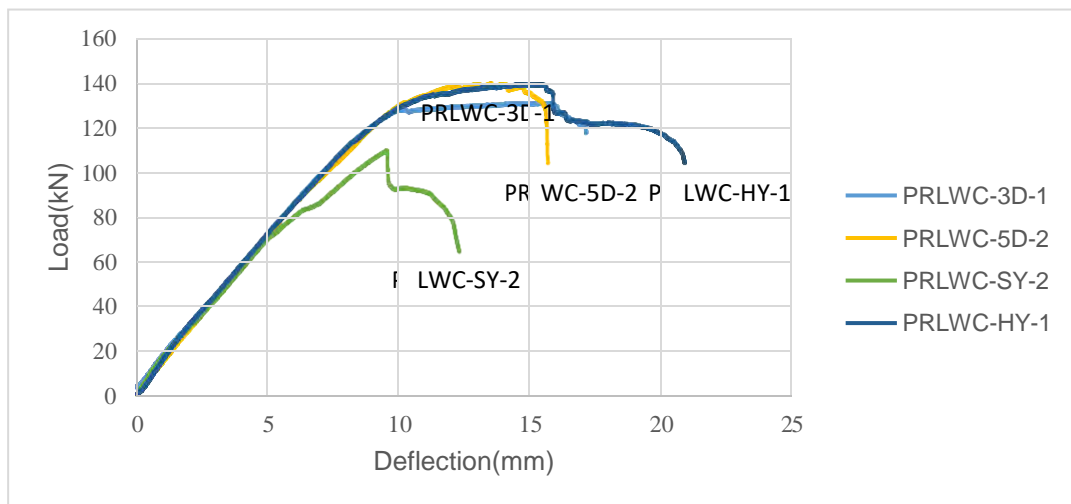
The ultimate load is defined as the maximum load reached by the tested beam before failure. However, the failure load is considered the maximum load reached before the first drop. Furthermore, the shear capacity values (i.e., $V_c = \text{Ultimate load}/2$) were summarized. The ultimate deflection corresponds to the ultimate load. The elastic stiffness values were determined by calculating the initial slope of the respective load deflection curves. Figure 4.3 shows the average ultimate load of all the six groups.

Variabilities in the partially replaced concrete beams is mainly attributed to the distribution of the NWA during the mix time and its distribution through the crack plane. The differences encountered in similar fiber reinforced beams of the same group might be attributed to the distribution of the fibers between the two beams during the mixing time, the distribution of the fibers within the beam itself and whether it is more abundant in one part when compared to the other. In addition, the number of fibers passing through the crack. Less fibers passing the crack plane, leads to less stress transfer through the crack faces and reduction of the load bearing capacity of the beam. Moreover, the alignment of the fibers plays an important role if the fibers are aligned parallel to the crack, it will not be bridging the stresses across the crack surface. Therefore, these fibers will not be fully utilized. However, polypropylene fiber reinforced beams showed same trend, less scatter. This might be attributed to the following:

- 1) The polypropylene fibers could be more uniformly distributed into the mix when compared to the steel fibers due to their simpler geometry.
- 2) Due to its lightweight, the count of the polypropylene fiber tends to be more when compared to the steel fiber, leading to more fibers in the crack plane, arresting the crack.



(a)



(b)

Figure 4.2: Load versus mid-span deflection responses for the tested beams: (a) Control beams, ALWC-C-2 and PRLWC-C-2; (b) Fiber reinforced beams, PRLWC-3-1, PRLWC-5D-2, PRLWC-SY-2 and PRLW-HY-1.

Table 4.2: Summary of the test results.

Groups	Beam ID	Ultimate load (kN)	Average ultimate load (kN)	Cracking Load (kN)	Shear Load (Vc) (kN)	Aver. shear load (Vc) (kN)	Ultimate deflection (mm)	Ave. ultimate deflection (mm)	Stiffness (kN) /mm)	Ave. stiffness
Group A ALWC	-C-1	52.4	54.2	52.4	26.2	25.35	4.71	5.50	11.157	10.97
	C-2	56		48.827	24.5		6.3		10.78	
Group B PRLWC	-C-1	46	54	45.35	23	23.75	6.31	6.37	10.48	10.445
	C-2	62		48.12	24.5		6.43		10.41	
Group C	-3D-1	130	122.5	130	65	61.25	16	14	13.45	12.635
	-3D-2	115		115	57.5		12		11.82	
Group D	-5D-1	106	122.5	106	53	61.25	10.1	12.05	12.17	12.615
	-5D-2	139		139.91	69.5		14		13.06	
Group E	-SY-1	98	103.5	98	49	51.75	8.96	9.23	11.3	10.94
	-SY-2	109		109	54.5		9.5		10.586	
Group F	-HY-1	139	128	139	69.5	64	15.6	13.15	13.41	13.41
	-HY-2	117		117	58.5		10.7		13.41	

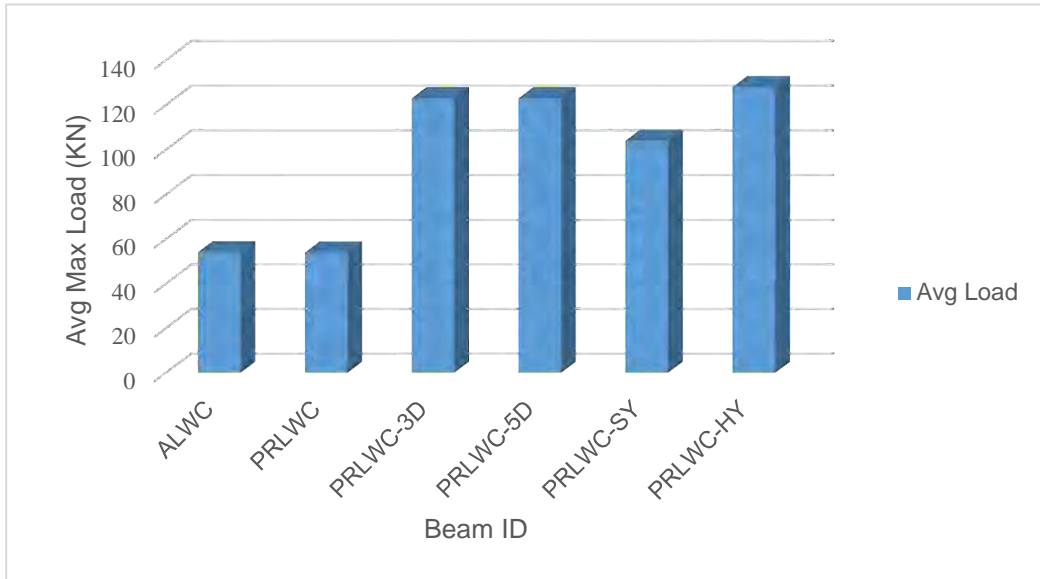


Figure 4.3: Average ultimate load of all the six mixes.

4.2.2. Strain Values. Seven strain gauges were used for each beam labeled as SG1 to SG7. SG1 and SG3 were placed in the right, and left shear spans at a distance of 20 cm from the respective support and of 10 cm from the base line of the beam, aligned diagonally, perpendicular to the expected crack direction inclined at an approximately 45 degrees angle. The strain gauges were also mounted on the bottom (SG4 and SG5) and the top steel (SG6 and SG7) bars to measure the strains in the steel.

4.2.2.1 Concrete Strain. Table 4.3 shows the summary of the maximum strain values in the concrete at ultimate loads for the six-beam groups. SG1 and SG3 are the diagonal tension strain values in the shear zone while SG2 represents the compressive strain values at the top of the mid span. Figure 4.4 presents the load vs strain curves for two beams (PRLWC-C-2 and PRLWC-3D-1), the rest of data are presented in Appendix B.

4.2.2.2 Steel Strain summary. Table 4.4 presents the maximum values of average top and average bottom steel strains and their corresponding stresses. The obtained strain values were plugged into the stress strain curves obtained for the steel bars, being tested in tension, to get the equivalent stresses. The obtained stresses are then compared with the average yield stress to find out as to whether or not the respective steel bars have reached to their yield point or not. SG4 and SG5 represent the bottom steel tensile strains while SG6 and SG7 represent the top steel compressive strains. As indicated earlier all of these strain measurements are taken at the critical

flexure section at the middle of the beam span. Figure 4.5 presents the load vs strain curves for two beams, figures from other beams are presented in Appendix C.

Table 4.3: Summary of maximum strain values in SG1, SG2, and SG3.

Groups	Beam ID	Ultimate load (kN)	Max Strain (SG1)	Max Strain (SG2)	Max Strain (SG3)
Group A	ALWC-C-1	52	0.0018	0.000172	0.00033
	ALWC-C-2	56	0.000117	0.00051	0.035
Group B	PRLWC-C-1	46	0.000304	0.0006712	0.028
	PRLWC-C-2	62	0.00327	0.00111	0.00324
Group C	3D-1	130	0.00095	0.003	0.0026
	3D-2	115	0.006	0.0007	0.035
Group D	5D-1	106	0.0031	0.000353	0.000912
	5D-2	139	0.00833	0.0024	0.008714
Group E	SY-1	98	0.00896	0.00118	0.00721
	SY-2	109	0.0101	0.017	0.0146
Group F	HY-1	139	0.00462	0.0015	0.0103
	HY-2	117	0.0002	0.00149	0.0247

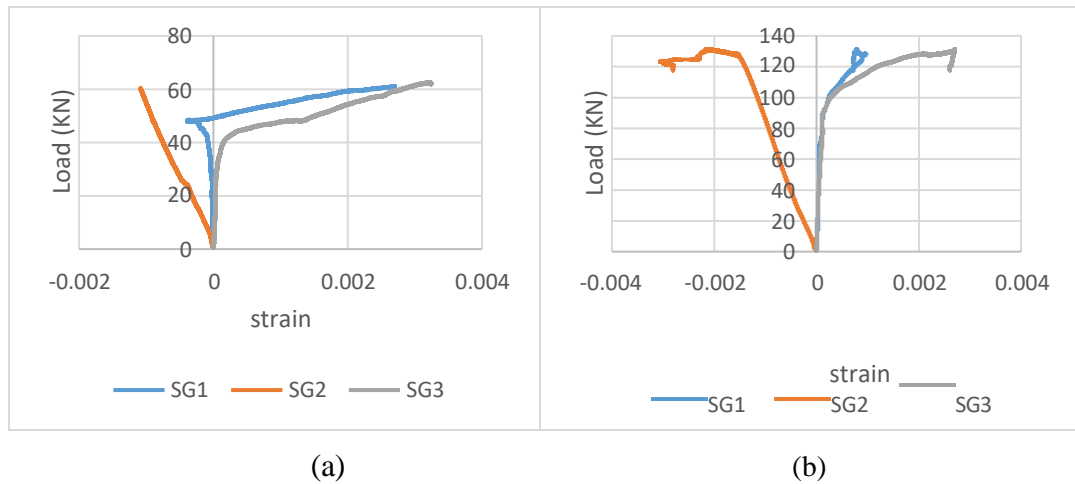


Figure 4.4: Load versus strain for beams (a) PRLWC-C-2, (b) PRLWC-3D-1.

Table 4.4: Summary of maximum strains in SG4, SG5, SG6, and SG7.

Groups	Beam ID	Maximum load (kN)	Max strain (SG4, SG5)	Yielded or not yielded (Y,N)	Max strain (SG6, SG7)	Yield strain	Yielded or not yielded (Y,N)
Group A ALWC-C	-1	52	0.000197	N	0.00177	0.00207	N
	-2	55	0.000345	N	0.00174	0.00207	N
Group B PRLWC-C	-1	46	0.000382	N	0.00154	0.00207	N
	2	62	0.000877	N	0.00152	0.00207	N
Group C	-3D-1	130	0.000827	N	0.0130	0.00207	Y
	-3D-2	115	0.000583	N	0.00403	0.00207	Y
Group D	-5D-1	106	0.0003	N	NA	0.00207	Y
	-5D-2	139	0.00066	N	0.0215	0.00207	Y
Group E	SY-1	98	0.00024	N	0.00291	0.00207	Y
	-SY-2	109	0.00047	N	0.00359	0.00207	Y
Group F	-HY-1	139	0.00064	N	0.01600	0.00207	Y
	-HY-2	117	0.00041	N	0.00380	0.00207	Y

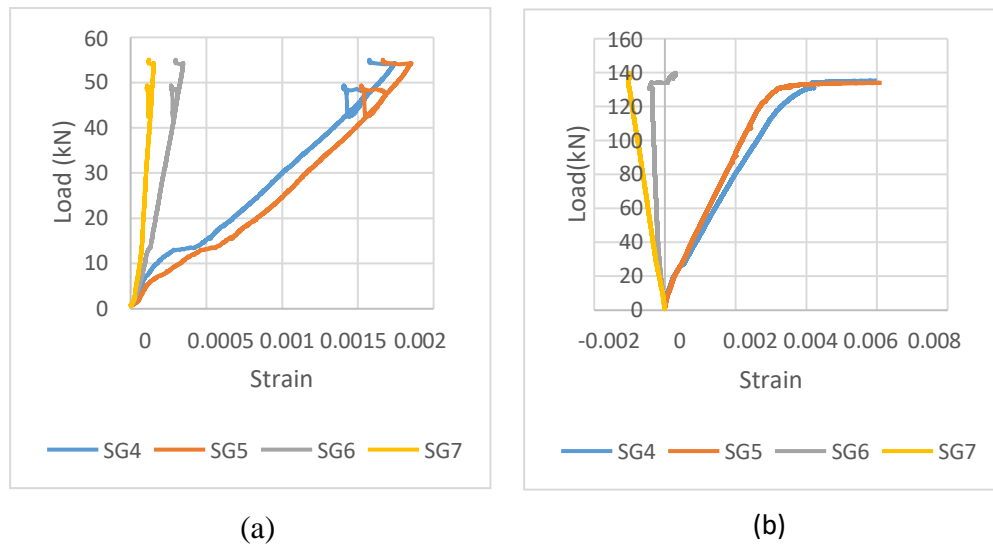


Figure 4.5: Load versus strain for beams (a) PRLWC-C-2, (b) PRLWC-3D-1.

4.2.3. Crack patterns. Crack patterns and the loads required to develop each crack (up to crack No. 8) were observed and recorded. Table 4.5 summarizes the loads at which each of the first 8 cracks were developed. Figure 4.6 illustrates the crack patterns and number of cracks of specimens ALWC-C-1 and PRLWC-5D-1, respectively. The crack patterns of the remaining 10 beams at the same loading conditions are provided in Appendix F.

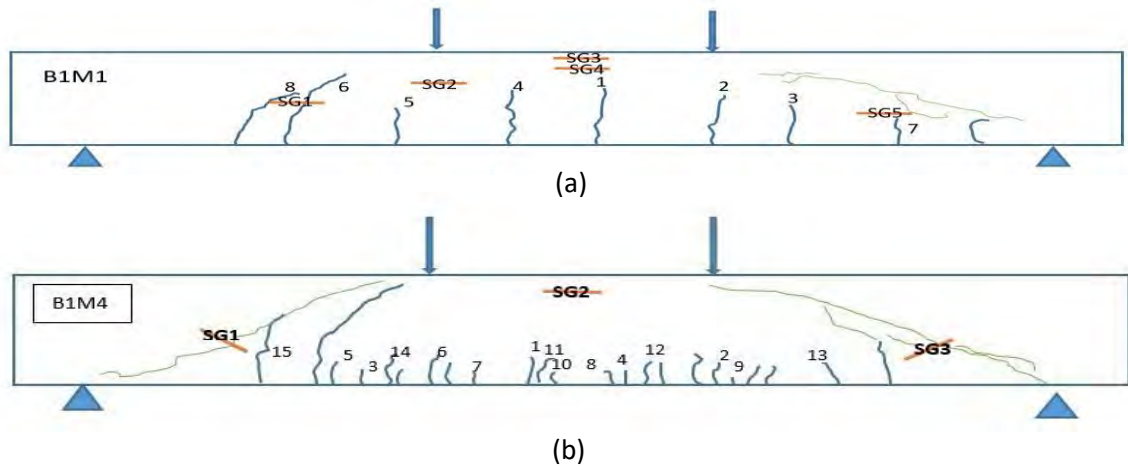


Figure 4.6: Crack pattern of beam (a) ALWC-C1 and (b) PRLWC-5D-1.

Table 4.5: Required loads to develop the cracks (up to crack No. 8).

Beam ID	Load (kN)								Maximum load (kN)
	Crack 1	Crack 2	Crack 3	Crack 4	Crack 5	Crack 6	Crack 7	Crack 8	
ALWC-C-1	29.41	30.67	31.64	33.21	34.18	35.04	42.84	51.18	52
ALWC-C-2	22.79	26.61	28.98	30.16	31.44	35.26	37.66	39.42	55
PRLWC-C-1	18.72	20.24	20.78	21.46	22.60	27.37	29.37	39.94	46
PRLWC-C-2	24.50	27.00	27.90	30.90	32.00	33.20	35.60	38.50	62
PRLWC-3D-1	41.49	45.22	45.92	52.30	56.25	78.69	80.52	85.72	130
PRLWC-3D-2	20.00	27.00	29.50	30.20	31.80	35.50	40.00	41.30	115
PRLWC-5D-1	21.58	22.82	23.85	24.67	27.92	30.51	32.17	33.93	106
PRLWC-5D-2	21.74	25.39	26.89	28.04	28.65	29.15	45.26	55.28	139
PRLWC-SY-1	20.20	22.83	23.65	25.08	26.75	30.01	42.26	49.86	98
PRLWC-SY-2	19.03	20.75	21.19	25.02	30.72	37.04	40.87	46.10	109
PRLWC-HY-1	32.20	33.10	40.30	41.89	42.40	42.98	52.65	57.58	139
PRLWC-HY-2	24.65	25.15	26.04	31.24	34.72	36.33	38.24	40.93	117

4.2.4. Initial cracking. The initial part of the load vs strain curves captured from concrete strain gauges were used to capture the initial crack load and crack width as shown in Figure 4.7 for SG1(the side where the dominant crack is observed) for PRLWC-C-2 beam. The initial crack load could be captured from the first bent that

occurs in the Load vs strain curve and the values are displayed in Table 4.6. It was noticed in few strain gages that after the initial crack occurred the strain gauge started to malfunction. The rest of the plots are provided in Appendix D.

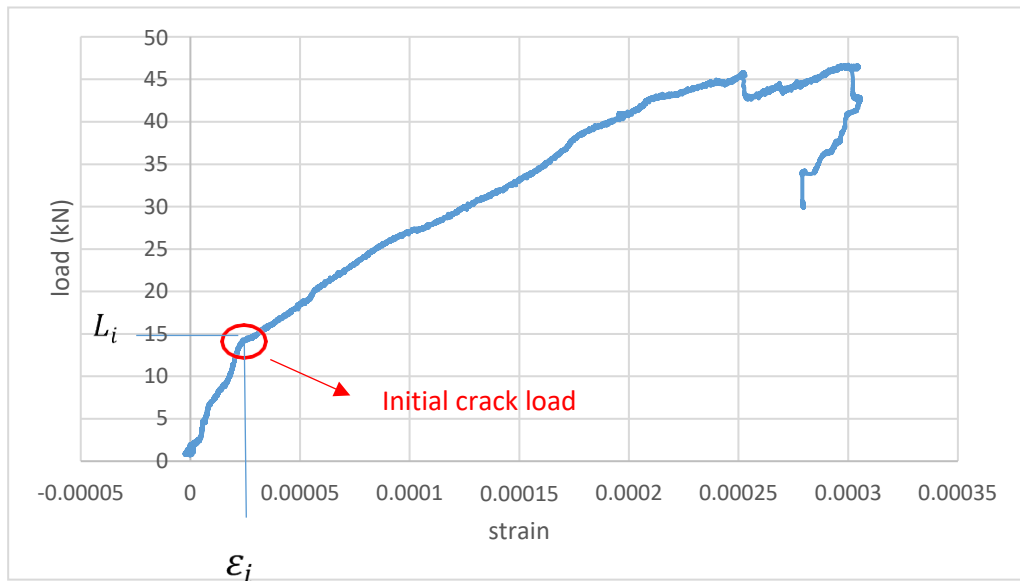


Figure 4.7: Initial part of the load vs strain curve for SG1 or beam PRLWC-C-2.

4.2.5. Modes of failure. The specimens were mainly designed to fail in shear as shown in Figure 4.8. Table 4.7 presents the mode of failure of all the tested specimens. The captured images of all the twelve beams that shows the modes of failure, cracks and crack angles are reported in Appendix E.



Figure 4.8: Mode of failure and shear angle of beam PRLWC-3D-2.

4.2.6. DIC results. DIC was a very helpful tool in capturing vertical and horizontal displacements, crack propagation and crack widths. VIC snap software was used to capture the deformed images during loading of the samples. Later, the collected images were analyzed using the VIC 2D software and the obtained results are presented in the following subsections.

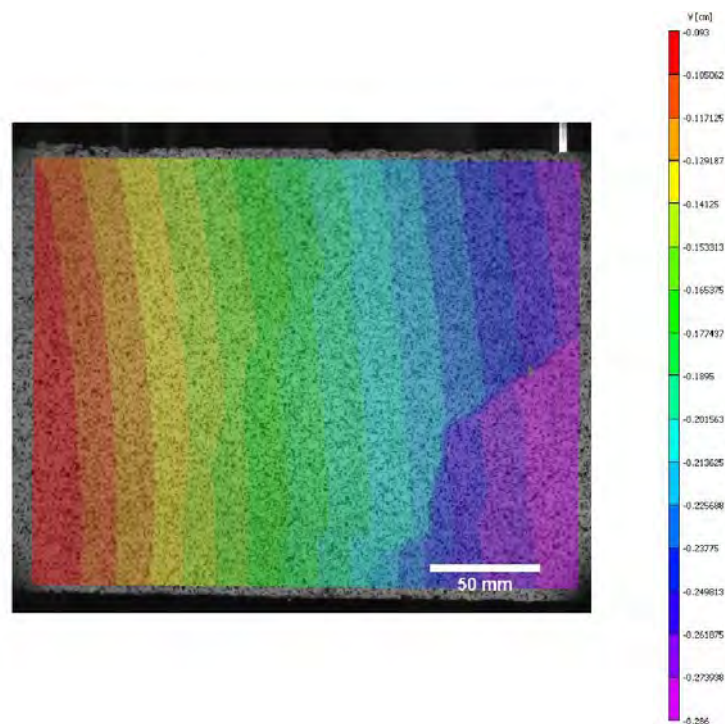
Table 4.6: Initial crack load captured from strain gauges.

Beam ID	Strain (ε_i)	Initial crack load L_i (kN)	Percentage of the ultimate load (%)
ALWC-C-1	0.0000728	12.68	24.38
ALWC-C-2	0.000109176	29.7	54
PRLWC-C-1	0.0000729	18	39.1
PRLWC-C-2	0.0000204	19.28	31.1
PRLWC-3D-1	0.000020944	23.55	18.11
PRLWC-3D-2	0.000088723	20.3	17.65
PRLWC-5D-1	0.0000358989	20.45	19.29
PRLWC-5D-2	0.0000708	21.85	15.72
PRLWC-SY-1	0.000061827	22.21	22.66
PRLWC-SY-2	0.0000165	24.8	22.75
PRLWC-HY-1	0.0000114	13.8	9.93
PRLWC-HY-2	0.0000797	19.7	16.84

Table 4.7: Modes of failure of all the tested beams.

Beam ID	Mode of failure
ALWC-C-1	Shear
ALWC-C-2	Shear
PRLWC-C-1	Shear
PRLWC-C-2	Shear
PRLWC-3D-1	Shear
PRLWC-3D-2	Flexure
PRLWC-5D-1	Shear
PRLWC-5D-2	Shear
PRLWC-SY-1	Shear
PRLWC-SY-2	Shear
PRLWC-HY-1	Shear
PRLWC-HY-2	shear

4.2.6.1 Vertical and horizontal displacement contour maps. Vertical and horizontal displacement contours at ultimate load were extracted from VIC-2D software. Figure 4.9 shows an example of ALWC-C-1 contours. The obtained contours are mainly used to show areas of higher displacements and how different parts of the beam are behaving relative to each other. Purple colour shows areas subjected to highest displacements. However, the red areas are representing lower displacements. Figure 4.9(a) shows vertical displacements in which, it was captured that as the distance from the load increases the displacement decreases, showing the lowest displacements near the supports. From Figure 4.9(b) it was noticed that the least displacement was observed at the top of the beam for the horizontal displacements.



(a)

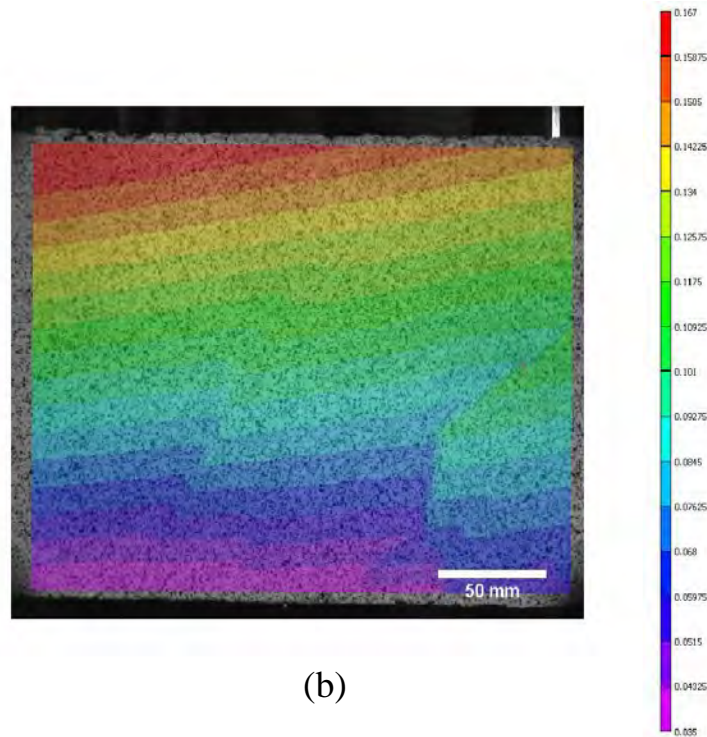


Figure 4.9: (a) Vertical and (b) horizontal displacement contours of ALWC-C-1 beam.

4.2.6.2 Crack initiation and propagation. From VIC 2D software, contours of different strain components, ϵ_{xx} , ϵ_{yy} and ϵ_1 , can be extracted. ϵ_{xx} can best capture the flexural cracks and ϵ_{yy} can capture the shear crack as shown in Figure 4.10 for beam ALWC-C-1 at ultimate load. In this work, ϵ_1 contours were used for all the beams, to capture both the crack components, to ensure consistency. Figure 4.10 shows the differences between the different strain components at the same load. It was clear that Figure 4.10 (c) was the most representative for the crack.

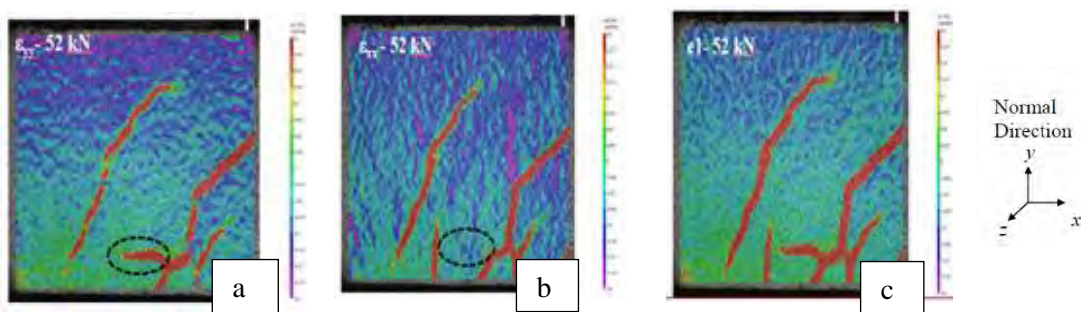


Figure 4.10: Different strain maps (a) ϵ_{xx} (b) ϵ_{yy} (c) ϵ_1 .

Figure 4.11 shows the initiation and propagation of crack with respect to load for ALWC-C-1 beam, rest of beams are shown in Appendix H. This makes it easy to capture the progression of the crack at any load value. For ALWC-C-1, flexure and shear crack initiation were captured at 6.2 kN and 41.5 kN respectively. Flexure crack turned into shear crack at load 41.5 kN. Shear crack propagated until the peak load was reached at 52.2 kN. As shear crack further propagated, load dropped, and crack started opening up until the beam failed⁴

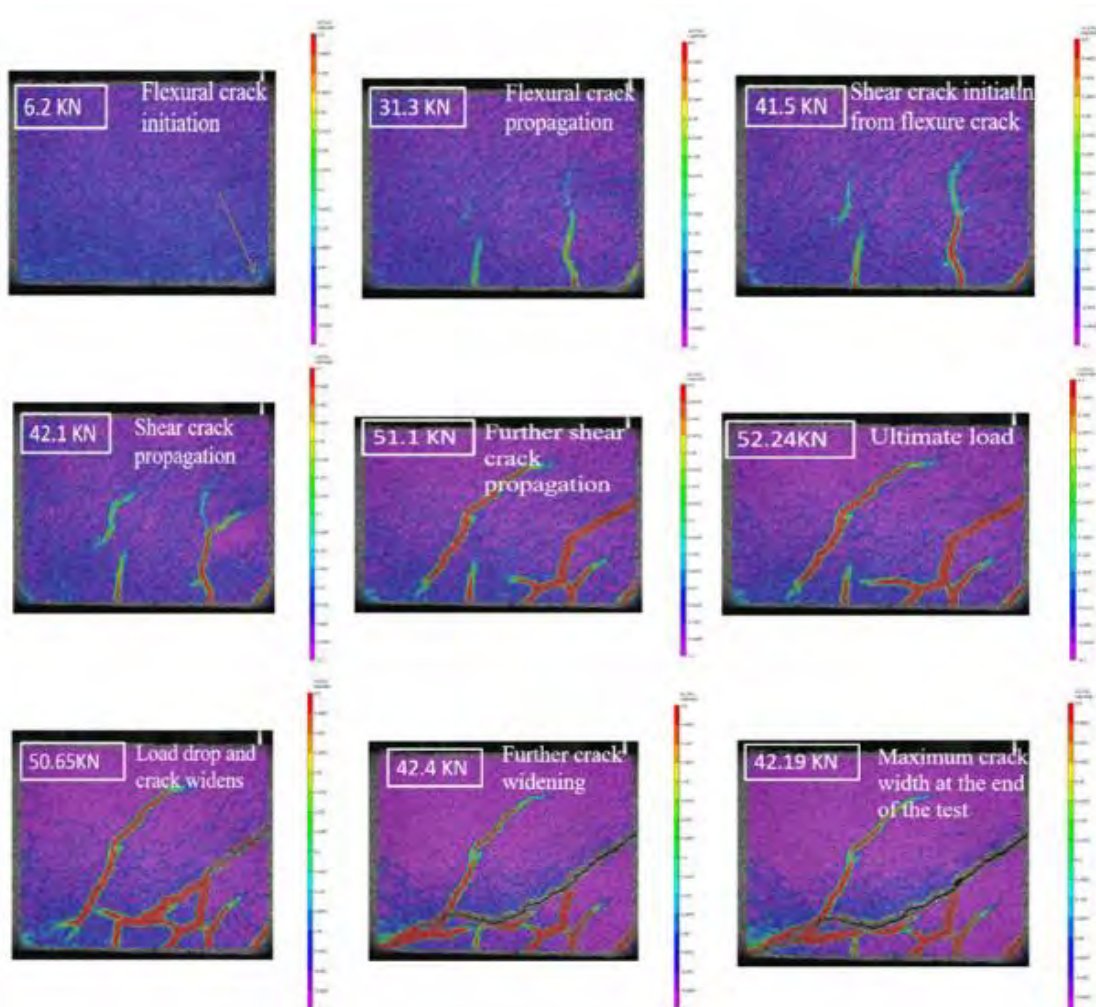


Figure 4.11: Shear and flexure crack initiation and propagation of ALWC-C-1 beam.

4.2.6.3 Crack Widths. Virtual extensometers were installed at several locations throughout the crack surface of the beams, to be able to measure displacements taking place across the cracks and calculate crack widths as a result. Figure 4.12 shows a plot of crack width vs time for ALWC-C-1 beam. Eight extensometers, E0 to E7, were virtually fixed to measure the crack width at different locations of the crack. The curves

shows that as the load increases the crack width increase. The crack started opening at time =7.6 min which is equivalent to load of 41 kN.

Figure 4.12 shows four stages for the crack propagation as discussed below.

- I. The first stage starts with the initiation of the crack at time $t = 7.6$ min, the crack then kept opening until the ultimate load was reached at a rate of 0.1333 mm/min.
- II. After the ultimate load was reached, a second stage started at which the crack started to grow at a faster rate of 1.17 mm/min and a small drop in the load was observed in the load deflection curve. However, by the end of stage II there was a loss of the aggregate interlock and there was a sudden jump in which the crack widened at a rate of 6.81 mm/min showing a brittle behavior, this was also noticed by a greater drop in the load deflection.
- III. The shear resistance was regained apparently due to the formation of new aggregate interlock in which there was a slight increase in the load. The rate at which the crack was opening was higher than stage II, since both the crack surfaces were further away from each other. By the end this stage, the crack suddenly opened at rate of 2.63 mm/min as the crack widened and as the interlocking got weaker. This was also reflected by a slight decrease in the load in the load-deflection curve.
- IV. At stage IV, due to the motion of the crack planes with respect to each other a weaker interlock mechanism was formed, reflected by a slight increase in the load and a slower rate of crack opening of 0.586 mm/min.

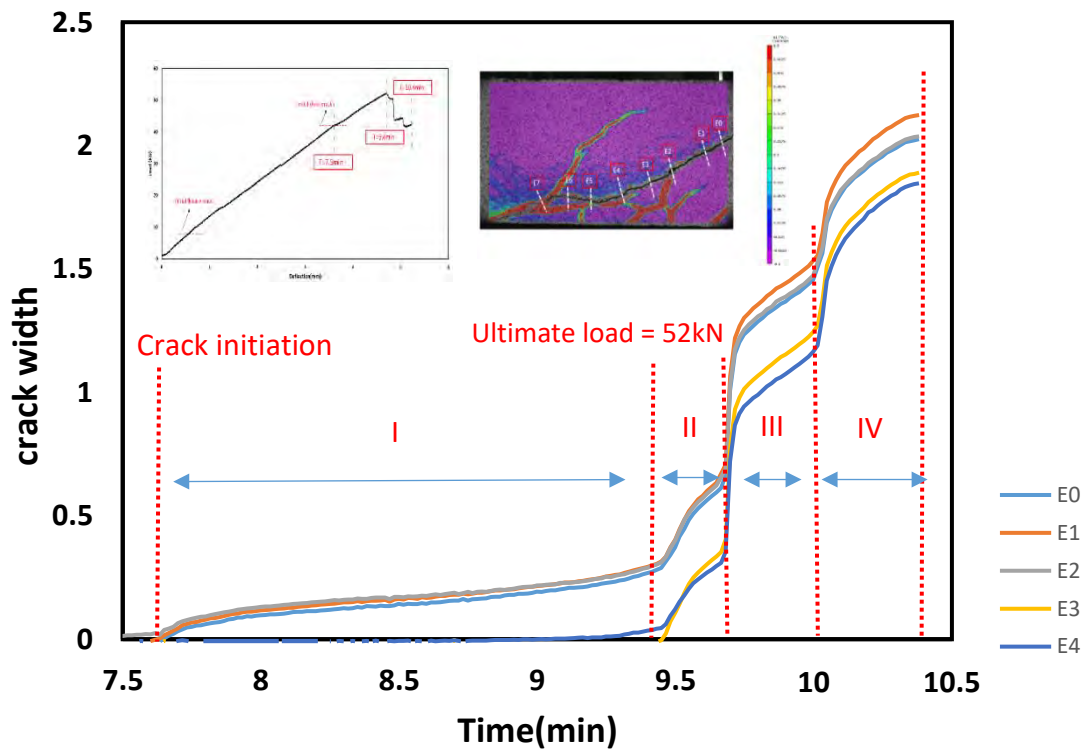


Figure 4.12: Crack vs time plot for beam ALWC-C-1.

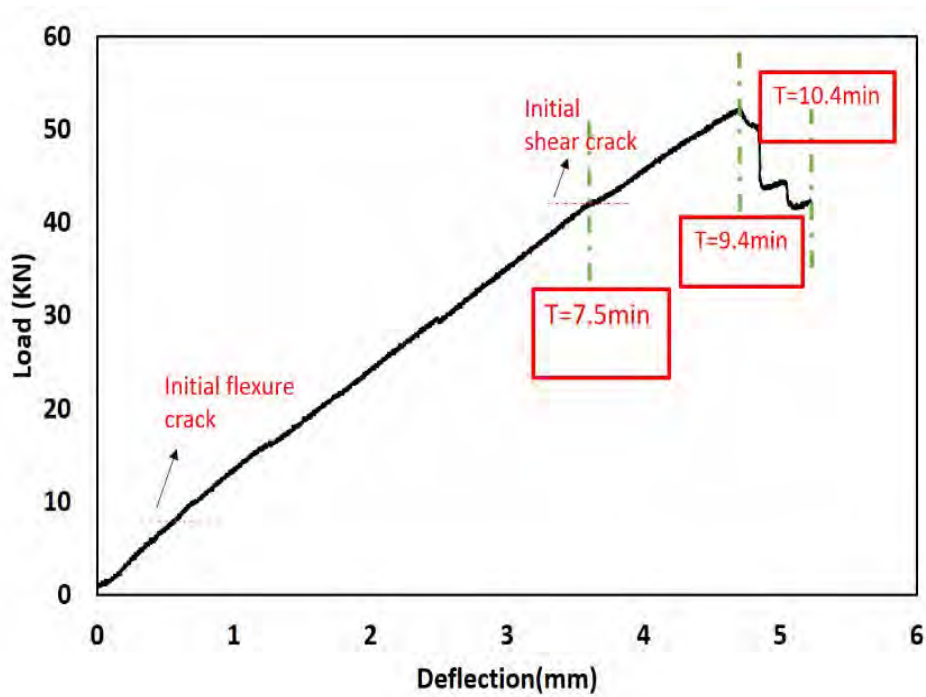


Figure 4.13: Load vs deflection for beam ALWC-C-1.

Chapter 5. Discussion of the Results

Effect of partial replacement of LWA with NWA, fiber type and steel fiber configuration are the factors considered in the investigation. The influence of these factors on the results will be discussed and presented in this chapter.

5.1. Material Evaluation Tests

The influence of the partial replacement of LWA with NWA on the compressive and flexural strength of partially replaced LWAC is discussed in the following subsections.

5.1.1. Effect of partial replacement on compressive strength. It was noticed from the results reported in Table 4.1 that the partial replacement of the LWC did not enhance its compressive strength. However, it led to a slight decrease of 7.1% in cube compressive strength. Also cylinder compressive strength reduced by 0.61%. On the other hand, Abdel Aziz et al. [63] noticed that the compressive strength increased by about 15, 30, 50 and 90%, when 35, 50, 60 and 100% NWA were used as a partial replacement of LWA; but, the percentages of NWA used in Abdel Aziz's study are higher than the 12% used in the current study. Therefore, the effect of the partial replacement was more pronounced. It is important to note that increasing the percentage of NWA leads to an increase in the concrete unit weight and the mix will no longer be classified as LWC mix.

5.1.2. Effect of partial replacement on flexural strength. For the flexural strength, the PRLWC showed 14.5% enhancement when compared to that of the reference samples. This therefore shows that the partial replacement had better influence on the flexural strength when compared to the compressive strength. This shows that the addition of a percentage of NWA to LWC has the potential to increase the flexural capacity. However, the added percentage was not sufficient to achieve higher improvement percentages.

5.1.3. Effect of the fiber addition on compressive strength. Results summarized in Table 4.1 showed a great enhancement in the cube compressive strength of the fiber reinforced mixes. Group C, D, E and F showed improvements of 30.7%, 42.3%, 21.1% and 36.5% respectively. In addition, the cylindrical compressive strength was enhanced by a percentage of 27.2%, 53.8%, 21.05%, and 45.41% respectively. The

5D steel fiber reinforced cubes showed the best performance, followed by the hybrid mix. However, results reported by other researchers showed only a slight increase in the compressive strength or no improvement. For instance, it was concluded by Gao et al. [43] noticed that adding steel fiber at different percentages, negligibly affects the compressive strength of lightweight concrete. On the other hand, Kayali et al. [46] showed that the addition of polypropylene fiber at percentage of 0.28% led to no improvement in the compressive strength. However, it had a slight improvement of 4.6% when 0.56% of the fiber was added. Furthermore, the addition of 1% of fiber adversely affected the compressive strength of the samples in which it led to a reduction of 10.7%. Balendran et al. [53] also observed that the addition of 1% of steel fiber to the lightweight concrete specimens had almost no effect on the compressive strength. O. kayali et al. [103] also reported that the use of steel and polypropylene fibers had no influence on the compressive strength of the fiber reinforced lightweight concrete at different percentages. Also, Libre et al. [104] concluded that the polypropylene fiber had no effect on the compressive strength of fiber reinforced light weight concrete. However, the addition of steel fiber led to an improvement of 47% for 0.5% of fiber. Bing Chen et al. [55] noticed that the addition of polypropylene fibers led to a slight decrease in the compressive strength. On the other hand, hybrid fibers significantly improved mechanical properties of lightweight concrete. Thomas et al. [105] concluded that the maximum increase in the compressive strength, of fiber reinforced concrete, due to the addition of steel fibers was found to be quite small (less than 10%) for different concrete grades (35, 65, and 85 MPa). Test results by Wu Yao et al. [76] showed that the fibers in general, when used in a hybrid form, could result in superior performance when compared to their individual fiber-reinforced concretes. On the other hand, it was also concluded that in the case of steel –Polypropylene fibers, it slightly increased strength compared to simple Polypropylene fibers and decreased strength compared to simple steel fibers at the same fiber volume fraction. Kang et al. [28] indicated that the compressive strength of SFRLC was increased by 13% for $V_f = 0.5\%$ and 20% for $V_f = 0.75\%$. This shows that the effectiveness of steel fibers is greater in lightweight concrete than in normal weight concrete.

5.1.4. Effect of fiber on flexural strength. The addition of the synthetic polypropylene fiber enhanced the flexural strength by 43%. Similar results were obtained by Libre et al. [104] in which it was shown that increasing the Polypropylene

fiber from 0.2% to 0.4% increased flexural strength by about 24% and 57% respectively for lightweight fiber reinforced concrete.

On the other hand, the addition of steel fibers in concrete mixes makes it distinguishable from plain mixes due to the steel fibers ability to absorb a large amount of energy and to withstand large deformations prior to failure. Therefore, it was clear that the 3D and 5D showed superior enhancement of 198.97% and 308.97% respectively, followed by the hybrid reinforced that increased the flexural strength to 209.48%. Overall, the 5D reinforced samples showed the best performance among the other samples. The effect of fiber reinforcement on the flexural strength is more pronounced when compared to compressive strength, since the fracture process of steel fiber-reinforced concrete consists of progressive debonding of fiber during which slow crack propagation occurs. Final failure occurs due to unstable crack propagation when the fiber pull out and the interfacial shear stress reach the ultimate bond strength.

Gao et al. [43] reported that an increase in steel fiber volume fraction from 0 to 2%, increases flexural strength from 9.6 to 90% for high strength lightweight concrete, it was concluded that flexural strength greatly depends on the fiber volume fraction and its aspect ratio. The increase in fracture strength with increasing fiber volume fraction initiates from a great number of fibers forming a bridge in the crack and a more tortuous crack propagation path. Libre et al. [104] also showed that increasing the steel fiber ratio from 0.5% to 1% increased flexural strength by about 67% and 198%, respectively.

5.2. Test to Determine Concrete Shear Capacity

Tests were performed on six groups named A, B, C, D, E and F, each group consists of two identical beams, to determine the shear capacity of the concrete. The goal is to investigate the effect of partial replacement of SCLWC with NWA and the addition of 3D steel fiber, 5D steel fiber, polypropylene fiber and hybrid fiber (Synthetic + 5D steel fiber) on the shear capacity of the partially replaced self-consolidated lightweight concrete.

5.2.1. Load _ Deflection response. The load-deflection curves of the test beams are presented in Appendix A. It is shown that all the beams exhibited linear behavior from initial loading up to the occurrence of the first crack. It is also noticed that stiffness of all the beams are comparable. After the formation of cracks, all the beams exhibited

nonlinear load-deflection characteristics. Comparing peak deflections at ultimate loads reveals that there is marginal improvement in the ductility of the partially replaced beams. However, a significant improvement was observed in the ductility of the fiber-reinforced beams. In addition, a dominating effect of fibers is to increase the shear cracking strength when comparing the shear cracking strength of the fiber-reinforced beams with that for the reference ones [28]. Figure 5.1 shows the average of the load deflection curves for each group.

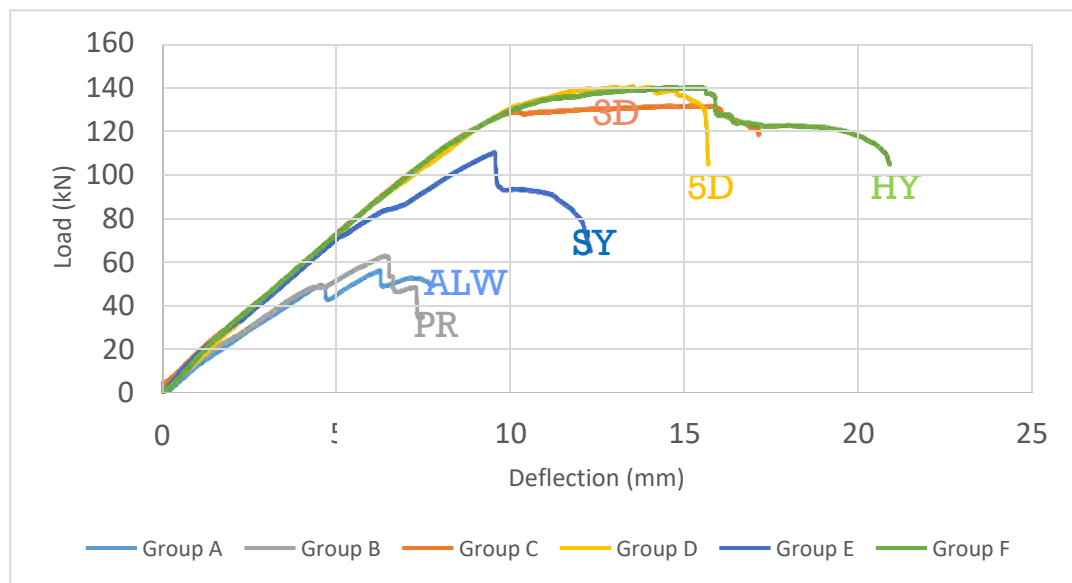


Figure 5.1: Average load versus mid-span deflection responses for all groups.

5.2.1.1 Effect of partial replacement on the load-deflection response. For beams without shear reinforcement, the aggregate interlock and friction between the crack faces is the mechanism for shear stress transfer and shear resistance. Group A and Group B beams are almost showing the same behavior in which the load kept on increasing until the aggregate interlock and friction between crack surfaces were lost and a drop in the load was noticed, as shown in Figure 5.1. Later, the shear resistance was regained apparently due to the formation of new aggregate interlock in addition to the dowel action provided by the longitudinal steel to realize a second peak. Later, the load again dropped as the crack widened and as the interlocking got weaker. Slight difference in behavior between the four beams can be mainly attributed to the aggregate distribution at the crack interface and the cement-aggregate interface. If more normal weight aggregates are available in the crack opening a rougher surface will be available

and more stresses could be transferred through the crack improving the shear capacity of the concrete beam.

5.2.1.2 Effect of fiber addition on the load deflection response. The addition of fibers to concrete beams significantly enhanced its properties. From the load deflection curves, Figure 5.1. It is noticed that the addition of fibers improved the cracking and ultimate shear capacity due to the significant amount of energy being absorbed in debonding and pulling out of fibers from the concrete matrix, in addition to the fiber ability to control and transfer stresses through cracks. However, the degree of enhancement differs depending on the fiber type, fiber geometry, fiber percentage and fiber orientation. In this study, the fibers used, at fixed percentage, are polypropylene fibers, 3D steel fibers, 5D steel fibers and hybrid mixture of polypropylene and 5D steel fibers, to study the synergetic effect of using these fibers together. All the fibers used in this work are macro fibers, therefore their effect was more pronounced at the macro scale post cracking behavior.

Utilizing the values given in Table 4.2, the percentages of improvement in the partially replaced lightweight concrete beam capacities were calculated. These improvement percentage values are presented in Table 5.2. Group C, D, E and F beams demonstrated the capability of carrying an average of 126.85%, 126.85%, 91.6 %, 137% higher ultimate loads respectively when compared to group B beams. On the other hand, they were able to carry higher deflections of 119.7%, 89.2%, 44.89% and 106.4% respectively. However, the stiffness of the fiber reinforced beams slightly increased by about 20%, 21%, 4.7% and 28.44%. Normalizing the results as shown in Table 5.1, to eliminate the effect of compressive strength, showed that the addition of fibers improved the shear capacity by 125%, 117%, 97.8%, and 130.7% respectively. Hybrid reinforced beams had the best performance followed by the 3D fiber then 5D and synthetic. Comparable results were obtained by Ding et al. [50] in which a 0.75% of steel fibers improved the maximum shear capacity by 82% for SCC beams. Moreover, Greenough et al. found that adding 1% of steel fibers enhanced the shear capacity by 128% for SCC beams [7]. In addition, Swamy et al. [14] test results indicated that SFRLWC with a steel fiber volume fraction of 1% showed significantly greater shear strength of 60% to 210% than equivalent beams without steel fibers. Furthermore, according to Kang et al. [9], the addition of steel fibers with V_f of 0.5% to 0.75% improves the resistance to structural damage and ultimate shear strength in

SFRLC by 25% to 45%. Furthermore, Kang et al. [28] showed that the increase in steel-fiber volume fraction results in a change in the failure mode from brittle to ductile. In addition, the steel-fiber volume fraction V_f of 0.5 % and 0.75% increases the shear capacities by 13% and 30%, respectively.

Table 5.1: V_c normalizes values for all the test beams.

Groups	Beam ID	$\frac{V_c}{\sqrt{f'_c}}$	Ave. $\frac{V_c}{\sqrt{f'_c}}$	% increase of $\frac{V_c}{\sqrt{f'_c}}$
Group A ALWC	-C-1	3.91	3.79	-
	C-2	3.66		
Group B PRLWC	-C-1	3.565	3.68	-2.9
	C-2	3.798		
Group C	-3D-1	8.812	8.30	125
	-3D-2	7.795		
Group D	-5D-1	6.888	7.99	117
	-5D-2	9.097		
Group E	-SY-1	6.902	7.28	97.8
	-SY-2	7.676		
Group F	-HY-1	9.22	8.49	130.7
	-HY-2	7.76		

Comparing the fiber reinforced beams to their reference beams (Group B); Figure 5.1 shows that all types of fibers contributed to a significant improvement on the shear strength of the beams. Due to the capability of the fibers to bridge the stresses across the crack, arresting the cracks, enhancing ductility and preventing catastrophic shear failures. The best performance was noticed for group F. This might be attributed to the effect of combining the two fibers together.

Looking closer to the load-deflection curves, it is noticed that for steel fiber reinforced concrete (especially the 3D fibers) that the response is a single-peak response. Prior the peak, the load increased proportionally with the increasing deflection, and then at the peak (concrete cracked), there was a slightly quick drop of load occurred before fibers began to contribute to the carrying capacity and led to a constant behavior in which the curve flattened with large strains registered for small increments of load. On the other hand, for the polypropylene fiber reinforced concrete (PFRC) as shown in Figure 5.1, the response noticed is a double peak response.

Table 5.2: Percentage of load increase for all the fiber-reinforced beams with reference to the control beams.

Groups	Beam ID	Fiber Type	% increase in maximum shear load
Group C	PRLWC-3D-1	Dramix(60/65) 3D steel fiber	140.7
	PRLWC-3D-2		112.9
Group D	PRLWC-5D-1	Dramix(60/65)5D steel fiber	96.3
	PRLWC-5D-2		157.4
Group E	PRLWC-SY-1	Strux(90/40) polypropylene fiber	81.48
	PRLWC-SY-2		101.9
Group F	PRLWC-HY-1	Dramix (60/65)5D+Strux (90/40) polypropylene.	157.4
	PRLWC-HY-2		116.7

The first response was a typical response of concrete under loading that the load increases proportionally with the deflection up to a peak, and then failure occurs due to cracking. The second response is the load recovery due to the onset of fiber bridging. The differences in the load-deflection responses of both fibers are essentially due to the properties of the fibers themselves. In SFRC, because of its high strength and stiffness, they were highly effective in terms of bridging instantaneously over the cracks at a very small deformation or crack opening, once the crack started to form. However, polypropylene fibers required much larger deformation or crack opening before the fibers could perform in response to the loading, due to lower strength and stiffness. Therefore, as a result of this, the recovery of load was delayed in the post-peak response of Polypropylene fiber reinforced concrete beams, similar conclusions were made by Sukontasukkul et al. [106]. In addition, the difference in the way steel and polypropylene fiber act in shear is also reported by Furlan et al. [107] in which stirrup stresses were lower in the case of steel fiber reinforced concrete than for a polypropylene fiber reinforced concrete.

It was expected that the 5D would show a better performance when compared to the 3D group due to its superior anchorage and tensile strength. However, Group C showed a better performance, they both achieved the same average ultimate load of 123kN but taking into account the effect of compressive strength, the 3D fiber showed higher percentage of improvement. This might be attributed to the following reasons:

- 1) The 5D fibers have high tensile strength and anchorage properties, however, it is not well utilized at the used percentage and concrete type, due to the weak concrete matrix; the effect of these superior properties could have been more pronounced at lower fiber percentages and different concrete constituents in which stronger matrix is achieved to result into a stronger bond between the fiber and the matrix.
- 2) Due to the more complex geometry of the 5D fiber, the uniformity of distribution decreases and the chances of having balling increases as compared to the 3D fiber reinforced beams.
- 3) For a given weight of the fiber, 5D steel fibers show less count. This means that for the case of the 3D fiber there might have been more fibers passing through the crack plane when compared to the 5D, transferring more stresses than the 5D scenario.

Comparing Group F beams with mixtures of steel and synthetic fibers, showed better performance compared to that of 5D steel fiber beams (Group D), and synthetic fiber beams (Group E) similar observations were made by Chen et al. [55].

The percentage of the 5D fibers in group F might have caused better utilization of the fibers across the cracks. Furthermore, the concept of hybridization was introduced to benefit from the advantages of both the steel and synthetic fibers. In the hybrid fiber system, the stiffer steel fibers improve the first crack stress and ultimate strength; while the flexible and ductile PP fibers led to improved ductility and post cracking toughness. Similar behavior was reported by Yao et al. [108] in which the toughness indices of the polypropylene fiber reinforced concrete showed a great improvement ranging from 25 to 163% depending on the type and percentage of the fiber used.

Therefore, it was clear that the performance of the hybrid-reinforced beams was better than the other types of fibers in terms of ductility, load bearing capacity and stiffness. Moreover, combining high modulus fibers, for example steel, with low modulus fiber, for example, polypropylene, the high modulus fiber, if properly bonded, would attain its optimal reinforcing capability at small to medium crack openings and the low modulus fiber, such as polypropylene, on the other hand, would develop its full reinforcement capability at large crack openings. These fibers, therefore, are expected to produce a composite with high toughness over a wide range of crack openings [109].

Comparing Group E, reinforced with Strux 90/40, with Group C and Group D, reinforced with steel fibers, the load it carried was less and it tolerated less deflection. This might be attributed to the following reasons:

- 1) The limited pull out capacity due to its lower anchorage and bond between the fiber and concrete matrix.
- 2) Less modulus of elasticity and tensile strength as compared to the steel fibers.

Tables 5.3 and 5.4 show comparison with results found in the literature, Table 5.3 provides a summarize of the mechanical properties of lightweight concrete and Table 5.4 summarizes results of lightweight concrete shear capacity.

5.2.2. Concrete strains. Concrete strains were measured for all the tested beams, to investigate the effect of concrete partial replacement and addition of fibers on the strain performance.

5.2.2.1 Effect of partial replacement on concrete strains. Comparing group B to Group A. It is noticed that the concrete strains are comparable, and the partial replacement had no effect on the concrete strain performance as shown in Table 4.4 and Appendix B.

5.2.2.2 Effect of fiber addition on concrete strains. Comparing group C, D, E and F to reference group B, it was noticed that there was no clear trend for the strain values.

Table 5.3: Summary of the material properties.

Material Properties						
Ref	Concrete type	Fiber type	Fiber %	% Improvement		Comments
				Compressive strength(cube or cylinder)	Flexural strength	
Gao et al.[43]	High strength lightweight concrete	Steel fiber	0.75	5.71	54	<ul style="list-style-type: none"> ▪ Mechanical properties of fiber reinforced concrete depends on the fiber aspect ratio. ▪
Balendran et al. [53]	Light weight high strength concrete	Steel fiber	1	1.11	182	<ul style="list-style-type: none"> ▪ The addition of fiber in normal weight concrete results in a much less increase in flexural strength than in lightweight concrete.
Kayali et al.[108]	Light weight concrete	Steel fiber Polypropylene	1.13 1	-6.17 -11.92	-	<ul style="list-style-type: none"> • Polypropylene fiber performs better at lower percentages
Libre et al.[110]	Light weight aggregate concrete	Steel fiber Polypropylene Hybrid	1 0.2-0.4 (1% steel- 0.4% pp)	54.54 (11.22 to - 8.55) 41.71	200 (23.8- 57.14) 247.6	<ul style="list-style-type: none"> • Lower percentages of polypropylene fibers show better compressive strength.
Chen et al[55]	High strength lightweight concrete	Steel Pp Steel+pp	1 1 0.5-0.5	9.8 -1.09 25.27	-	<ul style="list-style-type: none"> • The hybrid mix showed the best performance when compared to single types of fibers.
Kang et al.[28]	Light weight concrete	steel	0.5-0.75	13-20	-	<ul style="list-style-type: none"> • The compressive strength increase has been negligible to slight for SFRC with normal weight aggregates.
Current Study	PRLWSCC	Steel (3D)	0.75	30.7	198.97	<ul style="list-style-type: none"> • 5D steel fiber showed the best performance.
	PRLWSCC	Steel(5D)		42.3	308.97	
	PRLWSCC	PP		21.1	43.92	
	PRLWSCC	PP+5D		36.5	209.48	

Table 5.4: Summary of concrete shear capacity

Shear Capacity					
Ref	Concrete type	Fiber type	Fiber %	% Improvement	Comments
Kang et al.[28]	Light weight concrete	steel	0.5-0.75	13-30	<ul style="list-style-type: none"> Steel fiber is more effective in LWC than NWC Shows a high improvement in shear
Kang et al.[40]	Light weight concrete	Steel	0.5-0.75	25-45	<ul style="list-style-type: none"> Addition of fibers improves the resistance to structural damage and ultimate shear strength in SFRLC
Current Study	PRLWSCC	Steel (3D)	0.75	126.85	<ul style="list-style-type: none"> HY fiber reinforced mix had the best performance
	PRLWSCC	Steel(5D)		126.85	
	PRLWSCC	PP		91.6	
	PRLWSCC	PP+5D		137	

5.2.3. Steel strains. Steel strains were measured for all the tested beams to investigate the effect of concrete partial replacement and addition of fibers on the strain performance.

5231 Effect of partial replacement on steel strains. Strain values, Table 4.5, showed that the partial replacement of concrete resulted in a slight decrease in the steel stress by an average percentage 12.9%. This indicates that for the same load capacity, the addition of the NWA improved the bond between the steel bars and the surrounding concrete. This was also observed in the improved flexural strength of the concrete prisms. Overall, the stress in the steel bars were much less than the yielding point, due to the brittle behavior of the plain concrete beams.

5232 Effect of fibers addition on steel strains. As shown in Table 4.5, the strains in the top bars are too small and comparable in all beams. On the other hand, the stresses in the bottom bars increased in the fiber reinforced beams, due to the ductile effect the fibers added to the beams increasing the shear capacity and preventing sudden failures. For instance, stresses reached to the yield point in the three best performing beams (PRLWC-3D-2, PRLWC-5D-2 and PRLWC-HY-1) showing a delayed shear failure and more ductile behavior in which PRLWC-3D-2 beam failed in flexure.

5.2.4. Cracking behavior and mode of failure. The effect of the partial replacement and fiber addition on the tested beams was investigated.

5241 Effect of partial replacement on cracking behavior and mode of failure. As shown in Appendix E, the cracks in Group A beams were less than the cracks observed in Group B. However, these cracks propagated more towards the concrete compression zone and were more far apart, since there is no shear reinforcement to handle the stresses in the concrete section and the cracks could easily propagate through the lightweight aggregates due to their weak nature. On the other hand, the use of a percentage of normal weight aggregates inhibited the growth and propagation of cracks; this could be attributed to the ability of normal weight aggregate to resist cracking and improving the aggregate interlock.

5242 Effect of fiber reinforcement on the cracking behavior and mode of failure. As noticed from Appendix E, that the presence of fibers in concrete affected greatly the observed cracking pattern of the fiber reinforced beam. The flexural and shear cracks increased and spaced more closely. Moreover, there was less propagation

of the cracks in the compression zone. Failure was more ductile in practically all the fiber-reinforced beams. The shear crack angles ranged from 21 degrees to 59 degrees with no clear trend.

5.2.5. Initial cracking and crack widths. The initial cracking and cracks width were captured from the strain gauges located at the shear span of the concrete beams. As shown in Appendix D, the load vs strain curves were zoomed to be able to capture the initial behavior of the beam. The percentage of the initial crack to the ultimate load was calculated. It was clear that the percentage from the ultimate load was smallest, 9.9%, for the best performing beam (PRLWC-HY-1). This indicates that the beam sustained higher loads and took longer time to fail after the initiation of the first crack. On the other hand, the worst performing beam's (ALWC-C-2) initial load was 54% of the ultimate load; this in turn shows that the beam did not carry much load after the first crack initiated leading to a brittle failure. In addition, the initial crack width of PLWC-C-1 was 84% less than that of the ALWC-C-2. Other researchers obtained similar conclusions as well. For instance, Ayman et al. [87] observed that the addition of synthetic fibers reduces the crack width of lightweight reinforced concrete beams.

5.2.6. DIC observations summary. The results obtained from DIC could capture the behavior and propagation of the shear crack at different loading stages and timings of the test. The difference in behavior between the control beams and the fiber-reinforced beams were clearly observed from the crack width vs time plots.

The difference in the behavior between the control samples and the fiber-reinforced samples are clearly observed. The shear stresses in control specimens is mainly transferred by aggregate interlock. However, the fiber reinforced concrete beams have a combination of fiber bridging mechanism and aggregate interlock, showing a more ductile behavior. As shown in Figure 4.12 for Group A beam, after the ultimate load was reached, the load started to drop but the crack did not open suddenly due to the friction of the crack surfaces relative to each other and the aggregate interlock-taking place. Later, a sudden jump took place and the crack suddenly widened due to the loss of aggregate interlock showing a brittle behavior.

Group B beam encountered a sudden increase in the crack width at first peak. This demonstrates a brittle behavior in which the crack suddenly opens when the beam reaches its ultimate load. Between the first and second peak, the applied shear is then

carried partially by the friction between the two sliding faces of the crack planes and partially by aggregate interlock offered by the protrusions available on the crack plane. As a result, the load started picking up. As time passes, the surface asperities at contacts started to deform and the crack started to widen. The beam hit the second peak, and then a drastic increase in the crack width took place in the same instance, but at higher rate this time due to the loss of friction and aggregate interlock and due to wider crack opening.

For group C the crack opened at a constant rate showing ductile behavior. Since part of the shear stress is carried by the aggregate interlock mechanism due to the irregularities on the crack surface that lock with each other. The other part is carried by the fiber bridging mechanism. The crack kept on widening until it reached a second peak, the crack then opened at a faster rate. This might be attributed to the loss of aggregate interlock and yielding of some of the fibers crossing the crack. The difference in the crack width at different locations depends on the number and alignment of fibers crossing that area. In addition, it depends on the aggregate distribution at the crack plane. At the failure of the beam the crack suddenly opened at no time which is clearly shown from the jump taking place on the curve. The tensile stresses might have exceeded the pull out capacity of the fiber or the fiber has ruptured. In addition, the loss of aggregate interlock plays an important role.

Almost same behavior took place for all the fiber-reinforced beams. However, it is observed that the jump for the 5D reinforced beam is less than the 3D due to the higher pullout capacity. Moreover, for synthetic fibers the jump was not severe in most of the crack faces since the synthetic fiber is better distributed in the mix and the fiber count is much higher when compared to steel fiber. The best performing group is group F due to the synergetic effect of the 5D and polypropylene fibers. Table 5.1 shows a summary of the results obtained from DIC results.

5.2.7. Predication of the shear capacity using codes and proposed equations. Experimental shear capacity of the control beams is compared to the corresponding estimated ones from the American, the Canadian and the European codes as shown in Table 4.9. Reduction factor λ was applied according to the provisions of each code, to account for the effect of using lightweight aggregate. For the ACI and Canadian code the same reduction factors applied in which 0.85 was used for the

ALWC group and 0.868 was used for the PRLWC group (obtained by interpolation to account for the 12% replacement). A factor of 0.8 was used for the Euro2 ($f_{ck} < 50$ MPa).

Table 5.5: Experimental shear values versus predicted.

Beam ID	Vc experimental (kN)	Exp (Avg) (kN)	Vc ACI (kN)	Vc Canadian (kN)	Vc Euro 2 (kN)
ALWC-C-1	26.20	27.10	18.79	22.56	25.66
ALWC-C-2	28.00				
PRLWC-C-1	23.25	27.23	19.14	22.97	25.59
PRLWC-C-2	31.20				

Comparing the shear capacity from the experimental results with that predicted from the ACI, Canadian and Euro code 2 shown in Table 4.9. It was shown that the Euro code followed by the Canadian code is better matching the experimental results in this investigation as compared to ACI code as presented in Table 5.3 and Figure 5.2.

Table 5.6: Comparing the ratios of Vc experimental/Vc predicted from other codes.

Beam ID	$\frac{V_{cexp}}{V_{cACI}}$	Avg.	V_{cexp}	Avg.	$\frac{V_{cexp}}{V_{cEuro2}}$	Avg.
			$V_{cCanadian}$			
ALWC-C-1	1.23	1.44	1.02	1.2	1.13	1.055
ALWC-C-2	1.32		1.09		1.20	
PRLWC-C-1	1.09	1.42	0.94	1.19	1.02	1.065
PRLWC-C-2	1.52		1.27		1.37	

5.2.8 Experimental data vs predicted values from SFRC proposed equations. A comparison of predicted and experimental values of V_n (i.e. the contribution of the concrete and the fibers together) is shown in Table 5.7. The predicted values were found through the previously proposed equations by other researchers. It is essential to mention that those equations are only applicable to the steel fiber reinforced groups. A modification factor $\lambda = 0.868$ (obtained by linear interpolation) is applied to the ACI equation according to the ACI provision (ACI 318R-14) to account for the 12% of partial replacement.

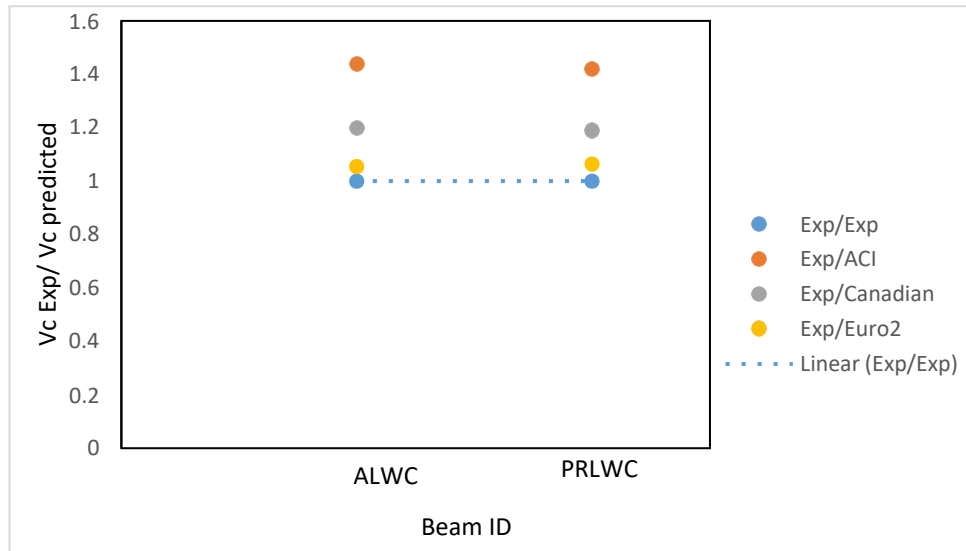


Figure 5.2: Ratios of Vc experimental/Vc predicted from other codes.

Comparing the shear values shown in Table 5.7 with the experimental results. It is clear that the results of the ACI modified equations best matches the experimental results followed by Kwak and Narayan equations. It is noticed from Table 5.8 and Figure 5.3 that Ashour's equation is very conservative when compared to other equations. All the proposed equations include parameters that accounts for the geometry, fiber volume and bond.

Table 5.7: Vn experimental vs Vn predicted from SFRC proposed equations

Beam Group	ACI short (kN)	ACI long (kN)	Experimental (kN)	ACI modified (kN)	Narayan (kN)	Ashour (kN)	Kwak (kN)	Khuntia (kN)
3D	25.44	26.06	61.25	58.04	56.45	44.91	57.91	45.45
5D	26.54	27.11	61.25	59.52	58.18	45.83	59.67	47.42

Table 5.8: Comparing the ratios of Vn experimental/Vn predicted from other studies.

Beam Group	$\frac{Vn\ exp}{Vn\ ACI\ modified}$	$\frac{Vn\ exp}{Vn\ Narayan}$	$\frac{Vn\ exp}{Vn\ Ashour}$	$\frac{Vn\ exp}{Vn\ Kwak}$	$\frac{Vn\ exp}{Vn\ Khuntia}$
Group C	1.05	1.085	1.363	1.057	1.35
Group D	1.03	1.053	1.336	1.026	1.29

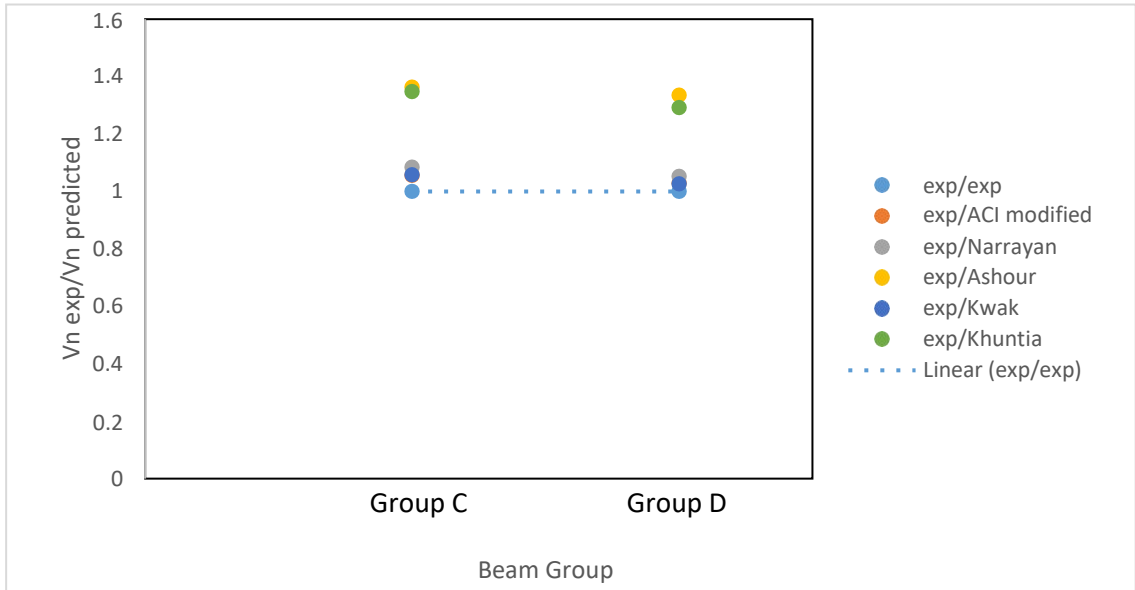


Figure 5.3: Ratios of V_n experimental/ V_n predicted from other codes.

5.2.9. Calculating a modification factor to account for lightweight concrete.

Table 5.9 shows the shear values of all the predicted code values excluding the effect of the reduction factor. The λ factor was calculated for all the four control beams by dividing the experimental with the code predicted. It was noticed that the Canadian and ACI code showed a reduction factor $\lambda > 1$ as shown in Table 5.10. This shows that despite using lightweight aggregate, beams showed superior performance to the extent that there was no modification factor needed and the experimental results were better than the predicted ones. Predicted values by the Canadian code was best matching the experimental results. On the other hand, for the Euro code a modification factor of 0.85 was needed to account for the effect of using lightweight aggregate.

Table 5.9: Shear values (V_c) of all code equations without applying reduction factors.

Beam ID	V_c experimental	Avg.	V_c ACI	V_c Canadian	V_c Euro 2
ALWC1	26.2	27.1	22.12	26.54	32.069
ALWC2	28				
PRLWC1	23.25	27.225	22.05	26.46	31.994
PRLWC2	31.2				

Table 5.10: λ values predicted based on different applied codes.

Beam ID	λ Exp/predicted ACI	λ avg ACI	λ Exp/ predicted Canadian	λ avg Canadian	λ Exp/ predicted Euro 2	λ avg Euro 2
ALWC1	1.18	1.225	0.987	1.021	0.817	0.845
ALWC2	1.27		1.055		0.873	
PRLWC1	1.05	1.230	0.878	1.028	0.726	0.850
PRLWC2	1.41		1.179		0.975	

5.2.10. Cost of fibers used in all the mixes. Table 5.8 shows the cost of using each type of fiber in the different concrete mixes. It was noticed that cost of the 5D steel fiber is about 108% higher than that of the 3D fiber. However, for the hybrid fibers the cost was 38% higher when compared to that of the 3D. Nevertheless, it is about 33.6% cheaper when compared to the cost of the 5D fiber alone. On the other hand, synthetic fibers had the highest unit price. However, the cost was less since less weight is used when compared to the steel fiber because the difference in the materials densities.

Table 5.11: Cost of the fibers used in each concrete beam of each mix.

Mix no.	Fiber type	Fiber unit price AED/Kg	Cost of 0.75% fiber (AED)
Mix 3	3D steel	6	57.6
Mix 4	5D steel	12.5	120
Mix 5	SY	35	39.31
Mix 6	HY	-	79.6

Table 5.12: A summary of the results obtained from the DIC results.

Beam ID	Load @ 1 st flexure crack (kN)	Time @ 1 st flexure crack (min)	Load @ 1 st shear crack	Time @ 1 st shear crack	Average Crack width @ ultimate load (mm)	Time @ ultimate load (min)	Average Crack width at failure (mm)	Crack width at failure/ def.	Time @failure (min)	Load at failure (kN)	Average Rate of cracking (mm/min)	Maximum strain at failure
ALWC-C-1	6.2	2.3	41.54	7.533	0.111	9.4	1.69	0.292	10.38	42.19	2.04	3.4
PRLWC-C-1	10.6	3.28	42.9	8.93	1.09	12.2	2.37	0.289	13.54	34.9	0.75	3.58
PRLWC-3D-2	60	9.7	77.2	12.2	0.334	20.98	4.64	0.2095	25.94	82	1.726	6.65
PRLWC-5D-1	10.4	0.966	48.5	5.995	0.848	16.85	2.92	0.264	18.35	82.7	0.557	5.6
PRLWC-SY-1	20.7	3.864	40	6.69	0.571	16.62	2.2	0.161	22.82	80.56	0.2	9.25
PRLWC-HY-1	27.8	2.83	114.7	13.92	0.118	17.2	4.37	0.209	34.8	96.5	1.2	7.6

Chapter 6. Conclusions and Recommendations

6.1. Conclusions

The main objectives of this research are to evaluate i) the effect of utilizing normal weight aggregate to partially replace lightweight aggregate and ii) the influence of fiber addition on the shear behavior of LWSCC beams. An experimental investigation was conducted on 12 beams representing six groups (A to F); each category consists of two beams. The first group, A, (two beams) was prepared using lightweight coarse aggregate, while the other groups (B to F) were cast using lightweight coarse aggregate with partial replacement of 12% of normal weight coarse aggregate. Different types of fibers with volumetric ratio of 0.75% were used in the evaluation. 3D steel fibers, 5D steel fibers, polypropylene synthetic fibers and Hybrid fibers (50% synthetic+50% 5D steel fibers) were used in groups C to F, respectively. In addition, an analytical investigation was conducted to compare the experimental results with those predicted from codes and equations found in the literature. The following conclusions may be drawn:

Effect of partial replacement of NWA and fibers on the mechanical properties of the lightweight aggregate mix

1. The partial replacement of the LWA with 12% of NWA resulted in 7.1% and 0.61% decrease in cube and cylinder compressive strength respectively when compared to the reference samples. However, the flexural strength was improved by 14.5% when compared to the reference samples. This indicates that the partial replacement had better influence on the flexural strength rather than the compressive strength.
2. For fiber-reinforced specimens, there is a great enhancement in the cube and cylinder compressive strength of the fiber-reinforced mixes. Group C, D, E and F showed enhancements of 30.7%, 42.3%, 21.1% and 36.5% respectively for the cube compressive strength and 27.2%, 53.8%, 21.05%, 45.41% respectively for the cylindrical compressive strength. Overall, 5D steel fiber reinforced samples showed the best performance, followed by the hybrid mix.
3. The addition of the synthetic polypropylene fiber showed an improvement of 43% when compared to the control samples. However, the addition of steel fibers in SCC mixes makes it significantly distinguishable from plain SCC by

its ability to absorb a large amount of energy and to withstand large deformations prior to failure. Therefore, it was clear that the 3D and 5D showed superior enhancement of 198.97% and 308.97% respectively, followed by the hybrid reinforced that increased the flexural strength to 209.48%. Overall, the 5D reinforced samples showed the best performance among the other samples.

4. The fiber-reinforced specimens did not have severe failure modes when compared to the control specimens. This is attributed to the fibers capability of bridging stresses across cracks. Therefore, the tested samples had preserved shape with less observed damage.

Effect of partial replacement of NWA and fibers on the concrete shear strength

5. The partial replacement of LWA with 12 % of NWA did not contribute to the ultimate shear capacity of the concrete. However, it showed an improvement in the ductility of the beams due to the improved aggregate interlock and the presence of more normal weight aggregates in the crack opening which contribute to transfer of the crack. Nevertheless, the results were scattered which could be attributed to the dependence of the failure mechanism on the distribution of the normal weight aggregate in the shear zone.

6. Groups C, D, E and F beams demonstrated the capability of carrying an average of 126.85%, 126.85%, 91.6 %, 137% higher ultimate loads; respectively, when compared to group B beams. On the other hand, they were able to carry higher deflections of 119.7%, 89.2%, 44.89% and 106.4%, respectively. This is attributed to the significant amount of energy that is absorbed in deboning and pulling out of fibers from the concrete matrix before the complete concrete failure occurs.

7. Normalizing the results as shown in table 4.2, showed that the addition of fibers improved the shear capacity by 125%, 117%, 97.8%, and 130.7% respectively, to eliminate the effect of the compressive strength. It was clear that hybrid mix showed the best performance. However, 3D showed better performance compared to the 5D.

8. Beams reinforced with 3D steel fiber (Group C) showed better performance when compared to that of the beams reinforced with the 5D steel fiber (Group D) this might be attributed to better distribution and utilization of the 3D fibers

9. The mixture of both synthetic and steel fibers in the hybrid-reinforced beams led to better performance than those with 5D steel fiber. Benefits from the two types of fibers were observed in the improved first crack stress, ultimate strength, ductility and post cracking behavior.
10. Steel fiber, both configurations, provided better performance than that of the synthetic fiber. Beams reinforced with synthetic fiber sustained less ultimate capacity and ductility when compared to the beams reinforced with steel fibers.
11. In the hybrid fiber system, the steel fibers improved the first crack stress and ultimate strength; while the flexible and ductile PP fibers led to improved ductility and post cracking toughness. Therefore, the performance of the hybrid-reinforced beams were better than the other types of fibers in terms of ductility, ultimate capacity and stiffness.
12. DIC was a helpful technique for understanding the strain contours and crack propagation within the beam section. The progression of crack with load was easily captured and applying virtual extensometers, the change of crack widths with time was monitored. The technique provided a tool to capture the benefit of the fiber addition in controlling the initiation and propagation of cracks.
13. The Euro code 2 equation showed the best match with the experimental results for the control specimens. On the other hand, values predicted by the ACI modified equation demonstrated comparable results to that for the steel fiber reinforced specimens.
14. From cost prospective, 3D steel fibers would be the ideal solution when compared to 5D and Hybrid at (50:50) ratio. Also considering, higher percentage of 3D fiber might also cost less when compared to the 0.75% of the 5D and hybrid.

6.2. Recommendations

The following recommendations are related to the implementation and use of fiber reinforced partially replaced lightweight concrete as a shear reinforcement can be considered for structural designers and future research work:

1. Partial replacement of the lightweight concrete seems to be promising but needs to be investigated further with higher percentages to increase its effectiveness.

However, this could lead to higher unit weight but will still give a lighter weight structure than the normal weight concrete.

2. All fiber types investigated in the study showed a high performance and great enhancement of the concrete shear capacity. Therefore, the idea of totally replacing the shear reinforcement with fibers needs to be further investigated so that it could be implemented in field.
3. The 0.75% of fibers recommended by the ACI (318-08) as a minimum shear reinforcement proved to give superior results. Therefore, more studies needs to be carried out with different type of concrete mixes to solidify its applicability.
4. Consider other combinations of different fiber types and percentages to get higher synergetic effects.

References

- [1] M. Mouli and H. Khelafi, "Performance characteristics of lightweight aggregate concrete containing natural pozzolan," *Building and environment*, vol. 43, no. 1, pp. 31-36, 2008.
- [2] H. P. J. Taylor, "Investigation of the forces carried across cracks in reinforced concrete beams in shear by interlock of aggregate," 1970. TRA 42.447, Cement and Concrete Association; p.22.
- [3] S. Yehia, M. AlHamaydeh, and S. Farrag, "High-strength lightweight SCC matrix with partial normal-weight coarse-aggregate replacement: Strength and durability evaluations," *Journal of Materials in Civil Engineering*, vol. 26, no. 11, pp.80-86, 2014.
- [4] C. Johnston, "*Fiber reinforced cements and concretes*, Gordon and Breach Science Publishers," ed: Amsterdam, 2001.
- [5] C. Cucchiara, L. La Mendola, and M. Papia, "Effectiveness of stirrups and steel fibres as shear reinforcement," *Cement and Concrete Composites*, vol. 26, no. 7, pp. 777-786, 2004.
- [6] M. Nehdi and J. D. Ladanchuk, "Fiber synergy in fiber-reinforced self-consolidating concrete," *Materials Journal*, vol. 101, no. 6, pp. 508-517, 2004.
- [7] T. Greenough and M. Nehdi, "Shear behavior of fiber-reinforced self-consolidating concrete slender beams," *Materials Journal*, vol. 105, no. 5, pp. 468-477, 2008.
- [8] Y. Ding, Z. You, and S. Jalali, "Hybrid fiber influence on strength and toughness of RC beams," *Composite Structures*, vol. 92, no. 9, pp. 2083-2089, 2010.
- [9] Y.-K. Kwak, M. O. Eberhard, W.-S. Kim, and J. Kim, "Shear strength of steel fiber- reinforced concrete beams without stirrups," *ACI Structural Journal*, vol. 99, no. 4, pp. 530-538, 2002.
- [10] R.Narayanan and I.Darwish, "Use of steel fibers as shear reinforcement," *Structural Journal*, vol. 84, no. 3, pp. 216-227, 1987.
- [11] C.-W. Tang, T. Yen, and H.-J. Chen, "Shear behavior of reinforced concrete beams made with sedimentary lightweight aggregate without shear reinforcement," *Journal of Materials in Civil Engineering*, vol. 21, no. 12, pp. 730-739, 2009.
- [12] G. Mphonde and G. C. Frantz, "Shear tests of high-and low-strength concrete beams without stirrups," *ACI Structural Journal*, vol. 81, no. 4, pp. 350-357, 1984.
- [13] C. Li, R. Ward, and A. M. Hamza, "Steel and synthetic fibers as shear reinforcement," *ACI materials*, vol 89, no.5, pp. 499-508,1992.
- [14] R.Swamy and H. Bahia, "The effectiveness of steel fibers as shear reinforcement," *Concrete International*, vol. 7, no. 3, pp. 35-40, 1985.
- [15] G. A. Rao and S. Injaganeri, "Evaluation of minimum shear reinforcement in reinforced concrete beams," *International Conference on Structural Engineering Construction and Management*, 2013.
- [16] Committee, A. C. Institute, and I. O. f. Standardization, "Building code requirements for structural concrete (ACI 318-08) and commentary," 2008: American Concrete Institute.
- [17] L. AASHTO, "Bridge design specifications," ed: American Association of State Highway and Transportation Officials, Washington, DC, 1998.
- [18] C. S. Association, *Design of concrete structures*. Mississauga, Ont.: Canadian Standards Association, 2004.
- [19] S. BIS, "Is 456: Code of practice for plain and reinforced concrete," *Bureau of Indian Standards, New Delhi, India*, 2000.

- [20] B. Standard, "8110: Part 1, Structural use of concrete—code of practice for design and construction," *British Standards Institute, London UK*, pp. 3-8, 1985.
- [21] S. Sinha, *Reinforced concrete design*. Tata McGraw-Hill Education, 2014.
- [22] R. Khaloo and N. Kim, "Influence of concrete and fiber characteristics on behavior of steel fiber reinforced concrete under direct shear," *Materials Journal*, vol. 94, no. 6, pp. 592-601, 1997.
- [23] C. Li, R. Ward, and A. M. Hamza, "Steel and synthetic fibers as shear reinforcement," *ACI materials*, vol 89, no.5, pp. 499-508, 1992.
- [24] G. N. J. Kani, "How safe are our large reinforced concrete beams?," in *Journal Proceedings*, 1967, vol. 64, no. 3, pp. 128-141.
- [25] Acheampong, C. Kankam, and J. Ayarkwa, "Shear behaviour of palm kernel shell reinforced concrete beams without shear Reinforcement: Influence of beam depth and tension steel," *Journal of Civil Engineering and Construction Technology*, vol. 7, no. 2, pp. 8-19, 2016.
- [26] K.-H. Yang and A. F. Ashour, "Aggregate interlock in lightweight concrete continuous deep beams," *Engineering Structures*, vol. 33, no. 1, pp. 136-145, 2011.
- [27] E. G. Sherwood, E. C. Bentz, and M. P. Collins, "Effect of aggregate size on beam-shear strength of thick slabs," *ACI Structural Journal*, vol. 104, no. 2, p. 180, 2007.
- [28] T. H. Kang, W. Kim, Y.-K. Kwak, and S.-G. Hong, "Shear testing of steel fiber-reinforced lightweight concrete beams without web reinforcement," *ACI Structural Journal*, vol. 108, no. 5, p. 553, 2011.
- [29] M. Mansur, K. Ong, and P. Paramasivam, "Shear strength of fibrous concrete beams without stirrups," *Journal of structural engineering*, vol. 112, no. 9, pp. 2066-2079, 1986.
- [30] R. N. Swamy, R. Jones, and A. T. Chiam, "Influence of steel fibers on the shear resistance of lightweight concrete I-beams," *Structural Journal*, vol. 90, no. 1, pp. 103-114, 1993.
- [31] J.-H. Hwang, D. H. Lee, H. Ju, K. S. Kim, S.-Y. Seo, and J.-W. Kang, "Shear behavior models of steel fiber reinforced concrete beams modifying softened truss model approaches," *Materials*, vol. 6, no. 10, pp. 4847-4867, 2013.
- [32] J.-K. Kim and Y.-D. Park, "Prediction of shear strength of reinforced concrete beams without web reinforcement," *ACI Materials Journal*, vol. 93, no. 3, pp. 213-222, 1996.
- [33] "Concrete in Practice: what, why and how?," N. R. M. C. Association, Ed., ed: National Ready Mixed Concrete Association, 2003.
- [34] T. AlJaafreh, "Strengthening of Lighweight Reinforced Concrete Beams Using Carbon Fiber Reinforced Polymers (CFRP)," Master of Science in Civil Engineering, Faculty of the Graduate School, The University of Texas at Arlington, Texas, USA, 2016.
- [35] E. C. Bentz, F. J. Vecchio, and M. P. Collins, "Simplified modified compression field theory for calculating shear strength of reinforced concrete elements," *ACI Materials Journal*, vol. 103, no. 4, pp. 614, 2006.
- [36] K.-K. Choi, P. Hong-Gun, and J. K. Wight, "Shear strength of steel fiber-reinforced concrete beams without web reinforcement," *ACI Structural Journal*, vol. 104, no. 1, pp. 12, 2007.
- [37] H. H. Dinh, "Shear behavior of steel fiber reinforced concrete beams without stirrup reinforcement," PHD. thesis, University of Michigan, USA, 2009.

- [38] J. Choi, G. Zi, S. Hino, K. Yamaguchi, and S. Kim, "Influence of fiber reinforcement on strength and toughness of all-lightweight concrete," *Construction and Building Materials*, vol. 69, no. 1, pp. 381-389, 2014.
- [39] D. de Lima Araújo, F. G. T. Nunes, R. D. Toledo Filho, and M. A. S. de Andrade, "Shear strength of steel fiber-reinforced concrete beams," *Acta Scientiarum Technology*, vol. 36, no. 3, pp. 389-397, 2014.
- [40] T. Kang and W. Kim, "Shear strength of steel fiber-reinforced lightweight concrete beams," in *Proceedings of the 7th International Conference on Fracture Mechanics of Concrete and Concrete Structures (FraMCoS-7)*, Jeju, Korea, pp. 23-28, 2010.
- [41] M. S. Shaikh, S. Kulkarni, S. Patil, and S. Halkude, "Effect Of Hybrid Fibre Reinforcement In Concrete Deep Beams," *Imperial Journal of Interdisciplinary Research*, vol. 3, no. 2, pp. 46-53, 2017.
- [42] J. A. Lamide, R. N. Mohamed, and A. B. Abd, "Experimental Results on the Shear Behavior of Steel Fiber Self-Compacting Concrete (SFSCC) Beams," *Jurnal Teknologi*, vol. 78, no. 11, pp. 103-111, 2016.
- [43] J. Gao, W. Sun, and K. Morino, "Mechanical properties of steel fiber-reinforced, high-strength, lightweight concrete," *Cement and Concrete Composites*, vol. 19, no. 4, pp. 307-313, 1997.
- [44] H. Jadhav and M. Koli, "Flexural behavior of hybrid fiber reinforced concrete beams," *International Journal of Structural and Civil Engineering Research*, vol. 2, no. 3, pp. 211-88, 2013.
- [45] H. Wang and L. Wang, "Experimental study on static and dynamic mechanical properties of steel fiber reinforced lightweight aggregate concrete," *Construction and Building Materials*, vol. 38, no. 1, pp. 1146-1151, 2013.
- [46] O. Kayali, M. Haque, and B. Zhu, "Some characteristics of high strength fiber reinforced lightweight aggregate concrete," *Cement and Concrete Composites*, vol. 25, no. 2, pp. 207-213, 2003.
- [47] N. Banthia and J. Sheng, "Fracture toughness of micro-fiber reinforced cement composites," *Cement and Concrete Composites*, vol. 18, no. 4, pp. 251-269, 1996.
- [48] B. Chen and J. Liu, "Properties of lightweight expanded polystyrene concrete reinforced with steel fiber," *Cement and Concrete Research*, vol. 34, no. 7, pp. 1259-1263, 2004.
- [49] R. Z. Al-Rousan, "Flexural Toughness Characteristics of Steel Synthetic Fibers-Lightweight Aggregate Concrete," *International Journal of Engineering Research*, vol. 8, no. 3, pp. 1536-1542, 2016.
- [50] Y. Ding, F. Zhang, F. Torgal, and Y. Zhang, "Shear behavior of steel fibre reinforced self-consolidating concrete beams based on the modified compression field theory," *Composite Structures*, vol. 94, no. 8, pp. 2440-2449, 2012.
- [51] P. Patil Sonali and M. Pawar Mukund, "Prediction of shear strength of steel fiber reinforced concrete beams without web reinforcement," *International Journal of Engineering Research and Technology*, vol. 4, no. 1, pp. 1319-1322, 2015.
- [52] H. Aoude, M. Belghiti, W. D. Cook, and D. Mitchell, "Response of steel fiber-reinforced concrete beams with and without stirrups," *ACI Structural Journal*, vol. 109, no. 3, pp. 359, 2012.
- [53] R. Balendran, F. Zhou, A. Nadeem, and A. Leung, "Influence of steel fibres on strength and ductility of normal and lightweight high strength concrete," *Building and environment*, vol. 37, no. 12, pp. 1361-1367, 2002.

- [54] S. Altoubat, A. Yazdanbakhsh, and K.-A. Rieder, "Shear behavior of macro-synthetic fiber-reinforced concrete beams without stirrups," *ACI Materials Journal*, vol. 106, no. 4, pp. 381, 2009.
- [55] B. Chen and J. Liu, "Contribution of hybrid fibers on the properties of the high-strength lightweight concrete having good workability," *Cement and Concrete Research*, vol. 35, no. 5, pp. 913-917, 2005.
- [56] H. Mazaheripour, S. Ghanbarpour, S. Mirmoradi, and I. Hosseinpour, "The effect of polypropylene fibers on the properties of fresh and hardened lightweight self-compacting concrete," *Construction and Building Materials*, vol. 25, no. 1, pp. 351-358, 2011.
- [57] M. Hassanpour, P. Shafigh, and H. B. Mahmud, "Lightweight aggregate concrete fiber reinforcement—a review," *Construction and Building Materials*, vol. 37, no. 1, pp. 452-461, 2012.
- [58] J.-Y. Wang, K.-S. Chia, J.-Y. R. Liew, and M.-H. Zhang, "Flexural performance of fiber-reinforced ultra lightweight cement composites with low fiber content," *Cement and Concrete Composites*, vol. 43, pp. 39-47, 2013.
- [59] H. Mattock, W. Li, and T. Wang, "Shear transfer in lightweight reinforced concrete," *PCI journal*, vol. 21, no. 1, pp. 20-39, 1976.
- [60] H. Higashiyama and N. Banthia, "Correlating flexural and shear toughness of lightweight fiber-reinforced concrete," *Materials Journal*, vol. 105, no. 3, pp. 251-257, 2008.
- [61] S. Yehia, M. AlHamaydeh, and S. Farrag, "High-Strength Lightweight SCC Matrix with Partial Normal-Weight Coarse-Aggregate Replacement: Strength and Durability Evaluations," *Journal of Materials in Civil Engineering*, vol. 26, no. 11, pp. 04014086, 2014.
- [62] D. V. B. Desai and M. A. Sathyam, "Some Studies on Strength Properties of Light Weight Cinder Aggregate Concrete," *International Journal of Scientific and Research Publications*, vol. 4, no. 2, pp. 1-13, 2014.
- [63] G. E. Abdelaziz, "A study on the performance of lightweight self-consolidated concrete," *Magazine of Concrete Research*, vol. 62, no. 1, pp. 39-50, 2010.
- [64] J. A. Bogas and A. Gomes, "Static and dynamic modulus of elasticity of structural lightweight and modified density concrete with and without nanosilica—characterization and normalization," *International Journal of Civil Engineering*, vol. 12, no. 2, pp. 268-278, 2014.
- [65] S. A. Ashour, G. S. Hasanain, and F. F. Wafa, "Shear behavior of high-strength fiber reinforced concrete beams," *Structural Journal*, vol. 89, no. 2, pp. 176-184, 1992.
- [66] J. Hanson, "Tensile strength and diagonal tension resistance of structural lightweight concrete," in *Journal Proceedings*, vol. 58, no. 7, pp. 1-40, 1961.
- [67] O. A. Harry and I. E. Ekop, "A Comparative Analysis of Codes Prediction of Shear Resistance in Beams without Shear Reinforcement," *American Journal of Civil Engineering and Architecture*, vol. 4, no. 1, pp. 39-43, 2016.
- [68] M. Khuntia, B. Stojadinovic, and S. C. Goel, "Shear strength of normal and high-strength fiber reinforced concrete beams without stirrups," *Structural Journal*, vol. 96, no. 2, pp. 282-289, 1999.
- [69] M. Zhang, M. Sharif, and G. Lu, "Impact resistance of high-strength fibre-reinforced concrete," *Magazine of Concrete Research*, vol. 59, no. 3, pp. 199-210, 2007.
- [70] Ezeldin and P. Balaguru, "Bond behavior of normal and high-strength fiber reinforced concrete," *Materials Journal*, vol. 86, no. 5, pp. 515-524, 1989.

- [71] J. Thomas and A. Ramaswamy, "Mechanical properties of steel fiber-reinforced concrete," *Journal of materials in civil engineering*, vol. 19, no. 5, pp. 385-392, 2007.
- [72] Alhozaimy, P. Soroushian, and F. Mirza, "Mechanical properties of polypropylene fiber reinforced concrete and the effects of pozzolanic materials," *Cement and Concrete Composites*, vol. 18, no. 2, pp. 85-92, 1996.
- [73] M. Nataraja, N. Dhang, and A. Gupta, "Stress-strain curves for steel-fiber reinforced concrete under compression," *Cement and concrete composites*, vol. 21, no. 5-6, pp. 383-390, 1999.
- [74] P. Song and S. Hwang, "Mechanical properties of high-strength steel fiber-reinforced concrete," *Construction and Building Materials*, vol. 18, no. 9, pp. 669-673, 2004.
- [75] Z. M. K. Al-Azzawi and K. Sarsam, "Mechanical properties of high-strength fiber reinforced concrete," *Engineering and Technology Journal*, vol. 28, no. 12, pp. 2442-2453, 2010.
- [76] W. Yao, J. Li, and K. Wu, "Mechanical properties of hybrid fiber-reinforced concrete at low fiber volume fraction," *Cement and concrete research*, vol. 33, no. 1, pp. 27-30, 2003.
- [77] Ezeldin and P. Balaguru, "Bond behavior of normal and high-strength fiber reinforced concrete," *Materials Journal*, vol. 86, no. 5, pp. 515-524, 1989.
- [78] Xu and H. Shi, "Correlations among mechanical properties of steel fiber reinforced concrete," *Construction and Building Materials*, vol. 23, no. 12, pp. 3468-3474, 2009.
- [79] N. Banthia and J. Sheng, "Fracture toughness of micro-fiber reinforced cement composites," *Cement and Concrete Composites*, vol. 18, no. 4, pp. 251-269, 1996.
- [80] Caggiano, S. Gambarelli, E. Martinelli, N. Nistic, and M. Pepe, "Experimental characterization of the post-cracking response in hybrid steel/polypropylene fiber-reinforced concrete," *Construction and Building Materials*, vol. 125, pp. 1035-1043, 2016.
- [81] G. J. Parra-Montesinos, "Shear strength of beams with deformed steel fibers," *Concrete International*, vol. 28, no. 11, pp. 57-66, 2006.
- [82] A. Achuthankutty, S. Ramadass, J. Thomas "Shear strength of RC beams containing hybrid steel fibers," *American Journal of Engineering Research*, vol. 2, pp. 48-52, 2013.
- [83] J. Choi, G. Zi, S. Hino, K. Yamaguchi, and S. Kim, "Influence of fiber reinforcement on strength and toughness of all-lightweight concrete," *Construction and Building Materials*, vol. 69, no. 1, pp. 381-389, 2014.
- [84] F. Altun and B. Aktaş, "Investigation of reinforced concrete beams behavior of steel fiber added lightweight concrete," *Construction and Building Materials*, vol. 38, no. 2, pp. 575-581, 2013.
- [85] H. Tanyildizi, "Statistical analysis for mechanical properties of polypropylene fiber reinforced lightweight concrete containing silica fume exposed to high temperature," *Materials & Design*, vol. 30, no. 8, pp. 3252-3258, 2009.
- [86] G. Campione, C. Cucchiara, L. La Mendola, and M. Papia, "Steel-concrete bond in lightweight fiber reinforced concrete under monotonic and cyclic actions," *Engineering Structures*, vol. 27, no. 6, pp. 881-890, 2005.
- [87] G. Campione, C. Cucchiara, L. La Mendola, and M. Papia, "Steel-concrete bond in lightweight fiber reinforced concrete under monotonic and cyclic actions," *Engineering Structures*, vol. 27, no. 6, pp. 881-890, 2005.

- [88] G. Campione and L. La Mendola, "Behavior in compression of lightweight fiber reinforced concrete confined with transverse steel reinforcement," *Cement and Concrete Composites*, vol. 26, no. 6, pp. 645-656, 2004.
- [89] R. Bagherzadeh, H. R. Pakravan, A.-H. Sadeghi, M. Latifi, and A. A. Merati, "An Investigation on Adding Polypropylene Fibers to Reinforce Lightweight Cement Composites (LWC)," *Journal of Engineered Fabrics & Fibers (JEFF)*, vol. 7, no. 4, pp. 13-21, 2012.
- [90] T. M. Nahhas, "Flexural behavior and ductility of reinforced lightweight concrete beams with polypropylene fiber," *J. Constr. Eng. Manage*, vol. 1, no. 1, pp. 4-11, 2013.
- [91] K. Aghaee and M. A. Yazdi, "Waste steel wires modified structural lightweight concrete," *Materials Research*, vol. 17, no. 4, pp. 958-966, 2014.
- [92] Caratelli, A. Meda, and Z. Rinaldi, "Monotonic and cyclic behavior of lightweight concrete beams with and without steel fiber reinforcement," *Construction and Building Materials*, vol. 122, no.1, pp. 23-35, 2016.
- [93] Ababneh, R. Al-Rousan, M. Alhassan, and M. Alqadami, "Influence of synthetic fibers on the shear behavior of lightweight concrete beams," *Advances in Structural Engineering*, vol. 20, no. 11, pp. 1671-1683, 2017.
- [94] J. A. Lamide, R. N. Mohamed, and A. B. Abd, "Experimental Results on The Shear Behaviour of Steel Fiber Self-Compacting Concrete (SFSCC) Beams," *Jurnal Teknologi*, vol. 78, no. 11, pp. 103-111, 2016.
- [95] M. Sahmaran and I. O. Yaman, "Hybrid fiber reinforced self-compacting concrete with a high-volume coarse fly ash," *Construction and Building Materials*, vol. 21, no. 1, pp. 150-156, 2007.
- [96] H. Aoude and M. Cohen, "Shear Response of SFRC Beams Constructed with SCC and Steel Fibers." *Electronic Journal of Structural Engineering*, vol. 14, no. 1, pp.71-83, 2014.
- [97] S. Iqbal, A. Ali, K. Holschemacher, and T. A. Bier, "Mechanical properties of steel fiber reinforced high strength lightweight self-compacting concrete (SHLSCC)," *Construction and Building Materials*, vol. 98, no. 1, pp. 325-333, 2015.
- [98] Bentur, S.-i. Igarashi, and K. Kovler, "Prevention of autogenous shrinkage in high-strength concrete by internal curing using wet lightweight aggregates," *Cement and concrete research*, vol. 31, no. 11, pp. 1587-1591, 2001.
- [99] Li, X. Ding, S. Zhao, X. Zhang, and X. Li, "Cracking Resistance of Reinforced SFRFLC Superposed Beams with Partial Ordinary Concrete in Compression Zone," *The Open Civil Engineering Journal*, vol. 10, no. 1, pp. 727-737, 2016.
- [100] "Synthetic macro fiber reinforcement ", G. A. T. Inc., Ed., ed. 62 Whittemore Avenue, Cambridge, MA 02140 USA, 2016. <https://gcpat.com/sites/gcpat.com/files/2017-08/STRUX%2090-40%20Datashet.pdf>, Feb. 2, 2017.
- [101] "Dramix: Reinforcing the Future," Bekaert, Ed., ed. Zwevegem, Belgium, 2012. <https://www.bekaert.com/en/products/construction/concrete-reinforcement/dramix-steel-fiber-concrete-reinforcement>, Feb. 2, 2017.
- [102] D. Suji, S. Natesan, and R. Murugesan, "Experimental study on behaviors of polypropylene fibrous concrete beams," *Journal of Zhejiang University-SCIENCE A*, vol. 8, no. 7, pp. 1101-1109, 2007.
- [103] O. Kayali, M. Haque, and B. Zhu, "Drying shrinkage of fibre-reinforced lightweight aggregate concrete containing fly ash," *Cement and concrete research*, vol. 29, no. 11, pp. 1835-1840, 1999.

- [104] N. A. Libre, M. Shekarchi, M. Mahoutian, and P. Soroushian, "Mechanical properties of hybrid fiber reinforced lightweight aggregate concrete made with natural pumice," *Construction and Building Materials*, vol. 25, no. 5, pp. 2458-2464, 2011.
- [105] J. Thomas and A. Ramaswamy, "Mechanical properties of steel fiber-reinforced concrete," *Journal of materials in civil engineering*, vol. 19, no. 5, pp. 385-392, 2007.
- [106] P. Sukontasukkul, "Toughness evaluation of steel and polypropylene fibre reinforced concrete beams under bending," *Thammasat Int. J. Sc. Tech*, vol. 9, no. 3, pp. 35-41, 2004.
- [107] S. Furlan Jr and J. B. de Hanai, "Shear behavior of fiber reinforced concrete beams," *Cement and concrete composites*, vol. 19, no. 4, pp. 359-366, 1997.
- [108] Y. Wu, "Flexural strength and behavior of polypropylene fiber reinforced concrete beams," *Journal of Wuhan University of Technology-Mater. Sci. Ed.*, vol. 17, no. 2, pp. 54, 2002.
- [109] N. Banthia and N. Nandakumar, "Crack growth resistance of hybrid fiber reinforced cement composites," *Cement and Concrete Composites*, vol. 25, no. 1, pp. 3-9, 2003.

Appendix A

Load versus Mid-span Deflection plots for the rest of specimens are shown in Appendix A.

Group A

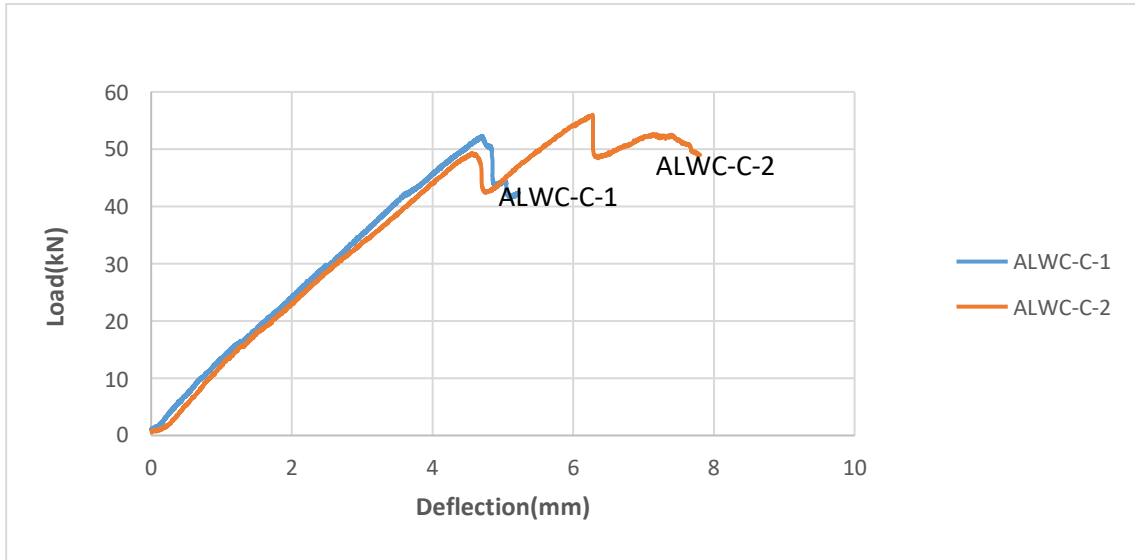


Figure A.1: Load versus mid-span deflection responses for Group A beams ALWC-C-1 and ALWC-C-2.

Group B

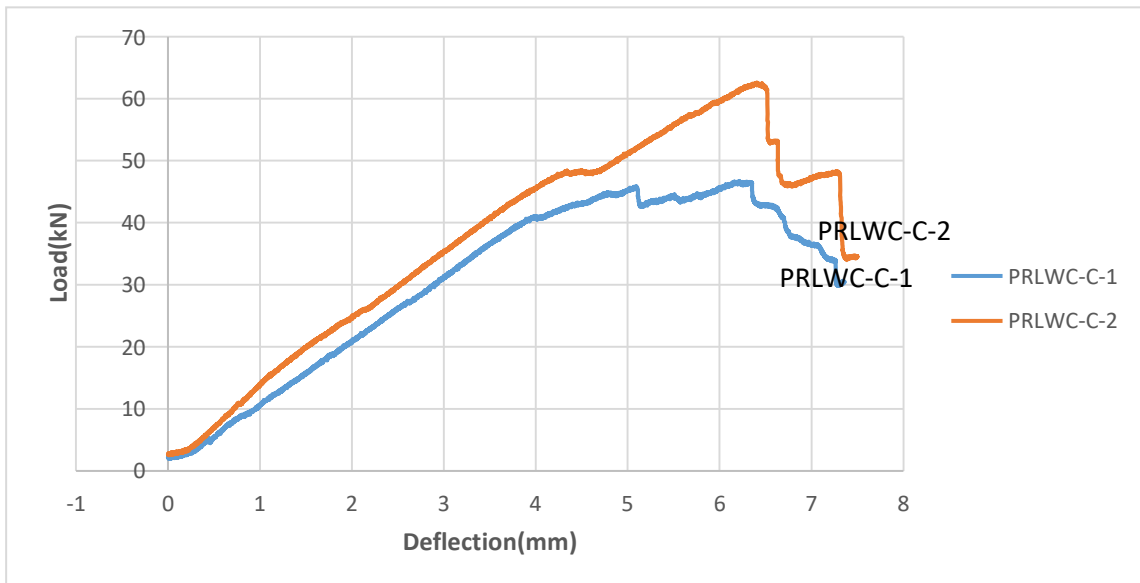


Figure A.2: Load versus mid-span deflection responses for Group B beams PRLWC-C-1 and PRLWC-C-2.

Group C

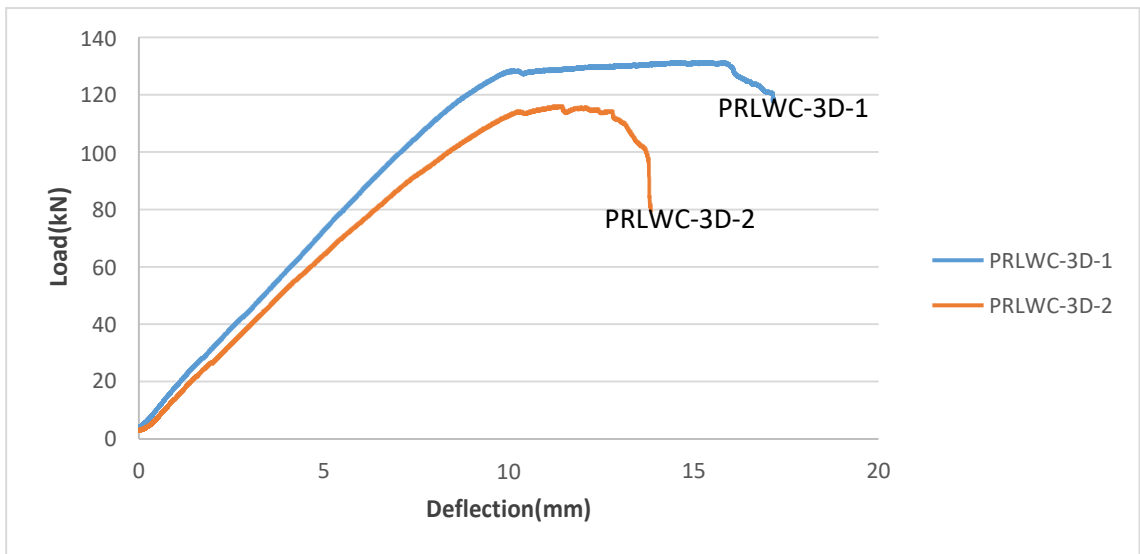


Figure A.3: Load versus mid-span deflection responses for Group C beams PRLWC-3D-1 and PRLWC-3D-2.

Group D

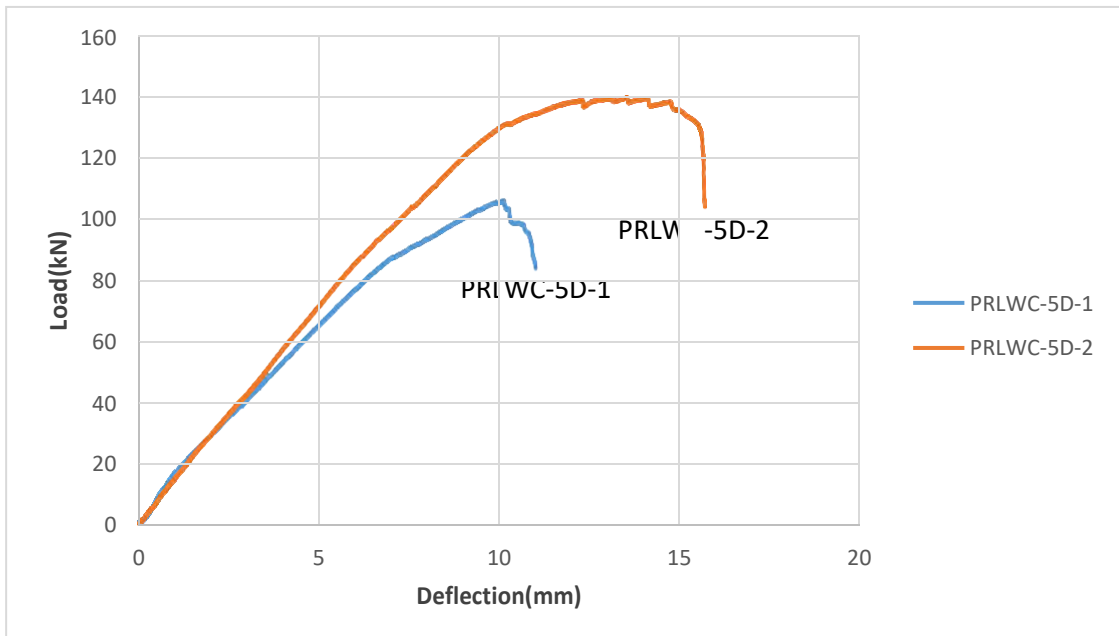


Figure A.4: Load versus mid-span deflection responses for Group D beams PRLWC-5D-1 and PRLWC-5D-2.

Group E

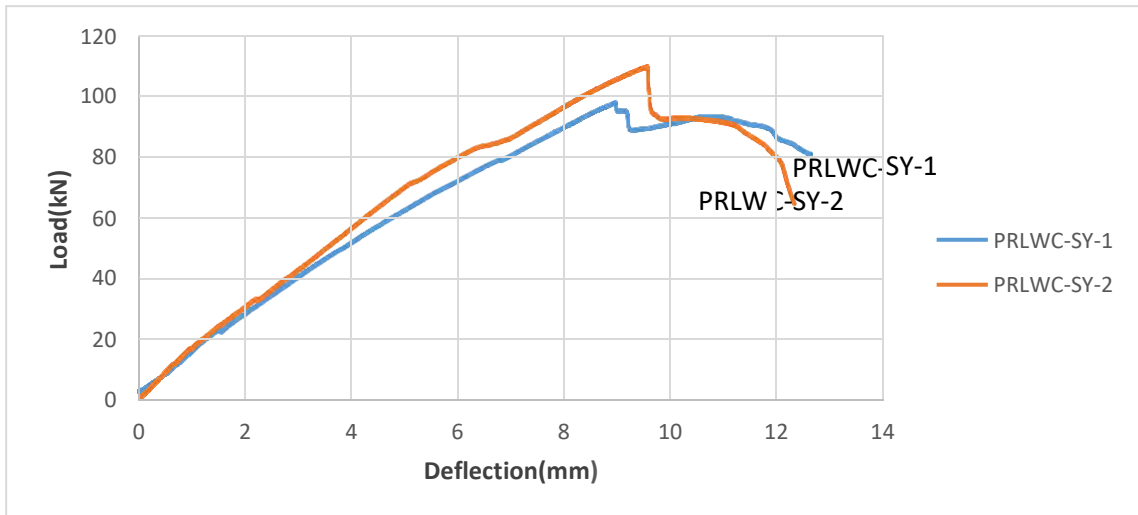


Figure A.5: Load versus mid-span deflection responses for Group E beams PRLWC-SY-1 and PRLWC-SY-2.

Group F

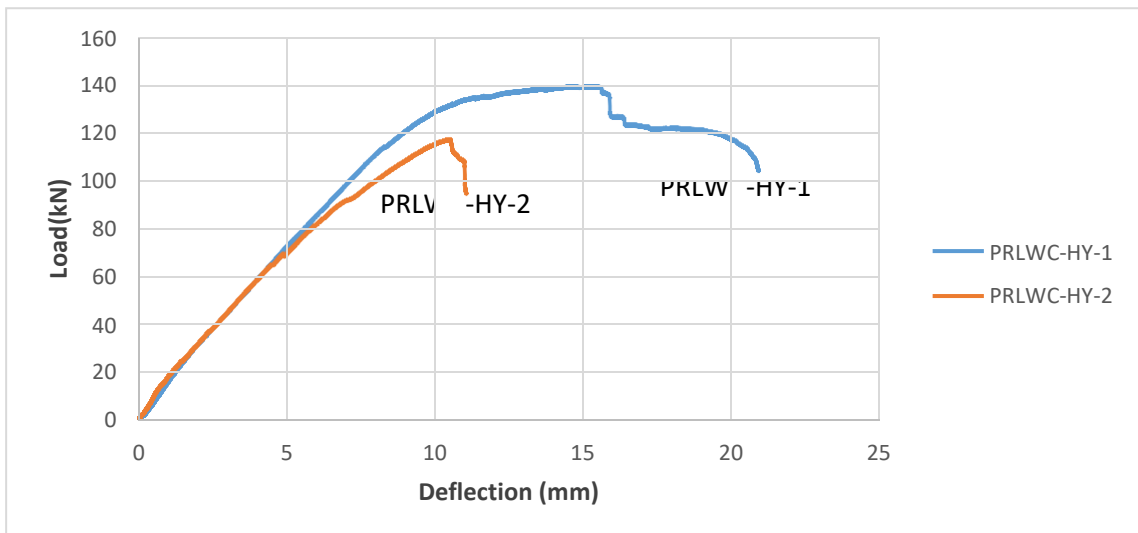


Figure A.6: Load versus mid-span deflection responses for Group F beams PRLWC-HY-1 and PRLWC-HY-2.

Appendix B

Load _ strain plots for the concrete strains for the rest of specimens are shown in Appendix B.

Group A.

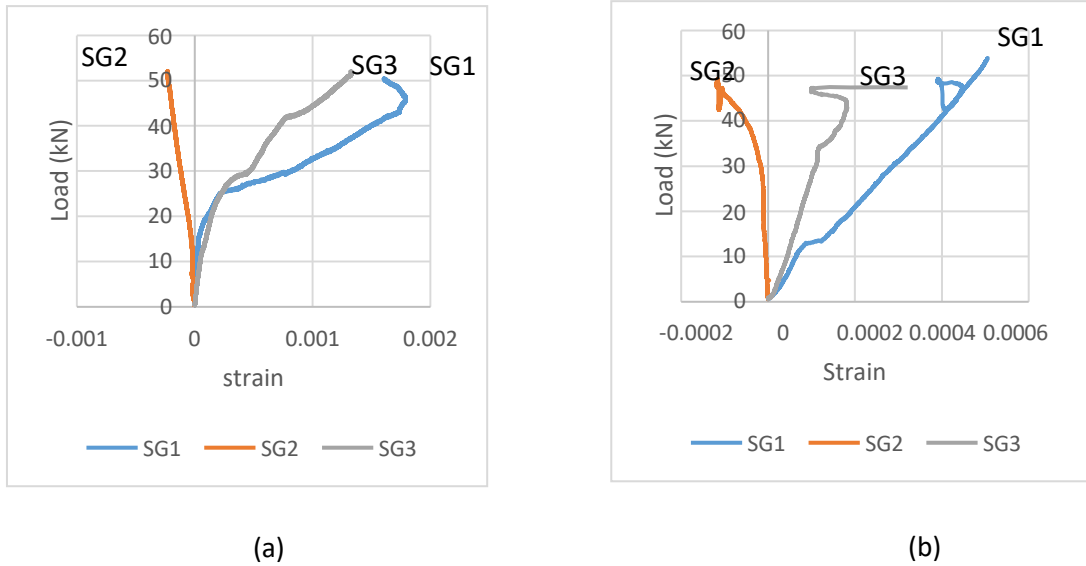


Figure B.1: Load versus strain responses for Group A beams (a) ALWC-C-1, (b) ALWC-C-2.

Group B.

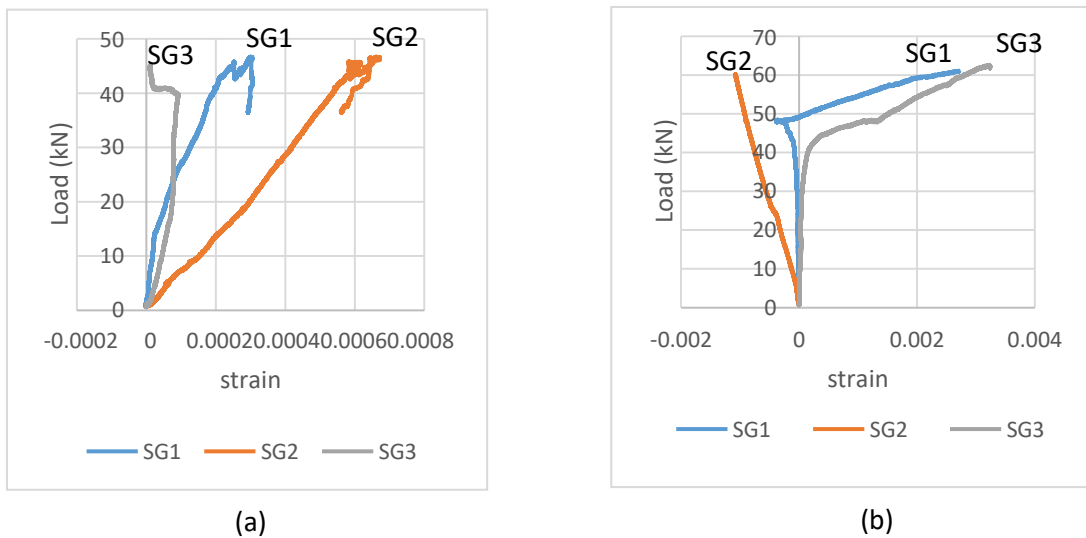
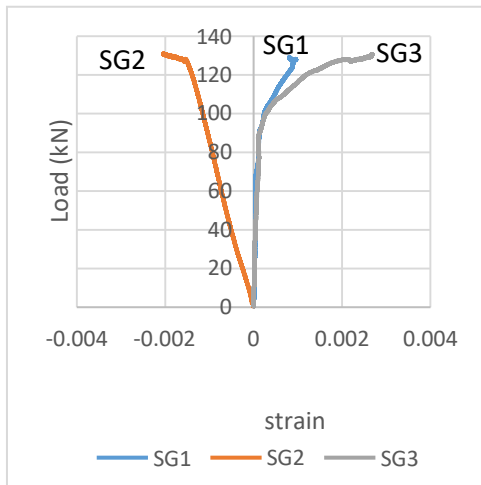
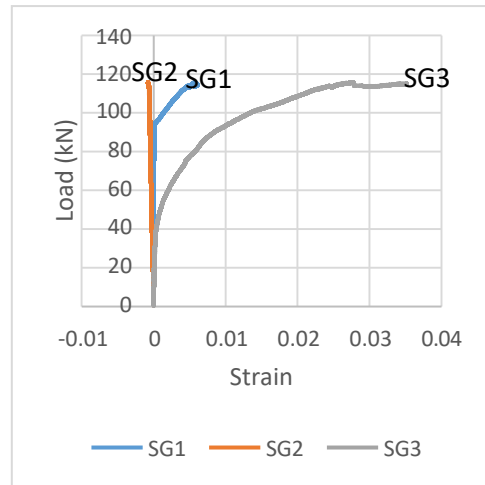


Figure B.2: Load versus strain responses for Group B beams (a) PRLWC-C-1, (b) PRLWC-C-2.

Group C.



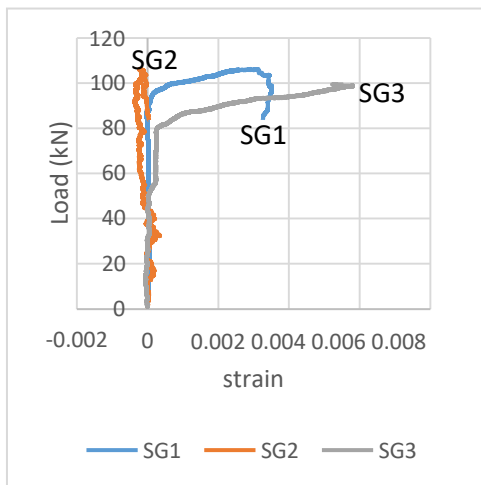
(a)



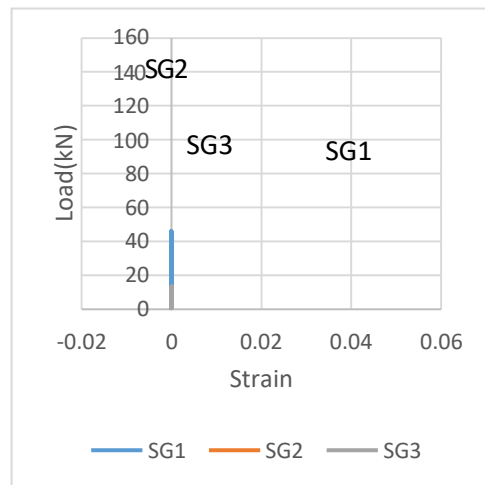
(b)

Figure B.3: Load versus strain responses for Group C beams (a) PRLWC-3D-1, (b) PRLWC-3D-2.

Group D.



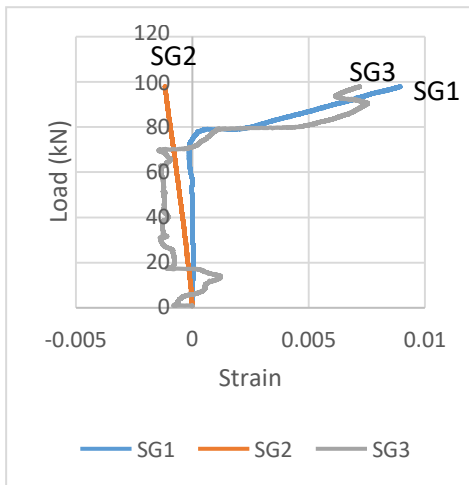
(a)



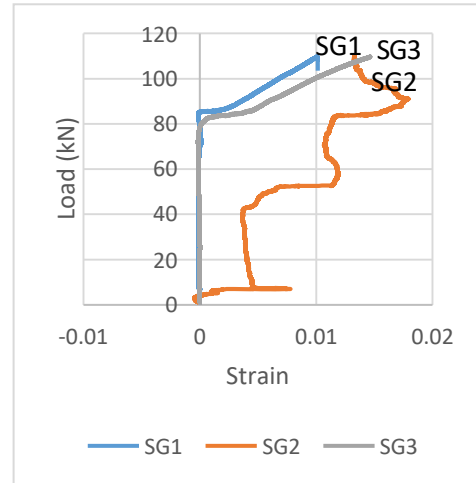
(b)

Figure B.4: Load versus strain responses for Group D beams (a) PRLWC-5D-1, (b) PRLWC-5D-2.

Group E.



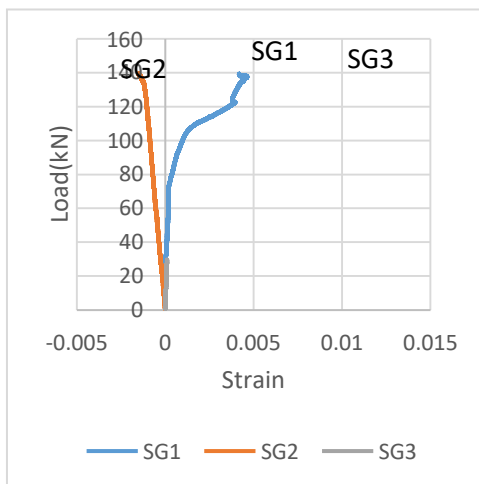
(a)



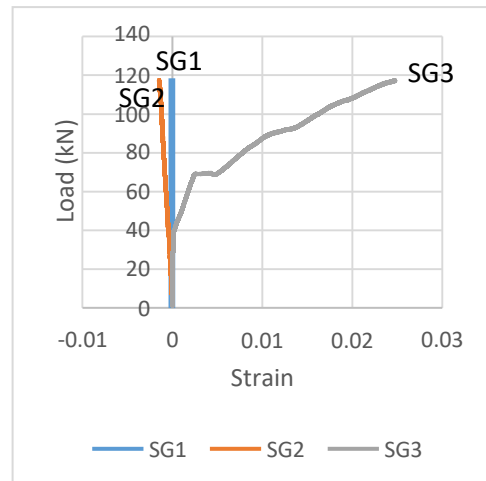
(b)

Figure B.5: Load versus strain responses for Group E beams (a) PRLWC-SY-1, (b) PRLWC-SY-2.

Group F.



(a)



(b)

Figure B.6: Load versus strain responses for Group F beams (a) PRLWC-HY-1, (b) PRLWC-HY-2.

Appendix C

Load _ strain plots for the concrete strains for the rest of specimens are shown in Appendix C.

Group A

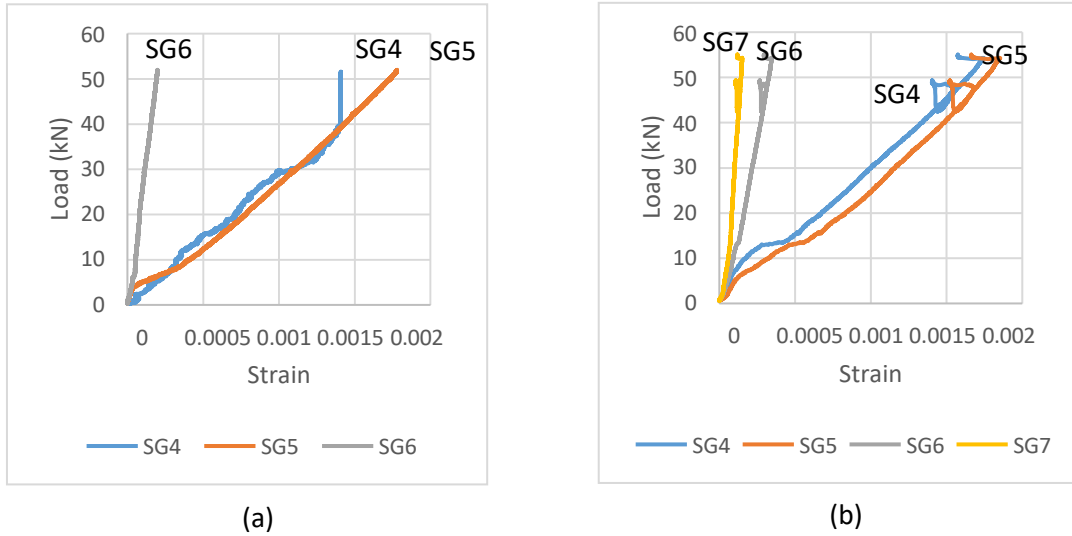


Figure C.1: Load versus strain responses for Group A beams (a) ALWC-C-1, (b) ALWC-C-2.

Group B

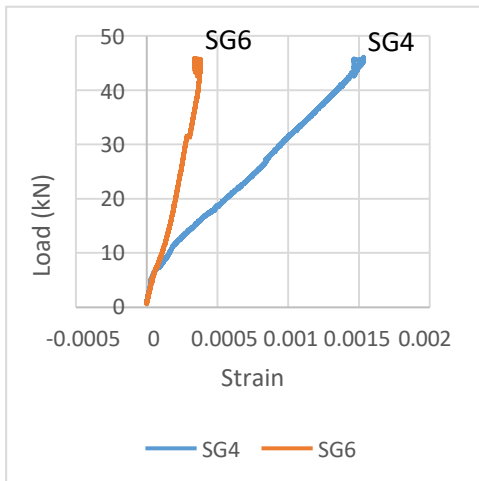


Figure C.2: Load versus strain responses for Group B beams (a) PRLWC-C-1.

Group D

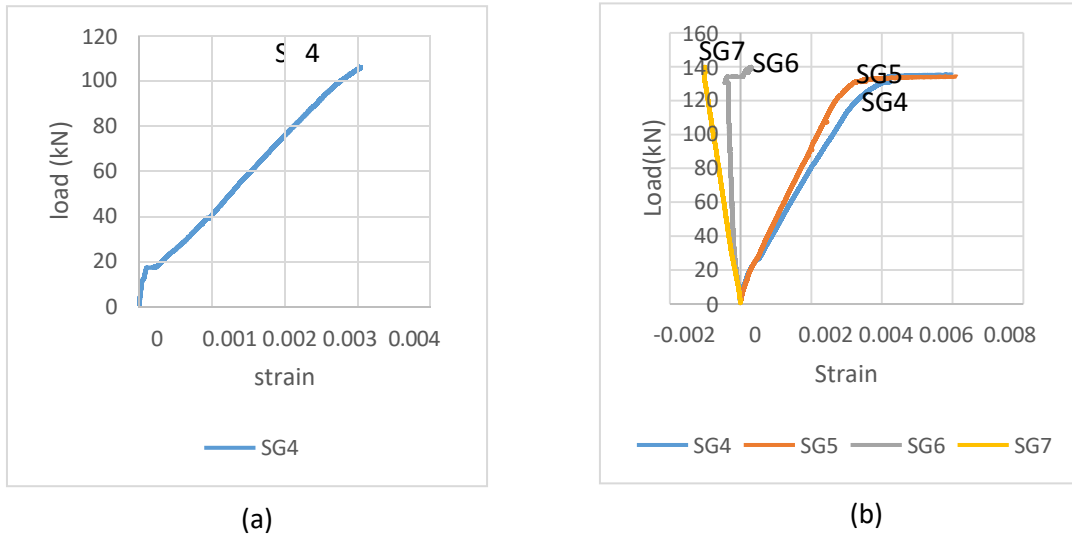


Figure C.3: Load versus strain responses for Group D beams (a) PRLWC-5D-1, (b) PRLWC-5D-2.

Group E

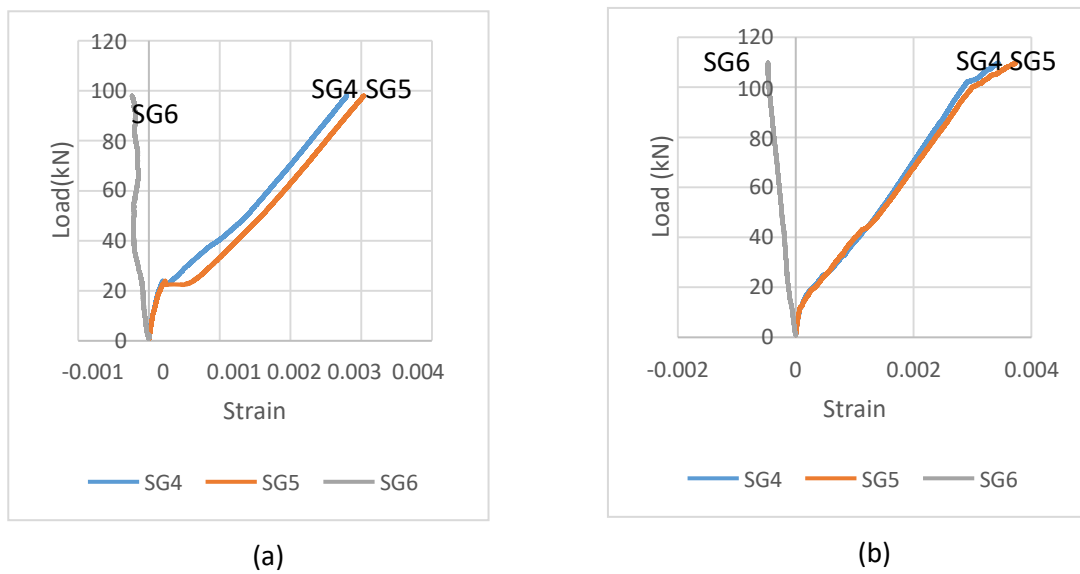
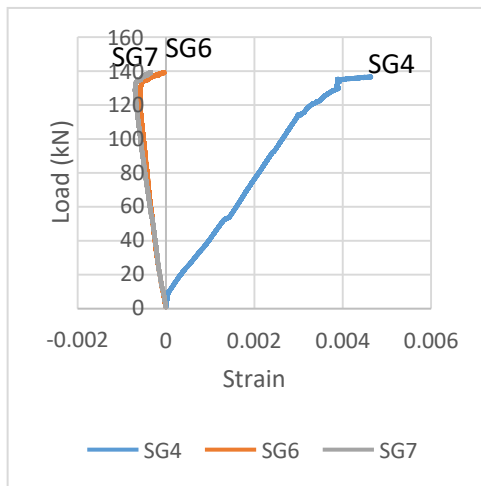
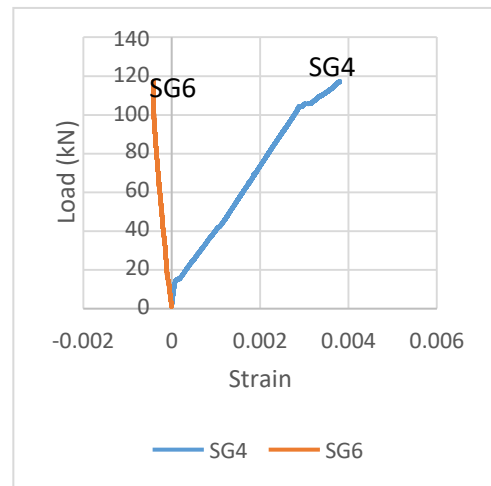


Figure C.4: Load versus strain responses for Group E beams (a) PRLWC-SY-1, (b) PRLWC-SY-2.

Group F



(a)



(b)

Figure C.5: Load versus strain responses for Group F beams (a) PRLWC-HY-1, (b) PRLWC-HY-2.

Appendix D

Load_strain initial responses for all the twelve teste beams a presented in Appendix D

Group A

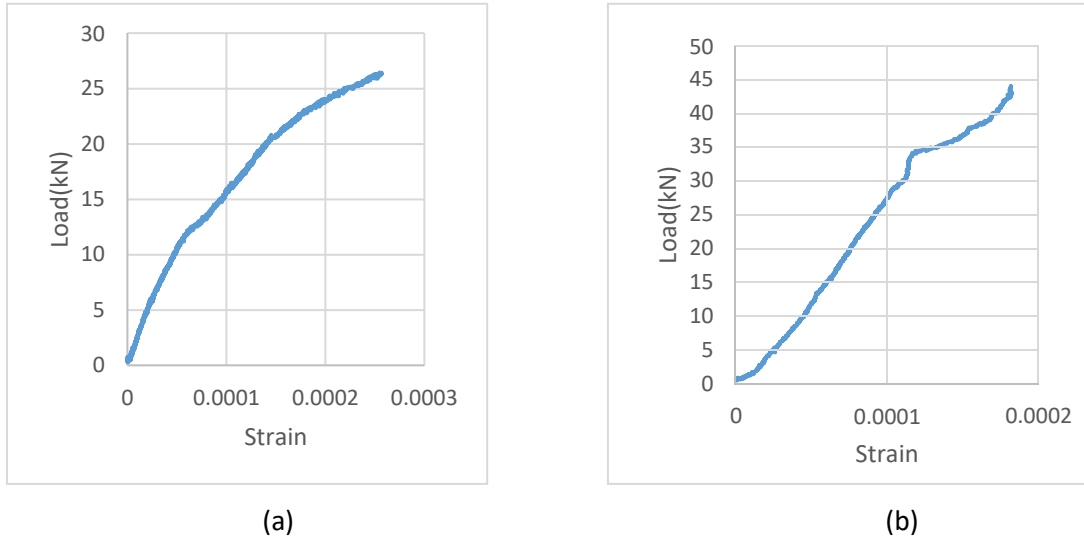


Figure D.1: Load versus strain initial responses for Group A beams (a) ALWC-C-1, (b) ALWC-C-2.

Group B

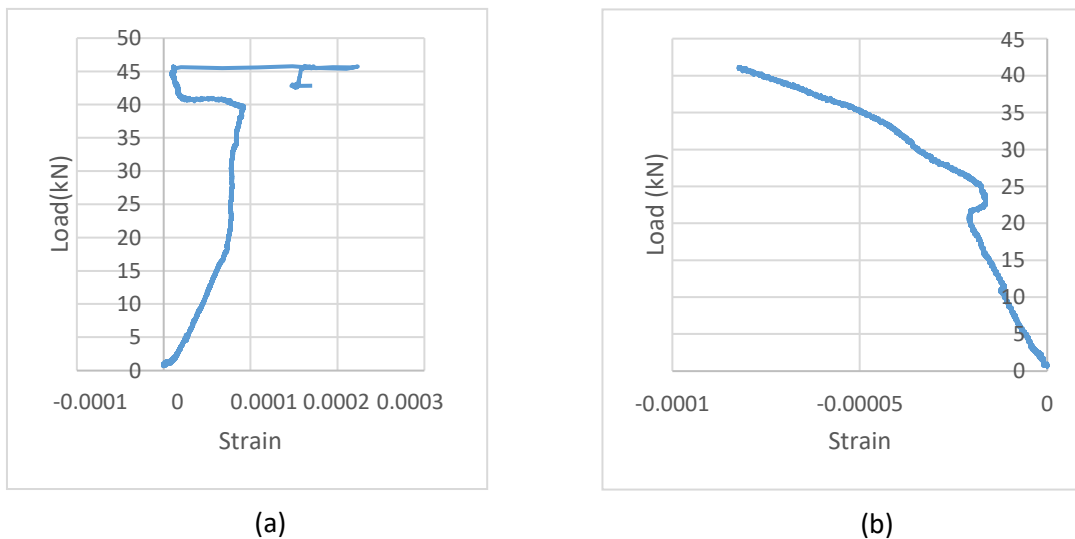
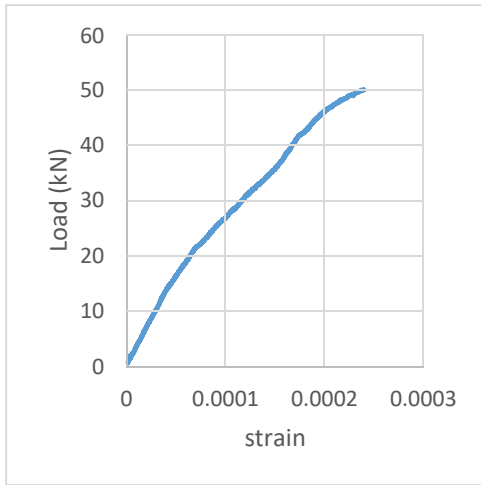
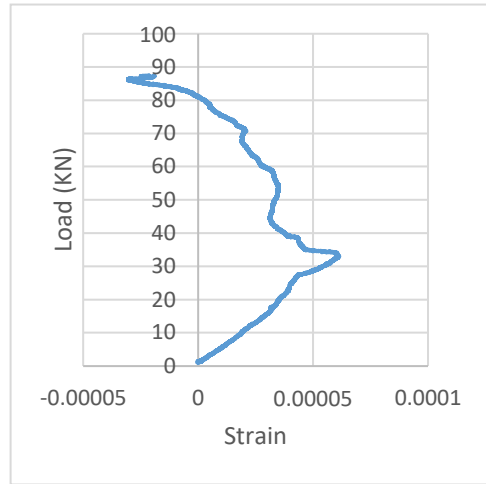


Figure D.2: Load versus strain initial responses for Group B beams (a) PRLWC-C-1, (b) PRLWC-C-2.

Group C



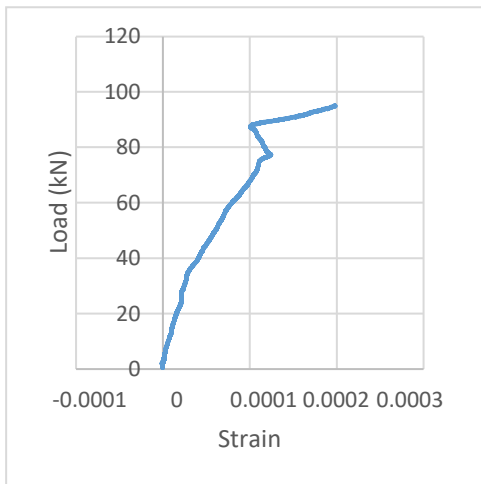
(a)



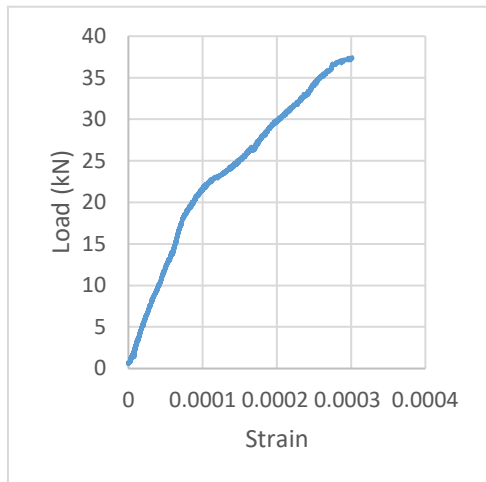
(b)

Figure D.3: Load versus strain initial responses for Group C beams (a) PRLWC-3D-1, (b) PRLWC-3D-2.

Group D



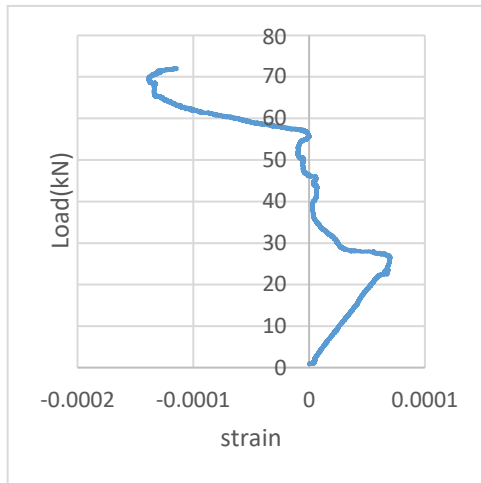
(a)



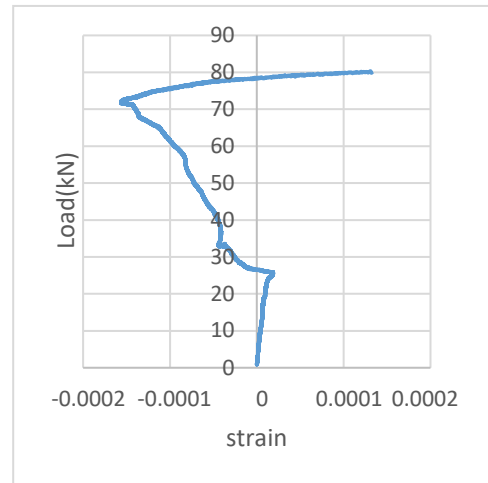
(b)

Figure D.4: Load versus strain initial responses for Group D beams (a) PRLWC-5D-1, (b) PRLWC-5D-2.

Group E



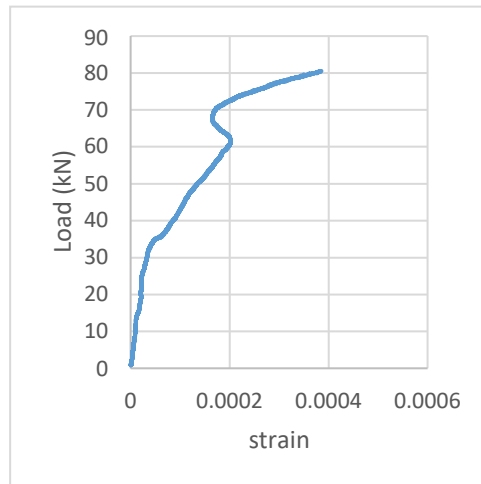
(a)



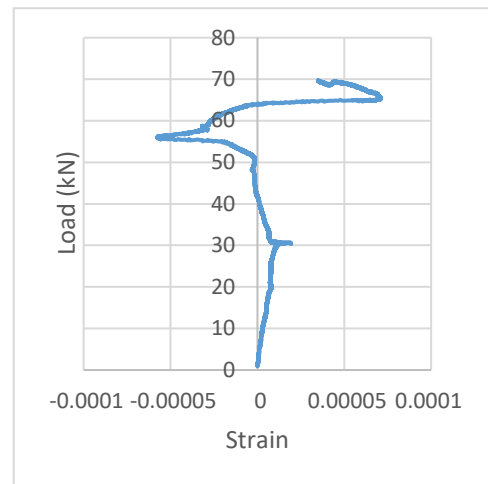
(b)

Figure D.5: Load versus strain initial responses for Group E beams (a) PRLWC-SY-1, (b) PRLWC-SY-2.

Group F



(a)

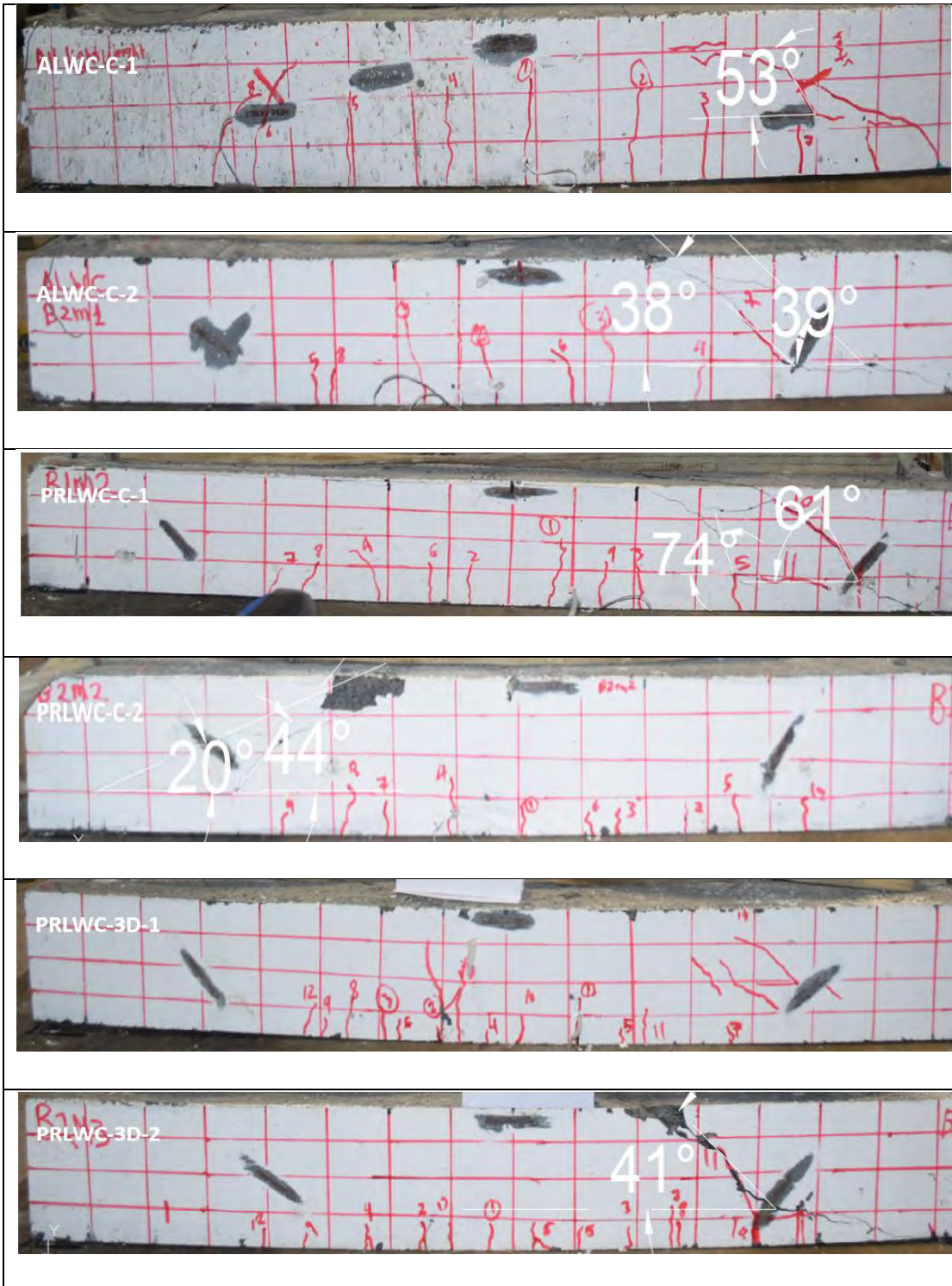


(b)

Figure D.6: Load versus strain initial responses for Group F beams (a) PRLWC-HY-1, (b) PRLWC-HY-2.

Appendix E

Modes of failure and angles of cracks of all the twelve beams are presented in Appendix E



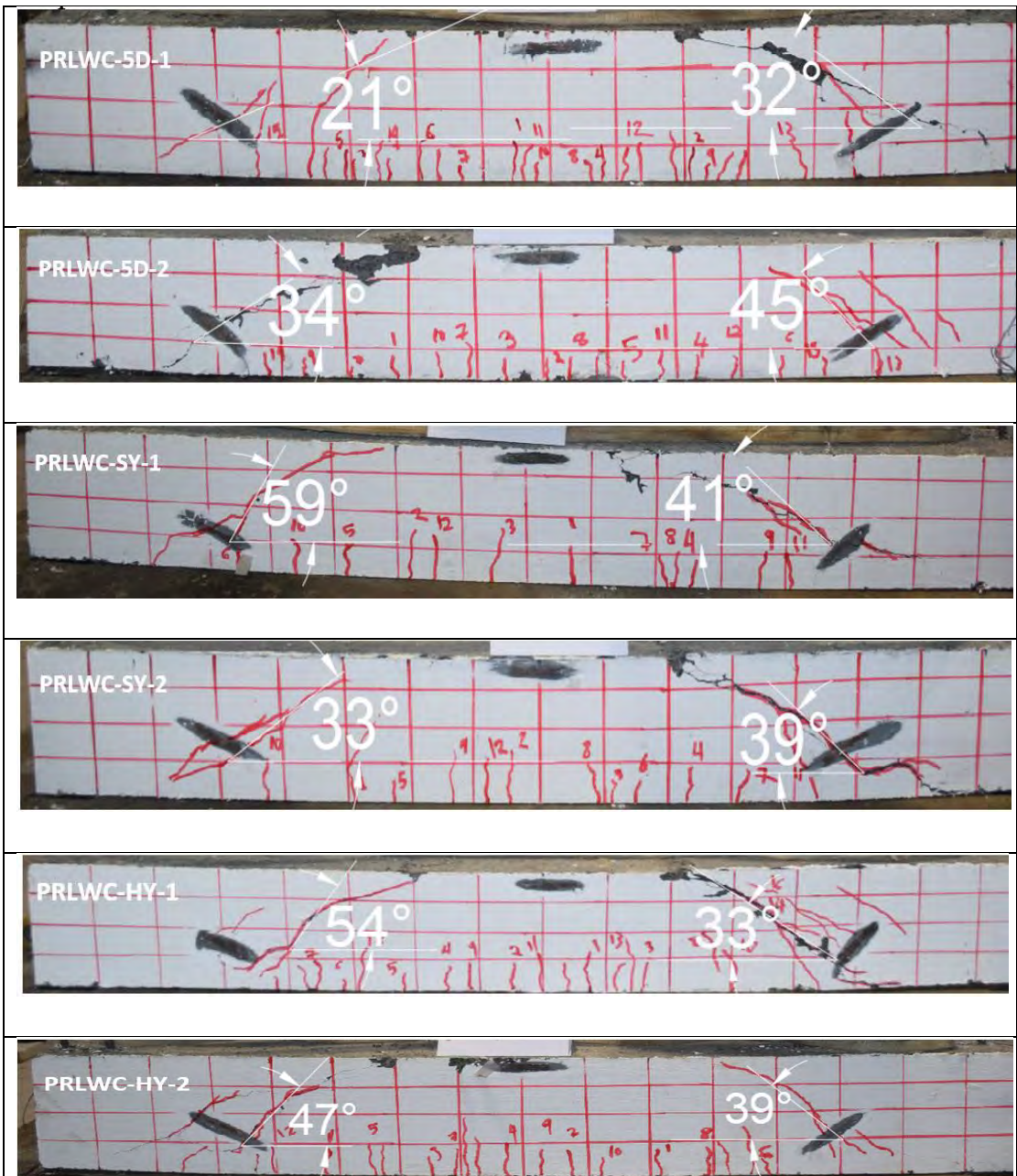
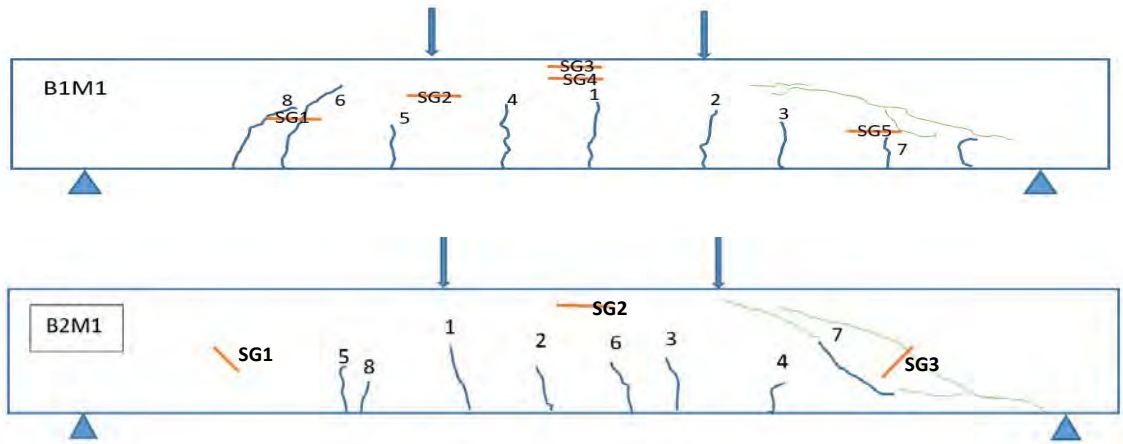


Figure E.1: Modes of failure and angles of cracks of all the twelve beams.

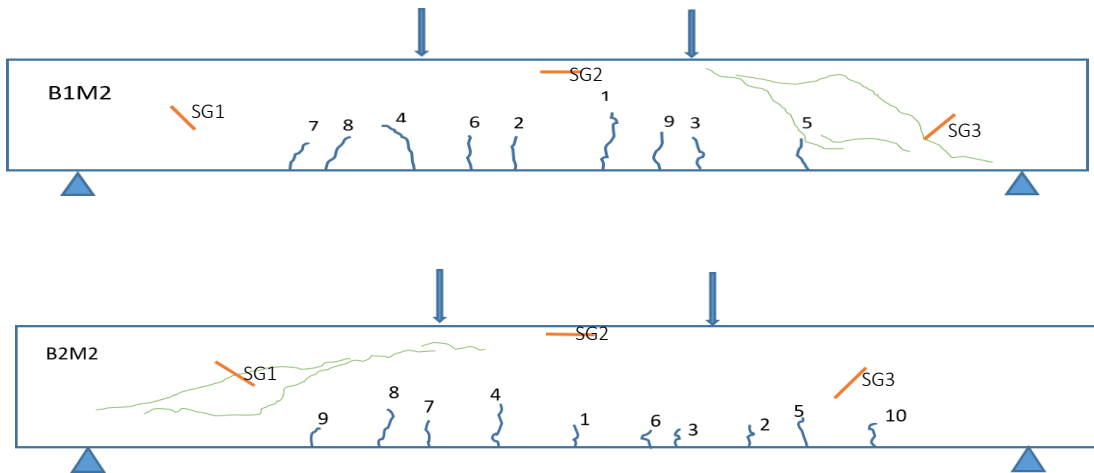
Appendix F

Schematic diagrams of all the twelve beams are shown in Appendix F.

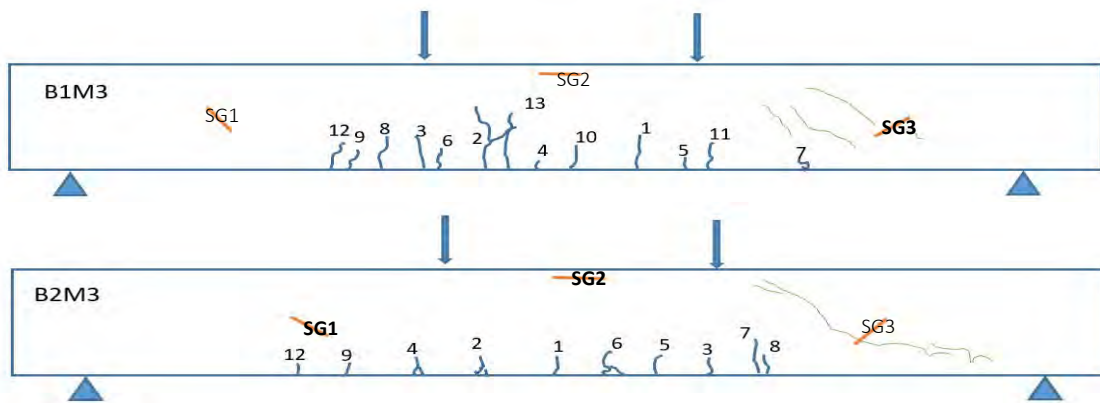
Group A



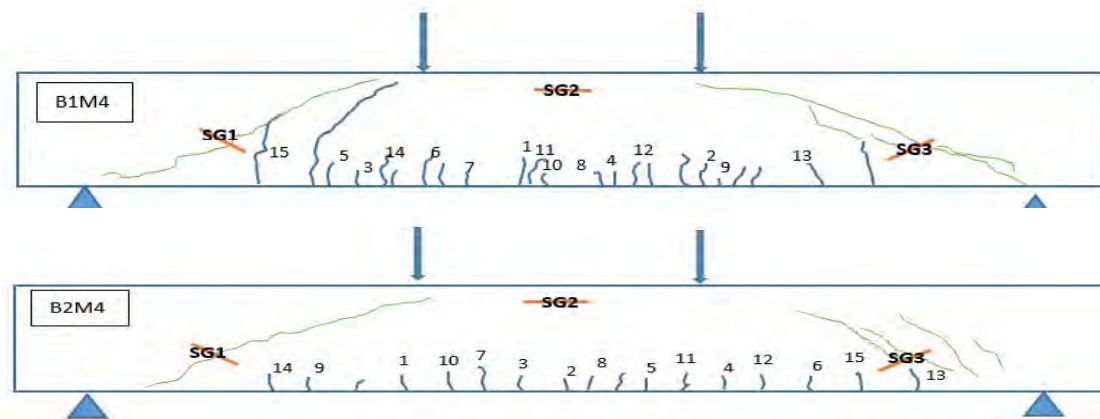
Group B



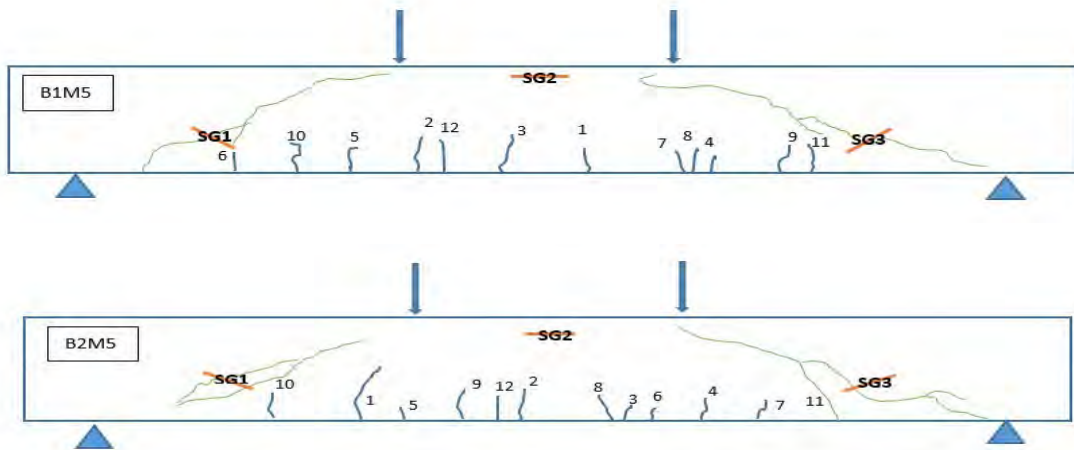
Group C



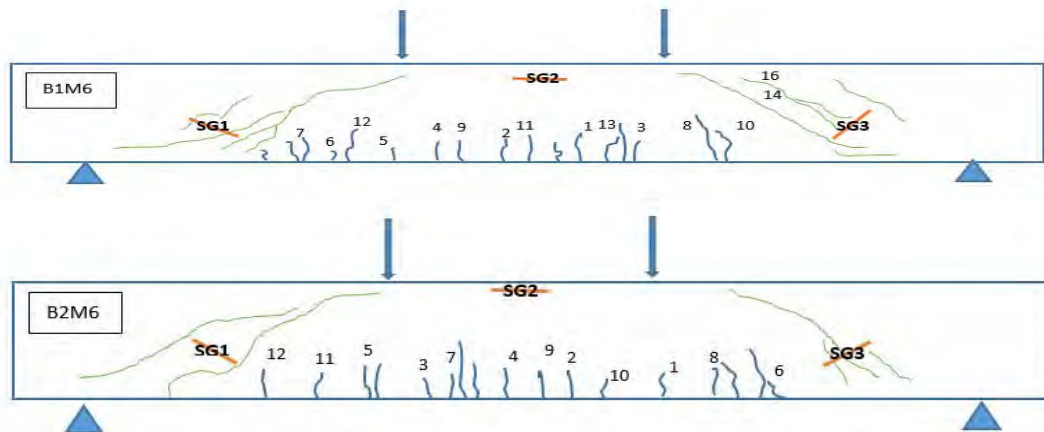
Group D



Group E



Group F



Appendix G

DIC results of the tested beams are shown in Appendix G

Crack initiation and propagation

Group A

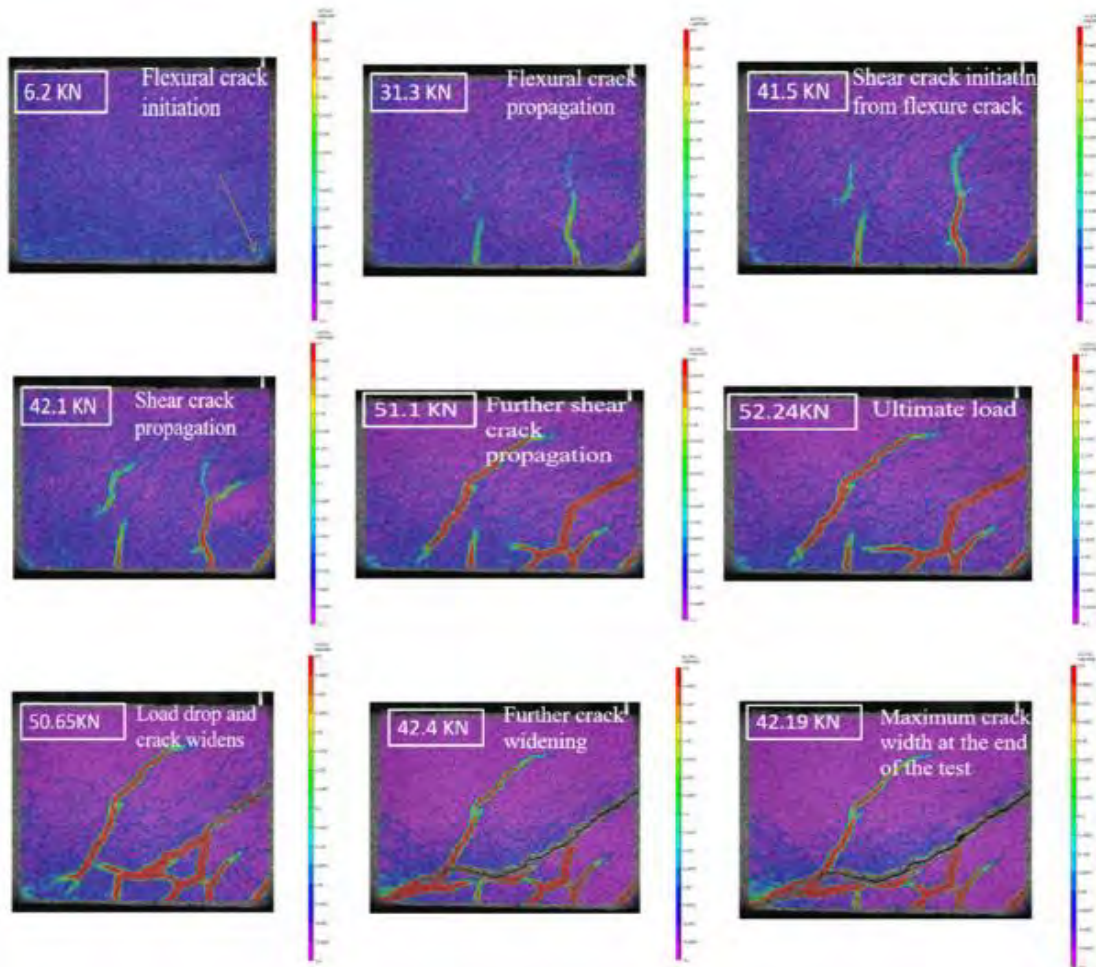


Figure G.1: Shear and flexure crack initiation and propagation of ALWC-C-1.

Group B

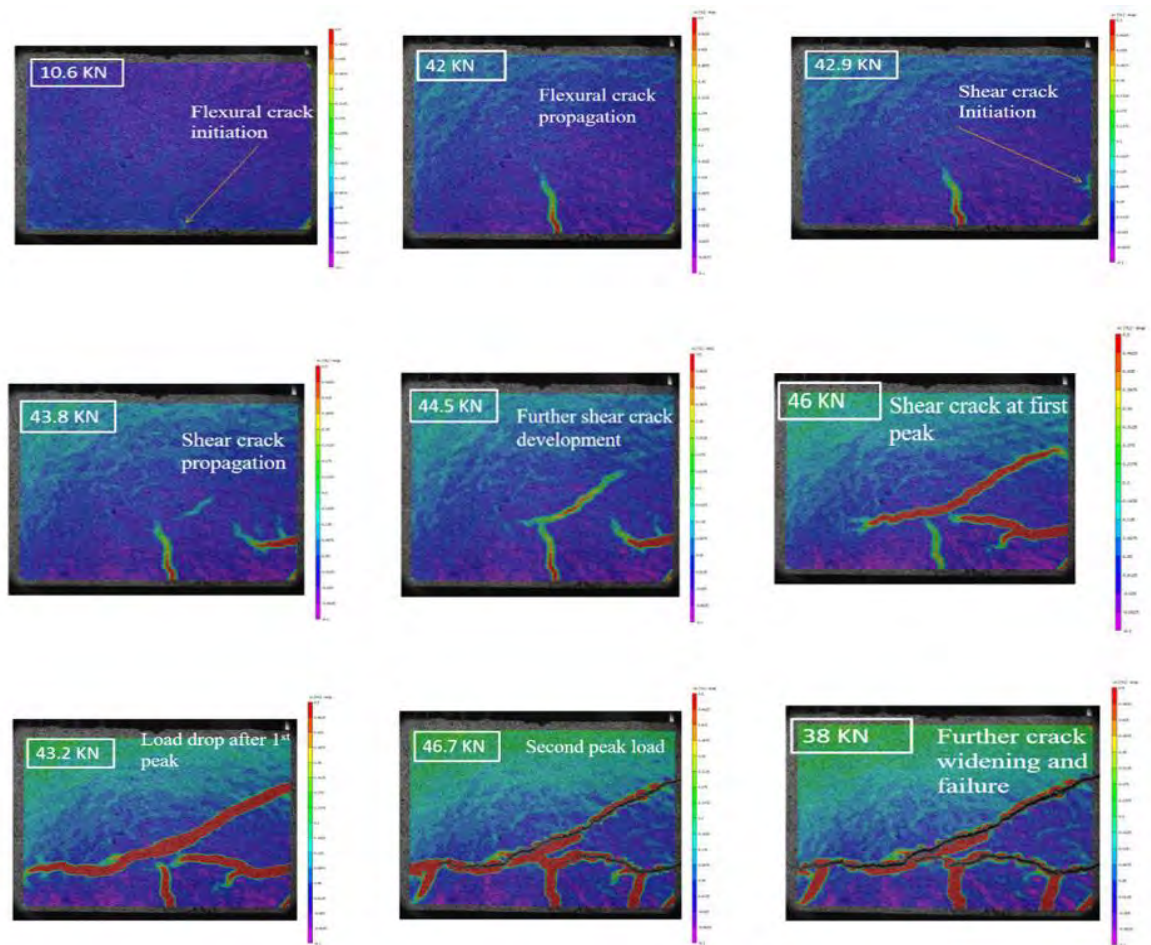


Figure G.2: Shear and flexure crack initiation and propagation of PRLWC-C-2.

Group C

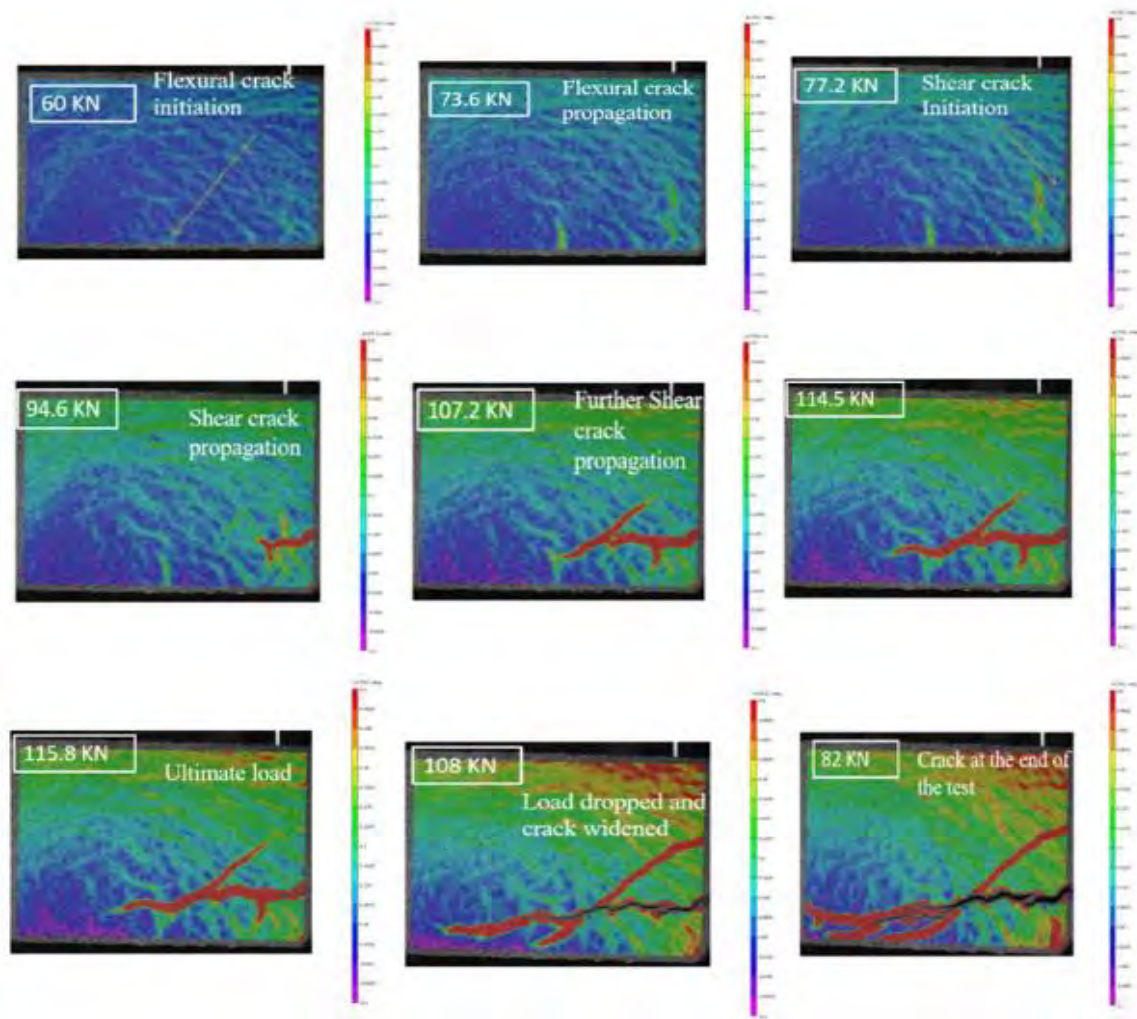


Figure G.3: Shear and flexure crack initiation and propagation of PRLWC-3D-2.

Group D

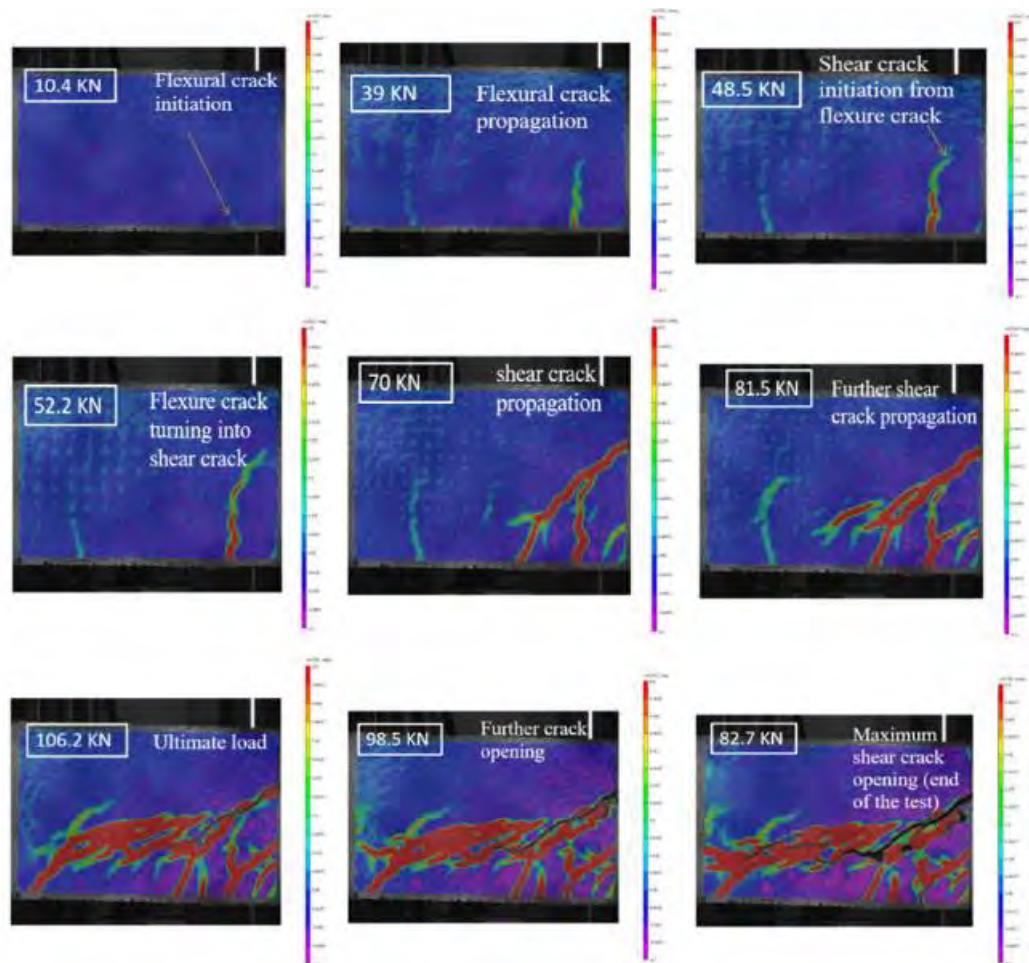


Figure G.4: Shear and flexure crack initiation and propagation PRLWC-5D-1.

Group E

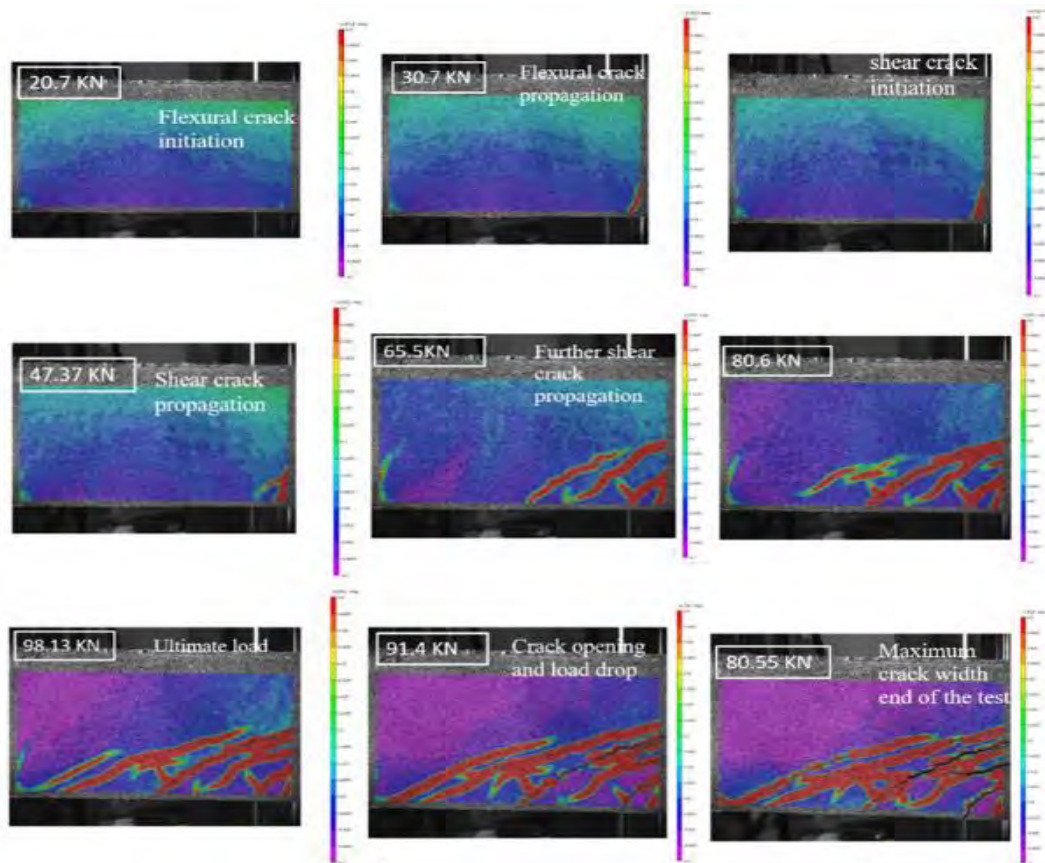


Figure G.5: Shear and flexure crack initiation and propagation for beam PRLWC-SY-1.

Group F

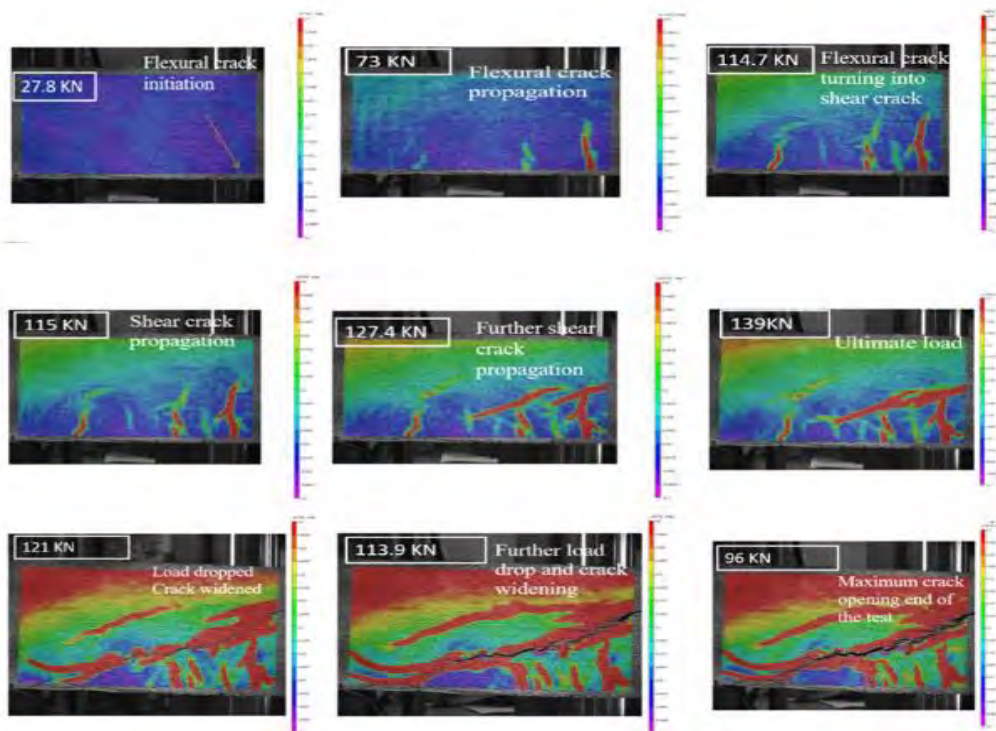


Figure G.6: Shear and flexure crack initiation and propagation for beam PRLWC-HY-1.

Crack widths.

Group A

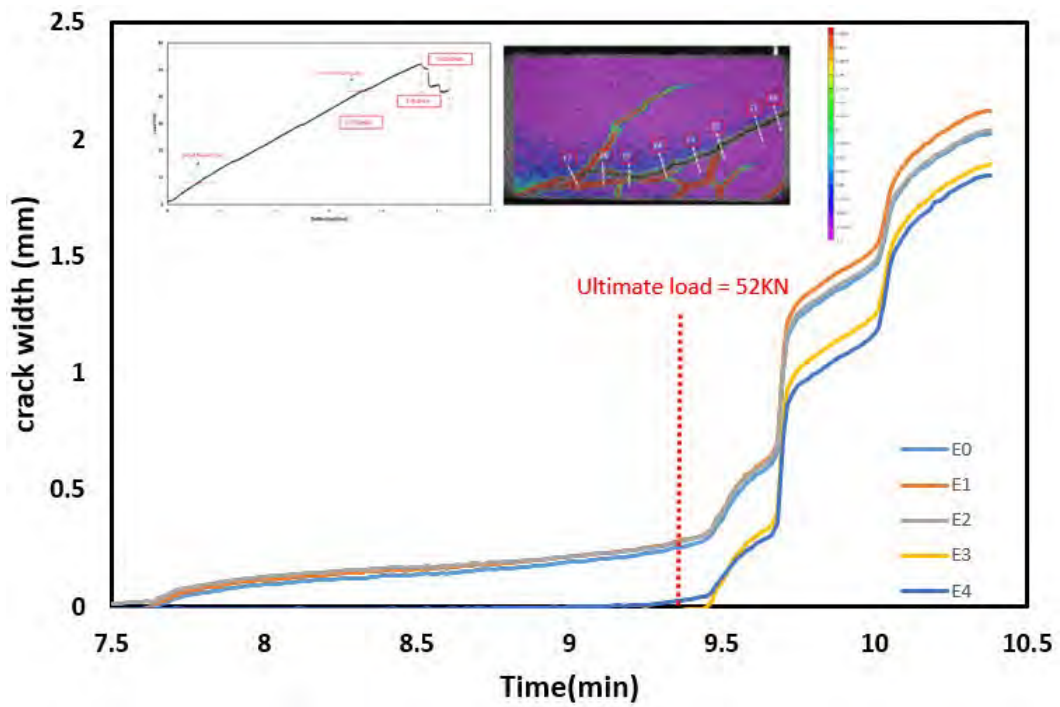


Figure G.7: Crack vs time plot for beam ALWC-C-1.

Group B

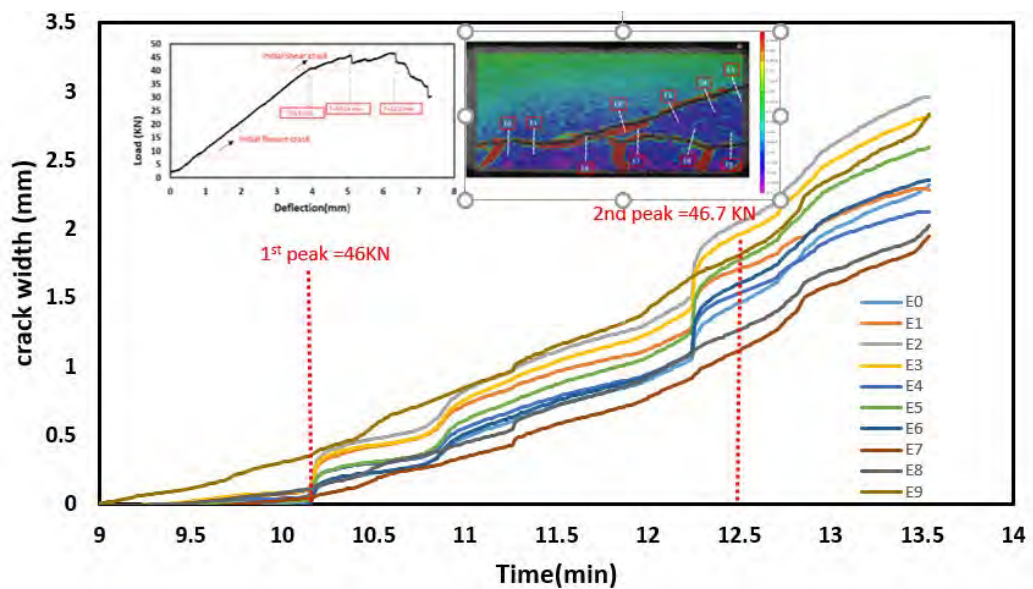


Figure G.8: Crack vs time plot for beam PRLWC-C-2.

Group C.

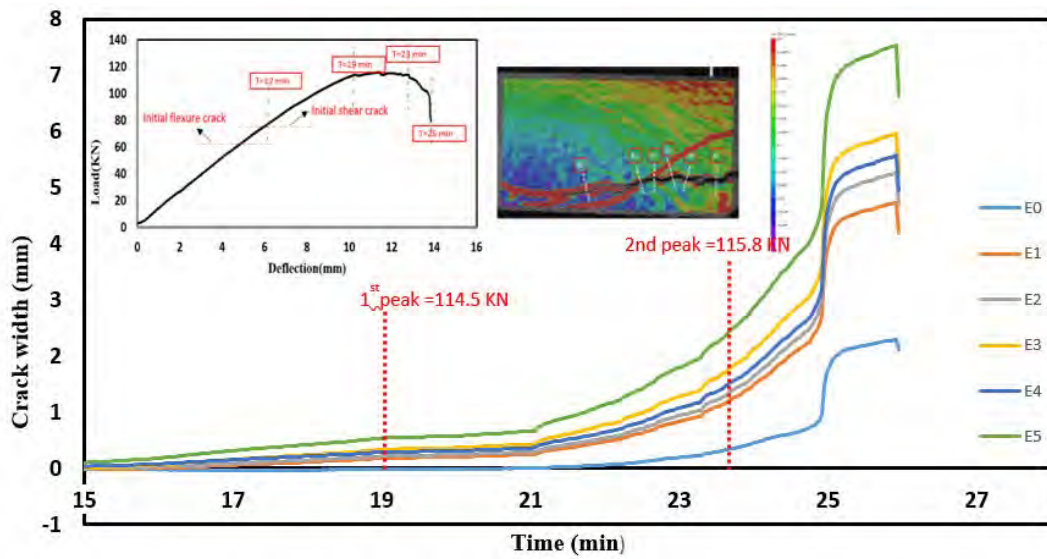


Figure G.9: Crack vs time plot for beam PRLWC-3D-2.

Group D

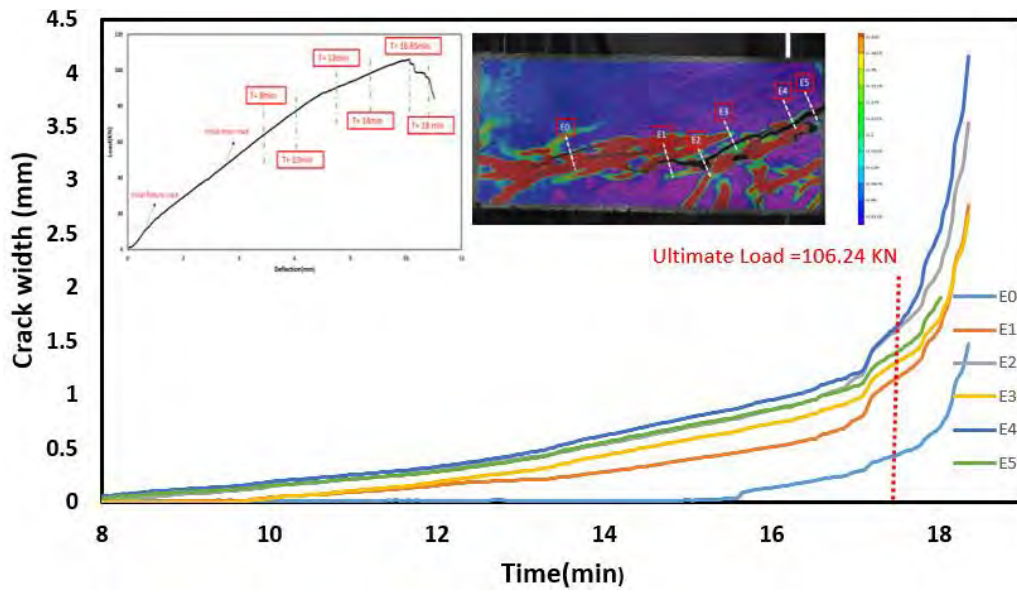


Figure G.10: Crack vs time plot for beam PRLWC-5D-1.

Group E

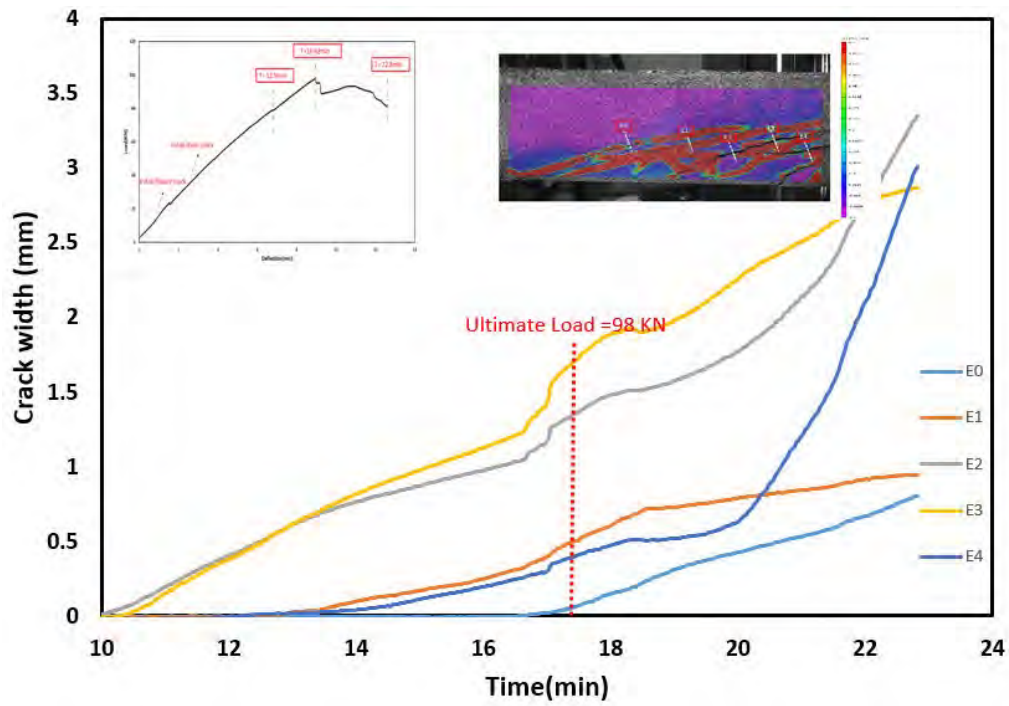


Figure G.11: Crack vs time plot for beam PRLWC-SY-1.

Group F

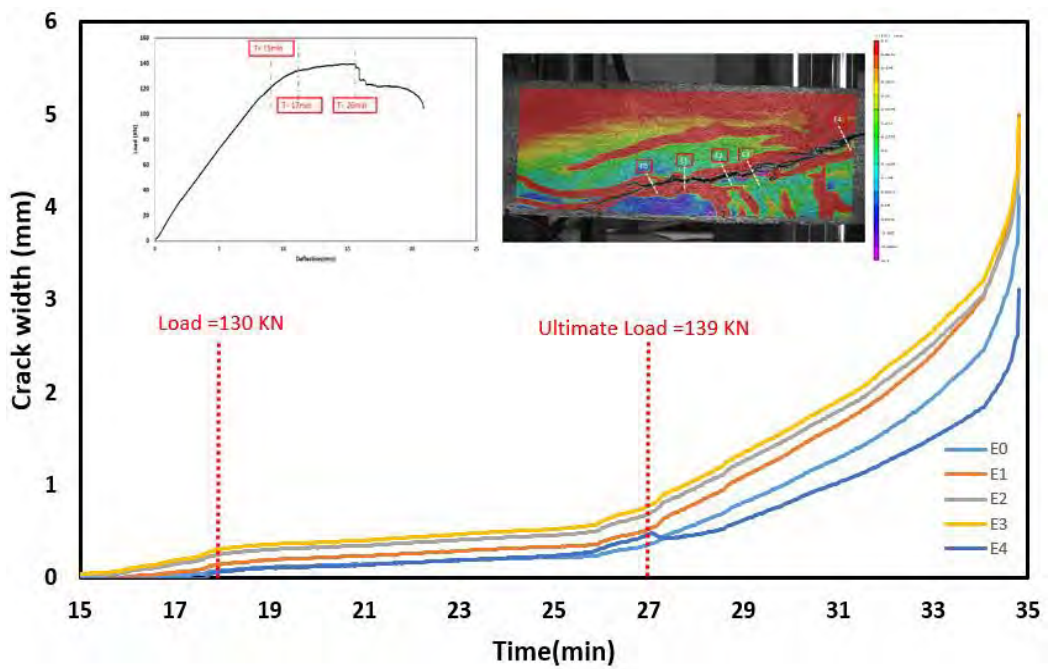


Figure G.12: Crack vs time plot for beam PRLWC-HY-1.

Appendix H

Sample calculations of SFRC proposed equations for 3D fiber reinforced concrete

Narayan and Darwish

$$V_n = \left[\left[0.24 f_{sp} + 80 \rho \frac{d}{a} \right] + v_b \right] b_w d$$

For the average of group C

- $f_{cuf} = 68 \text{ MPa}$
- $f'_c = 54.4 \text{ MPa}$
- $a = 500 \text{ mm}$
- $d = 159 \text{ mm}$
- $\rho = \frac{336}{159 \times 150}$
- $b_w = 150 \text{ mm}$
- $(L_f/D_f) = 65$
- $V_f = 0.75/100$
- df (bond factor) = 1

Substituting in eq. (2)

$$F = 65 \times \frac{0.75}{100} \times 1 = 0.4875$$

$$V_n = \left[\left[0.24 \frac{68}{20 - \sqrt{0.4875}} + 0.7 + \sqrt{0.4875} + 80 \frac{336}{150 \times 159} \frac{159}{500} \right] + 0.41 \times 4.15 \times \right.$$

$$\left. 0.4875 \right] 150 \times 159 = 56.49 \text{ KN.}$$

Ashour equation for $a/d > 2.5$

$$\begin{aligned} V_n &= \left[\left(2.11 \sqrt[3]{\frac{f'_c}{f_c + 7F}} \left(\rho \frac{d}{a} \right)^{0.333} \right) \right] b_w d = \\ &= \left[\left(2.11 \sqrt[3]{\frac{54.4}{54.4 + 7 \times 0.4875}} \left(\frac{336}{150 \times 159} \frac{159}{500} \right)^{0.333} \right) \right] 150 \times 159 \\ &= 44.93 \text{ KN.} \end{aligned}$$

Modified ACI equation

$$V_n = [(0.7 \sqrt{f'_c} + 7F) \frac{d}{a} + 17.2 \rho \frac{d}{a}] b_w d = (0.7 \sqrt{54.4} + 7 \times 0.4875) \frac{159}{500} + 17.2 \times \frac{336}{150 \times 159} \times \frac{159}{500} \times 150$$
$$\times 159 = 66.87 \text{ KN.}$$

To account for lightweight V_n is multiplied by a reduction factor of 0.868

$$V_n = 0.868 \times 66.87 = 58.04 \text{ KN}$$

Kwak equation

$$V_n = 3.7 e f_{sp}^2 \left(\frac{d}{a} \right)^{\frac{1}{3}} + 0.8 v_b = 3.7 \left(\frac{68}{20 - \sqrt{0.4875}} + 0.7 + \sqrt{0.4875} \right)^{\frac{2}{3}} \left(\frac{336}{150 \times 159} \times \frac{159}{500} \right)^{\frac{1}{3}} + 0.8 \times 4.15 \times 0.4875 = 57.91 \text{ KN.}$$

Khuntia equation

$$V_n = (0.167 \alpha + 0.25 F_1) \sqrt{f'_c} = (0.167 \times 1 + 0.25 \times 0.4875 \times 0.75) \times \sqrt{54.4} = 45.45$$

Note: - the lightweight effect is already counted for in the equation.

Where f_{sp} = estimated using the splitting tensile strength of SFRC as shown in the following equation.

- $f_{sp} = f_{cuf} / (20 - \sqrt{F}) + 0.7 + \sqrt{F}$
- e = arch action factor = 1 for $a/d > 2.8$, and $e = 2.8d/a$ for $a/d \leq 2.8$.
- a/d = shear span-to-depth ratio.
- ρ = flexural reinforcement ratio.
- F = fiber factor = $(L_f/D_f) \sqrt{v_f}$.
- f_{cuf} = cube strength of fiber concrete = $1.2 f'_c$, MPa (psi);
- f'_c = concrete compressive strength, MPa (psi);
- L_f = fiber length, mm (in.);
- D_f = fiber diameter, mm (in.);
- v_f = volume fraction of steel fibers;
- df = bond factor = 0.5 for round fibers, 0.75 for crimped fibers, and 1 for indented fibers;
- v_b = fiber pullout stress = $0.41 \tau F$, MPa (psi); and τ = average fiber matrix interface bond stress, taken as 4.15 MPa (600 psi)
- α = arch action factor = 1 for $a/d \geq 2.5$, and $\alpha = 2.5d/a \leq 3$ for $a/d < 2.5$
- F_1 = fiber factor = $\beta v_f (L_f/df)$
- β = factor for fiber shape and concrete type = 1 for hooked or crimped steel fibers, 2/3 for plain or round steel fibers with normal concrete, 3/4 for hooked or crimped steel fibers with lightweight concrete.

Appendix I

Beam design calculations are presented in Appendix I.

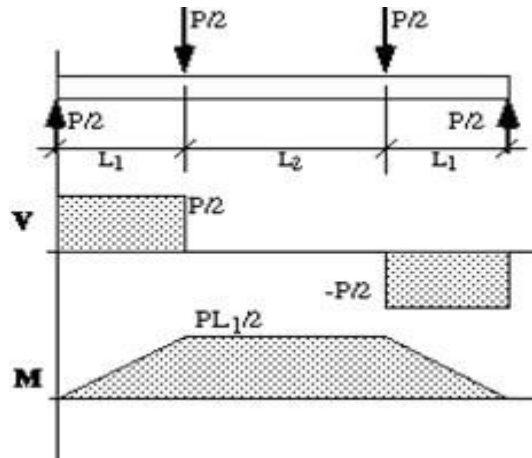


Figure I.1: Shear and bending moment diagram

3#12 bars are assumed

$$A_s = 339 \text{ mm}^2$$

$$V_c = 0.17\sqrt{f'_c} b d$$

$$\frac{p \text{ shear}}{2} = 0.17\sqrt{f'_c} b d$$

$$p \text{ shear} = 2 * 0.17\sqrt{f'_c} b d = 2 * 0.17\sqrt{40} * 150 * 157 = 43044.6 \text{ N}$$

$$a = \frac{A_s f_y}{0.85 f'_c b} = \frac{339 * 420}{0.85 * 40 * 150} = 27.9$$

$$p \text{ moment} = \frac{2A_s f_y (d - \frac{a}{2})}{L1 (\text{shear span})} = 81464 \text{ N}$$

pmoment \gg *pshear* therefore the assumed steel is ok

$$\rho = \frac{A_s}{bh} = \frac{339}{150 * 200} = 1.13\%$$

Vita

Mariam Elshazly was born in Kyoto, Japan. She graduated from Westminster school, Dubai, United Arab Emirates, as a school topper. She received her Civil and Environmental Engineering B.Sc. degree with highest honors in January 2016 from the University of Sharjah, United Arab Emirates. During her undergraduate studies, she had been the university swimming team captain. In the same year, 2016, she was enrolled in the master program in structural and materials engineering at the department of civil and environmental engineering at the American University of Sharjah (AUS). She was granted a Teaching Assistant Scholarship, through which she assisted her professors in delivering various specialty courses and laboratory assignments. Mariam continued her sports career as a member of the AUS swimming team where she added extra medals and trophies to her earlier ones. In the course of her master program, she published a paper in the FIB Congress, Melbourne, Australia, 2018.

She pursued two internship programs: the first was through the Yuksel and Chodai Joint Venture of the 3rd Bosphours Bridge and Marmara motorway project in Istanbul, Turkey, 2015; the second was in vrije universiteit of Brussels (VUB), Belgium, 2018, where she was involved in various structural and materials research programs, as an assistant to the principal researchers.